POLITECNICO

MILANO 1863

Topologic Optimization of Magnetic Circuits in Loudspeakers

TESI DI LAUREA MAGISTRALE IN
MUSIC AND ACOUSTIC ENGINEERING - INGEGNERIA INDUSTRIALE E DELL'INFORMAZIONE

Author: **Bruno Sciarrone**

Student ID: 10594610
Advisor: Prof. Giuseppe Bertuccio
Co-advisors: Grazia Spatafora
Academic Year: 2022-23

Abstract

Finite-element analysis (FEA) has become a widely used tool in transducer development, allowing at the design stage to faithfully simulate the end result while avoiding extra costs of manufacturing or physical prototyping.

This thesis work was done in Faital S.p.a, a european leader in loudspeaker manifacturing for automotive and audio Hi-Fi, and proposes an optimization methodology for the magnetic circuit of three different models of loudspeakers is proposed, through the use of 2D FEM models, analyzing the performance through three different indicators chosen a priori, concerning the Bl curve, its symmetry and the amount of material used.

All FEM models are set up in COMSOL Multiphysics ® and consequently graphical results are extracted from the software. The proposed result can be considered as a first step in the complete optimization process for the magnetic circuit, as other construction variables are not considered, such as the size of the magnet or the width of the air gap, so the final result leaves room for improvements, which can be made in a second design phase, after validation of the results presented in a subsequent prototyping phase.

Keywords: FEM, loudspeaker, magnetic circuit, topology optimization.

Abstract in lingua italiana

L'analisi ad elementi finiti è diventato uno strumento ampiamente utilizzato nello sviluppo di trasduttori, permettendo nella fase di design di simulare fedelmente il risultato finale evitando costi extra di manifattura o di realizzazione di prototipi fisici.

Questo lavoro di tesi è stato svolto in Faital S.p.a, azienda leader europea nella produzione di altoparlanti per l'automotive e per l'audio professionale, in cui propongo una metodologia di ottimizzazione per il circuito magnetico di tre diversi modelli di altoparlanti, tramite l'utilizzo di modelli FEM 2D, analizzando la performance tramite tre diversi indicatori scelti a priori, riguardanti la curva di Bl, la simmetria di quest'ultima e la quantità di materiale utilizzato.

Tutti i modelli FEM sono settati in COMSOL Multiphysics ® e conseguentemente i risultati grafici sono estratti dal software. Il risultato proposto può essere considerato come una prima fase del processo di ottimizzazione completo per il circuito magnetico, in quanto altre variabili costruttive non vengono prese in considerazione, come la dimensione del magnete o la larghezza del traferro, quindi il risultato finale lascia spazio a miglioramenti, che possono essere effettuati in una seconda fase di design, dopo la validazione dei risultati presentati in una successiva fase di prototipazione.

Parole chiave: FEM, altoparlanti, circuito magnetico, ottimizzazione topologica

Contents

6   Conclusions and Future Developments   103

1 | Loudspeaker Fundamentals

1.1. Loudspeakers History

Loudspeakers have been used for many years to convert electrical audio signals into sound waves. The invention of the loudspeaker is accredited to Johann Philipp Reis in 1861, but the refined version in 1876 invented by Alexander Graham Bell opened up a whole new world for the people living in the 19th century. Continuous effort eventually led to the discovery of the moving-coil loudspeaker in 1898, and in 1924 the moving-coil-loudspeaker in his latest fashion, that we also use today, was discovered [7]. The history of modern loudspeakers can be considered starting in 1925: this was the year when Rice and Kellogg developed the moving coil cone loudspeaker: what Rice and Kellogg developed is still the essence of the modern moving coil loudspeaker. The demands to the quality of speakers have not slowed down, and the actual design of a unit is not simple: designing one and optimising it for the best sound is a difficult process. Cost, size, and many other factors contribute to the overall quality.

1.2. Loudspeaker Working Principles

The basis of the dynamic loudspeaker is the electromotive force, also known as *Lorentz force*, which involves an electrical conductor in a magnetic field when an electrical current is passed through it. In most dynamic transducers, such as loudspeakers, the conductor consists in a *moving coil* placed inside a magnetic field generated by the *magnetic circuit.* This is composed by the permanent *magnet* and *the soft iron parts* that guide the magnetic flux generated by the magnet to the air gap. The instantaneous Lorentz force acting on a coil wire element $\vec{dl}$ in a magnetic field $\vec{B}$ is described by Equation (1.1) [8]:

$$d\tilde{F}(t) = \int_{\delta\Sigma} i(t)d\tilde{l} \; x \; \tilde{B} \tag{1.1}$$

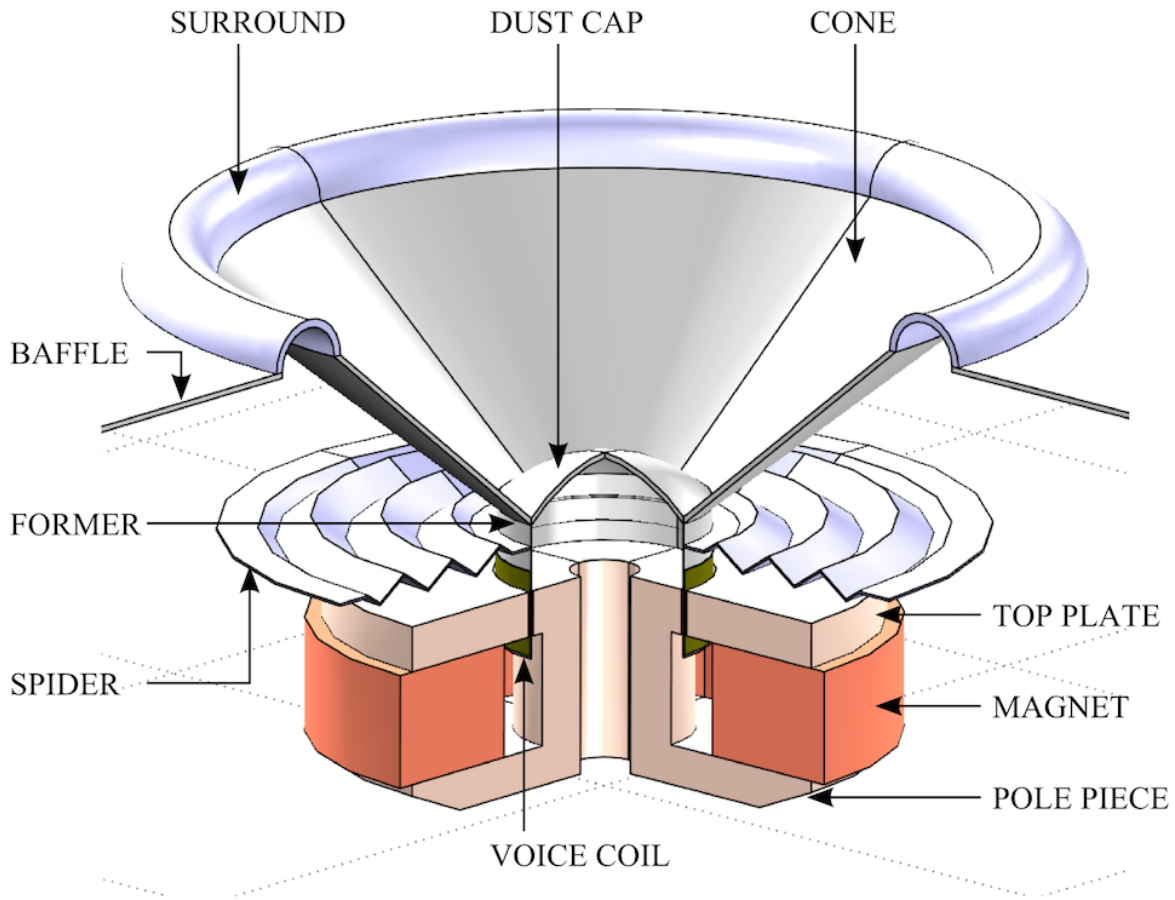Where $i(t)$ is the current, translated into mechanical excitation.

Figure 1.1: Loudspeaker Components [24]

In the figure 1.1 , can be seen all loudspeaker driver components [7]. The *cone*, attached to the moving coil, transforms this movement into air pressure waves, while the *suspensions* provide the recall forces that keep the moving parts in the rest position. The *surround* is the external suspension attached to the cone while the *spider* is the internal one, glued to the former which the moving coil is wounded onto. A dust cap is then normally placed in the apex of the cone in order to prevent the ingress of dust and any abrasive dirt, and may also be used as an air pump to cool the voice coil when the cone assembly moves in and out [24]. Loudspeaker comprehend acoustics, mechanics and electromagnetism as its working principles, and managing this topics during the design stages can be really useful. In this thesis, we will focus especially on the electromagnetic features related to magnetic circuit.

1.3.   Magnetism Fundamentals

Magnetic circuit characteristics play an important role on the overall performance and the behaviour of the magnetic field, and some of these depend on the initial design or the shape of its components. Some of these parameters regarding mostly the shape of the magnetic circuit are:

- *Magnet Type and Size*: The magnet's size and strength are important factors in determining the loudspeaker's overall performance, including its sensitivity and power handling.

- *Voice Coil Gap*: The distance between the voice coil and the magnetic pole piece affects the loudspeaker's sensitivity and power handling. A larger gap can result in lower sensitivity but higher power handling, while a smaller gap can result in higher sensitivity but lower power handling.

- *Pole Piece Shape*: The shape of the pole piece can affect the distribution of the magnetic field and the linearity of the speaker's response.

- *Back Plate Shape*: The shape of the back plate can affect the distribution of the magnetic field and the linearity of the speaker's response, as well as its power handling capabilities.

There are then some basic properties of the magnet required in the design stage that have to be taken into account when building the magnetic circuits, these are:

- *BH Curve*: As shown in Figure 1.10, the magnetic flux density in the magnet increases as the current in the coil increases gradually to magnetize the magnet until it finally reaches saturation at a certain point. If we focus on ferromagnetic materials, they can be divided in two main categories:

  - *Soft Materials*: characterized by a very high permeability and low coercivity (< 1000 A/m), which makes them easy to magnetize and demagnetize. These materials are used as flux conduits to confine and direct flux, and as flux amplifiers. The most commonly used are soft iron, alloys of iron-silicon, nickel-iron and soft ferrites.

  - *Hard Materials*: having a very low permeability and high coercivity ($> 10\,000$ A/m), they are very difficult to magnetize and demagnetize. Such materials are referred to as permanent magnets because once magnetized they tend to remain so. Commercially available hard materials include ferrites, alnico, samarium-cobalt (SmCo), neodymium-iron-boron (NdFeB) and bonded magnets.

In ferromagnetic materials, neighbour atoms tend to align their magnetic moments creating larger structures called magnetic domains, separated by domain walls. In a non-magnetized specimen, these do- mains are isotropic, thus resulting in $\vec{B} = \vec{0}$. But if we apply an external magnetizing force field to a sample of magnetic material, the dimension of the magnetic domains aligned to the direction of $\vec{H}$ start to grow and, with sufficient high values, destroy and rebuild the domain walls, creating a different distribution of magnetic domains with a total magnetization $\vec{M} \neq \vec{0}$ when the external field $\vec{H}$ is zero. The material has become a permanent magnet, and its residual flux density is called remanence (abbreviated with Br). If we further increase $\vec{H}$, all the magnetic domains will be aligned to it and the resulting magnetization $\vec{M}$ reaches saturation. The constitutive law of bulk magnetic properties is expressed in [7]:

$$\tilde{B} = \mu_0(\tilde{H} + \tilde{M}) \tag{1.2}$$

with μ_0 the vacuum permeability.

If we want to express the same equation in terms of the already cited magnetic permeability μ_r the same equation can be written as [7]:

$$\tilde{B} = \mu_0\mu_r(\tilde{H}) \tag{1.3}$$

The figure 1.2 shows the BH curve, also called *Hysteresis Loop Curve*, that is non linear and depends on prior state of magnetization.
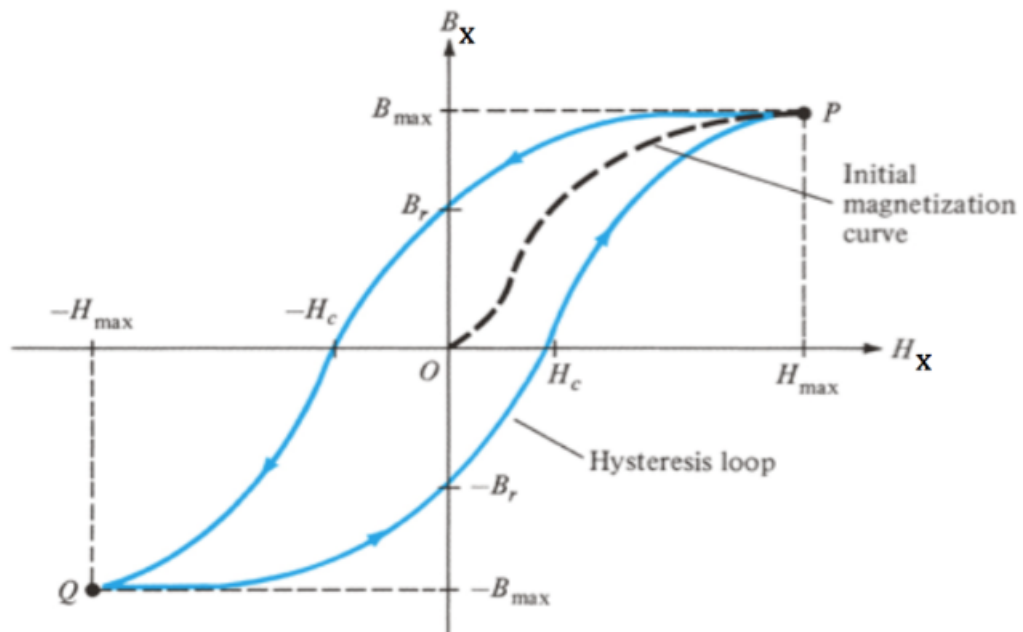
Figure 1.2: BH Curve [7]

The H_c point seen in the figure is where $\vec{H}$ is equal to 0, and is called *coercivity*. An important parameter for hard materials is the maximum energy product *BMax*. The energy product function is graphically defined as the area of the largest rectangle that can be drawn between the origin and the saturation demagnetization BH curve. This function is important for the strength of a permanent magnet material. A magnet that has an energy product near the maximum energy product has best magnetizing capabilities. The point of actual magnetization of the magnet on the demagnetization curve is defined as *working point*.

- *Self-Demagnetization Field*: Although the magnetic field generated on the surface of a magnetized magnet faces the S pole from the N pole, a magnetic field, represented as H_d in figure 1.3, acts in the opposite direction to the magnetization direction *I* inside the magnet.

    This internal magnetic field is known as a demagnetization field and since it acts in a direction to demagnetize the magnet, it is always represented in the second quadrant of the *BH Curve* when a magnet is used. The curve in this section is known as the demagnetization curve. This demagnetization field varies according to the proportions of the magnet, becoming smaller the longer and narrower the magnet is in the magnetization direction. In practice, the impact of this demagnetization field is often represented by the slope $\frac{B_d}{H_d}$, which is the ratio of the demagnetization field to the magnetic flux density.

This ratio is known as the permeance coefficient [21]:

$$P = \frac{B_d}{H_d} \tag{1.4}$$

The straight line traced by the permeance coefficient is known as the operating line and the intersection point of this line with the demagnetization curve is known as the operating point.
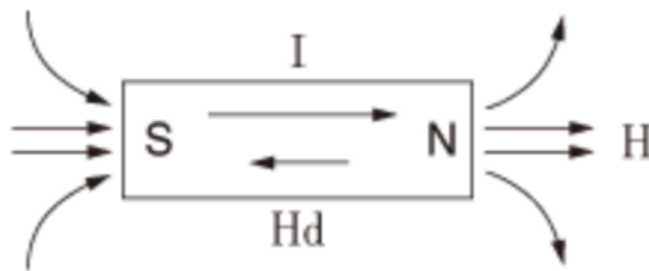

Figure 1.3: Self-Demagnetization Field [21]

- *External Field*: The operating point of a magnet will move and the magnetic force will change when a magnetic field is applied from the outside or when a piece of soft iron is brought near the magnetized magnet.
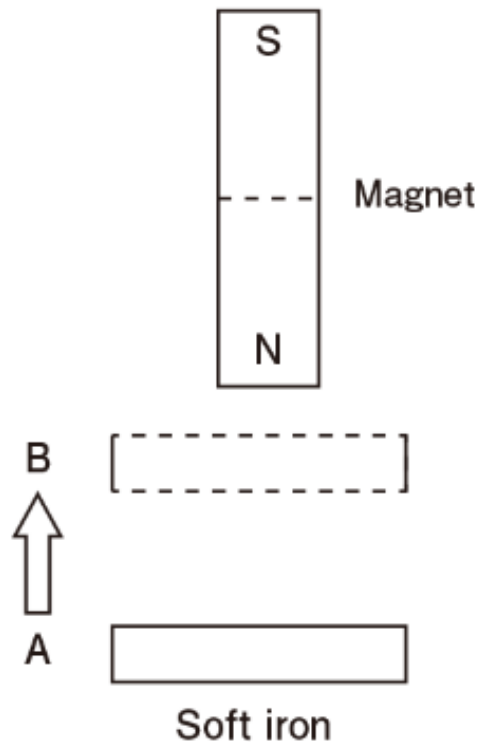
Figure 1.4: Soft iron near a magnet [21]

As shown in Figure 1.4, the magnetic force of a rod magnet changes when a piece of soft iron is brought near the magnet. This is because the soft iron magnetized by the magnet creates a magnetic field on the outside which acts in a direction to strengthen the magnetic force of the magnet. When analyzing this action with the demagnetization curve, the permeance coefficient of the magnet changes depending on the position of the soft iron. Assuming that the permeance coefficient at Position A is I, the permeance coefficient at Position B will become larger and change to II due to a reduction in the length of the vacant space.
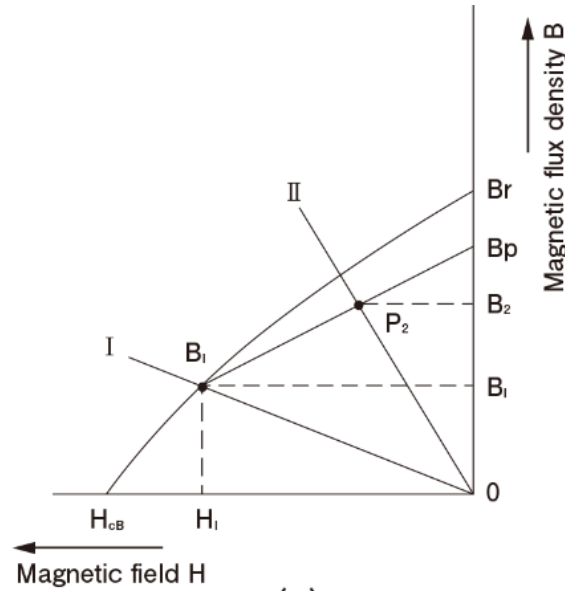
Figure 1.5: Recoil Magnetic Permeability [21]

At this point, the operating point will follow a separate path from the demagnetization curve starting from point P_1 to reach point P_2 as shown in Figure 1.5. This path from P_1 to B_p can be approximated by a straight line known as a recoil line. The gradient of this straight line is [21]:

$$\mu_r = \frac{B_p - B_1}{H_1} \tag{1.5}$$

known as the *recoil magnetic permeability*. μ_r is a material constant and this gradient is roughly the slope of the tangent to the demagnetization curve at the point B_r. In a ferrite magnet, μ_r usually shows a value of between 1.05 and 1.2. When the operating point moves from point P_1 to P_2 the magnetic flux density increases from B_1 to B_2.

Care is required in measuring and evaluating magnetic forces as the magnetic force changes when a piece of soft iron is located near the magnet.

1.3.1. Functioning Analysis

It is important to remember that the sole purpose of the magnetic assembly is to provide a concentrated magnetic field for the voice coil to operate in [3].

All of the physical parts are selected and assembled to achieve the desired field strength as efficiently as possible. The magnetic field in which the loudspeaker voice coil operates fills the air gap between the two pole pieces. The center pole piece is joined directly to

one end of the magnet. The magnetic lines of force are carried from the opposite end of the magnet through the heavy pot structure to the outer pole piece.

Although the arrows indicate the path of the magnetic lines of force, the magnetic field does not "flow" or fluctuate, but remains constant.

The electrical audio signal from the amplifier is carried to the terminal posts and through the flexible wires to the voice coil, producing a varying current in the coil and consequently a varying magnetic field around the coil.

This varying magnetic field interacts with the fixed held of the magnet, thus causing the entire cone assembly of the speaker to move in and out.

The instantaneous Lorentz force that acts on a coil is proportional to a quantity called *flux density*, measured in Tesla(T), which as the name suggests, is also represented by the density per square meter of magnetic flux lines, or when looking at a 2D cross-section, by the number of flux lines intersecting the coil. The flux lines are virtual lines along which the magnetic flux flows, starting from one magnetic pole and closing on the opposite pole, like an electric current flowing from one electric pole of a battery to the opposite pole.

Ideally, we want all the flux lines to pass through the air gap where the moving coil is located, for maximum efficiency, but in reality, some will close outside of it and constitute a loss of magnetic energy that is not available in the air gap.

Just as current in an electrical circuit with many resistances in parallel will flow more easily through resistances with lower values, magnetic flux will flow along paths with lower 'magnetic resistance.' This 'magnetic resistance' is called *reluctance*, and depends on the relative magnetic permeability, a measure of the resistance a material offers to the creation of a magnetic field within the material itself when it is immersed in an external magnetic field. The distribution of flux in the circuit is therefore determined by the local value of relative permeability in the soft iron parts: the higher the relative permeability, the lower the reluctance, and the greater the number of lines of flux that will pass through that area. And the longer the path that is found at a specific value of relative permeability, the greater the reluctance.

At the same time, soft iron parts permeability plays an important role in non-linear distortion, in fact, the less is relative permeability the less is the distortion amount, and consequently a cleaner sound reproduction. It is always a match between efficiency and linearity, with the magnet volume fixed.

1.3.2. Magnetic Circuit Components

The essential parts of the magnetic circuit of a loudspeaker are a set of concentric pole pieces (formed by the center pole piece and top plate), a magnet, and the additional iron

(the pot) needed to carry the magnetic flux from the magnet to the pole pieces. Also the air gap increase the reluctance of the magnetic circuit. The amount of air increases the reluctance of the circuit, thereby increasing the amount of current that we could put in a coil before we reach saturation. Also, the air gaps help the magnetic flux to expand outside the magnetic circuit. The physical size, shape, and arrangement of these various parts will vary, depending upon the overall design of the particular loudspeaker.
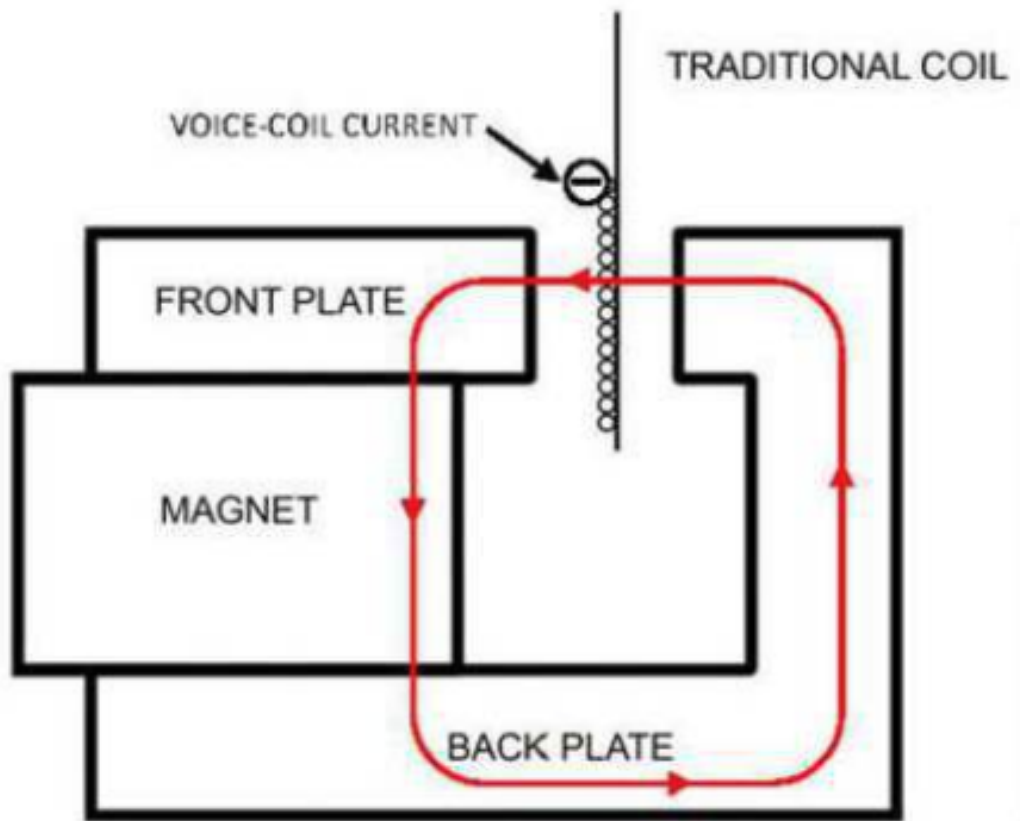

Figure 1.6: Magnetic Circuit with Air Gap [25]

Magnet

The goal of the magnet and the magnetic circuit in loudspeakers is to create a radial magnetic field in an annular gap in which the coil moves, called the air gap. [23] The gap has a finite volume due to its radial spacing and its length along the coil axis. If the gap spacing is increased, the reluctance goes up and the length of the magnet has

to be increased to drive the same amount of flux through the gap. If the gap length is increased, the flux density B goes down unless a magnet of larger cross-sectional area is used. Thus, the magnet volume tends to be proportional to the gap volume. With the evolution of loudspeakers, the evolution of magnets' technology followed, and the first evolution was when the coil of the motor stator was replaced by an Alnico permanent magnet. Permanent magnet speakers use a permanent magnet and allow us to eliminate the field coil.
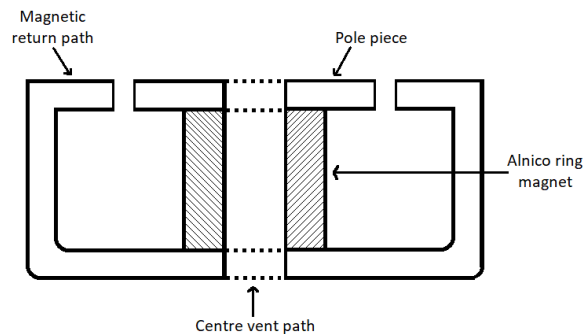
Figure 1.7: Alnico Magnet [23]

The main problem with Alnico magnets was that, due to the demagnetization curve of these kind of magnets, loudspeakers' shape was long and cumbersome. It was only during the 60's, with the introduction of hard-ferrite magnets, that loudspeakers' height was reduced. Hard ferrites are the reason why loudspeaker became more accessible. Besides, the magnetic circuit is designed to reach flux density values on the order of 1.5T in the air gap, corresponding to the iron saturation.
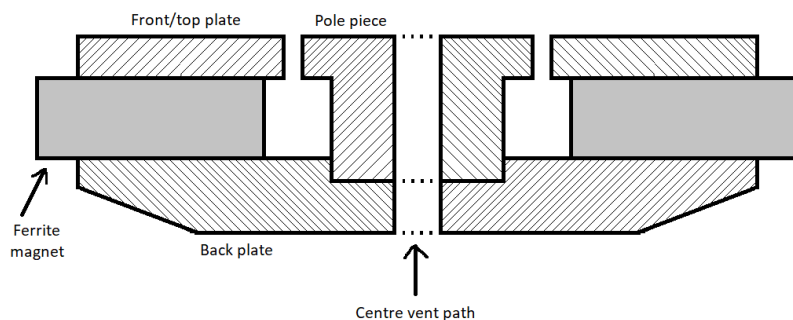
Figure 1.8: Ferrite Magnet [23]

The last step of the innovation process was obtained in the eighties, when the neodymium magnet was discovered. With such NdFeB permanent magnets, the size and weight of the devices decreased dramatically: they led the way to miniaturization.

The phenomenon is enhanced by the fact that these magnets are so powerful that it is sufficient to have cylindrical flat magnets located in the device center.
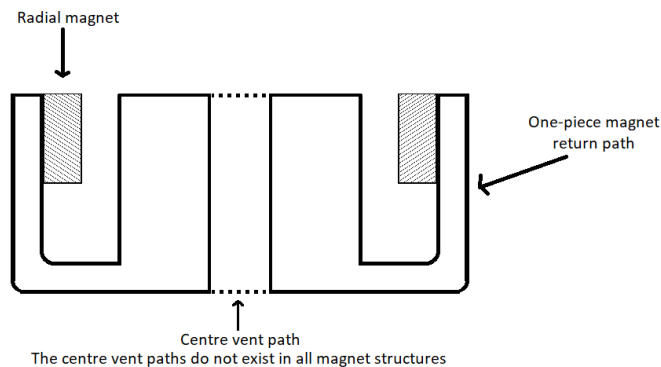

Figure 1.9: Neodymium Magnet [23]

The structure of electro-dynamic loudspeakers did not change throughout the years, except for the shape of the permanent magnet that was reduced and made better in terms of perfomance.

However, is well known that this structure has some drawbacks, like nonlinearities in the behavior and distorsion in sound reproduction. A few years ago, a new concept of magnet-only loudspeaker, also called "ironless loudspeaker", has been proposed to decrease the non-linearities of the loudspeaker motors. Such loudspeakers are called magnet-only because their magnetic circuit is totally made of rare-earth permanent magnets, such as NdFeB magnets.

Polar Plates and Magnet Types

The magnetic flux in the air gap is concentrated by means of the soft iron parts, but there will always be a certain amount of *fringe flux* extending above and below the gap. Any flux extending around the magnetic structure as a whole is referred to as *leakage flux*. The role of the magnetic circuit is to create a flux density as large as possible in the air gap. Also other requirements should be considered, such as the magnetic field uniformity

in the moving range of the voice coil and minimum leakage flux [7]. The magnet may be long and thin or short and squat; it may be a slug, a ring, or even a "W".
The most common shape is the ring magnet type, that is divided in three categories:

- The *underhung* design, lies completely within the axial range of uniform magnetic flux density. Such a structure is expensive, due to the metal and magnet requirements, but it completely engages a short voice coil over its normal travel and is often used in high linearity drivers of moderate to high efficiency.
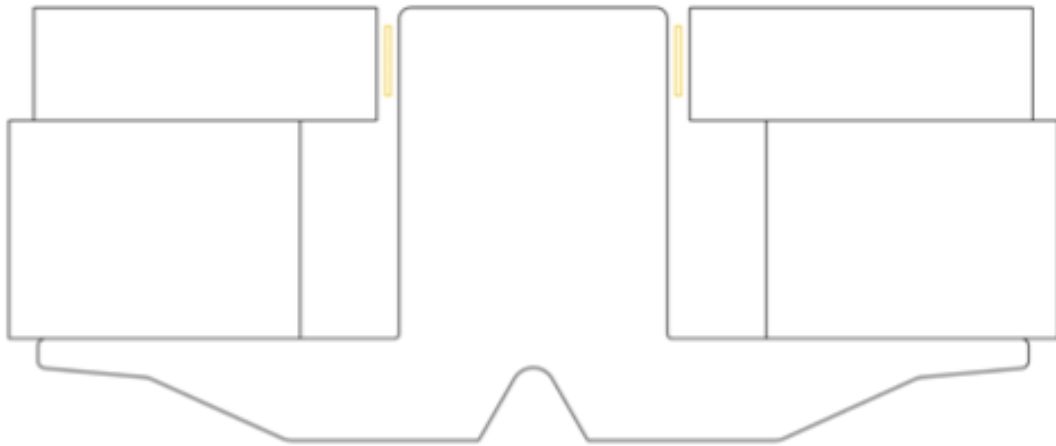

Figure 1.10: Underhung Design [7]

- The overhung design shown at 1.11 provides constant flux engaging a portion of the voice coil over a fairly large excursion range. The compromise here is that a large percentage of the voice coil lies entirely outside the flux field at all times. This design approach may be applicable for drivers intended for high linearity, but with relatively low efficiency.
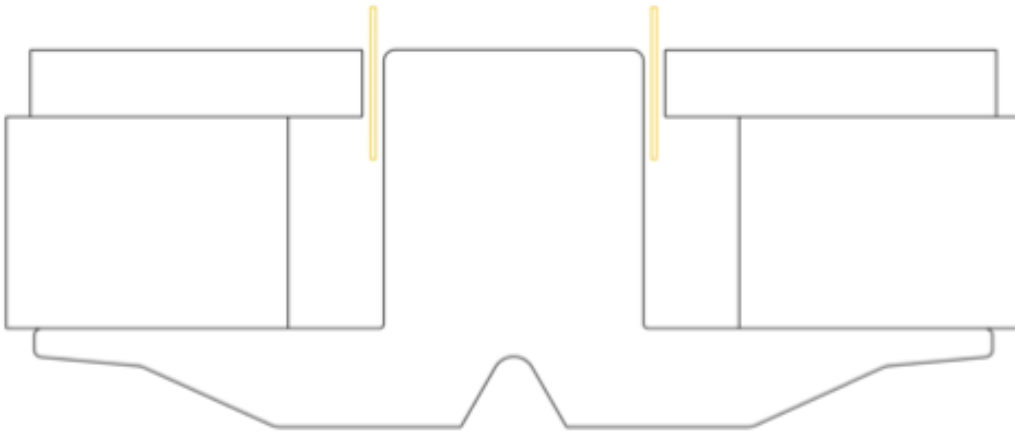
Figure 1.11: Overhung Design [7]

- The equal length configuration, that concentrates all of the flux in the coil at its rest position. It is evident that even moderate excursions of the voice coil will result in some loss of total flux engaging the voice coil, thus producing distortion. This design is common in very high efficiency drivers used for musical instrument amplification, where some degree of distortion may indeed be sonically beneficial.
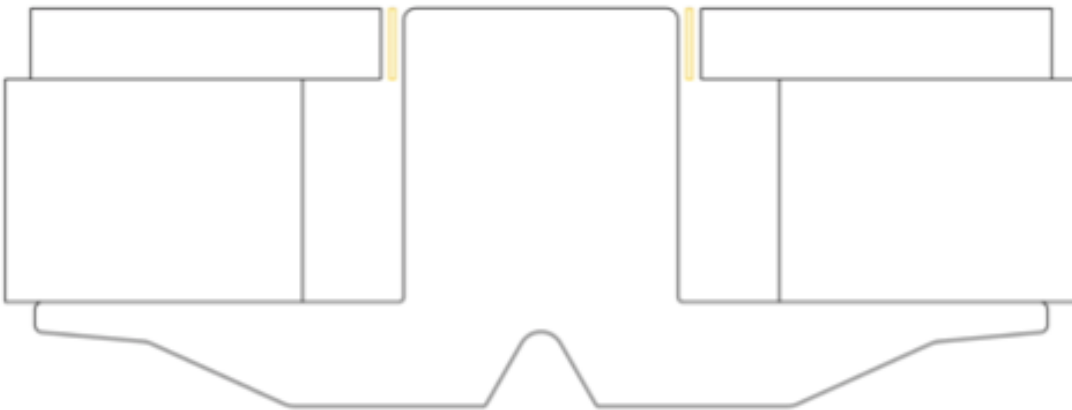

Figure 1.12: Equal Length Configuration [7]

Flux Components

Flux modulation refers to changes in the static magnetic flux density. The source of the modulation is the current through the voice coil that induces small local loops of current in the iron adjacent to the voice coil, primarily causing heat and loss of efficiency [6]. This effect is minimized through the use of shorting rings placed near or inside the gap and through the use of demodulation caps placed on the pole piece. They also play an important role in the modulation of the voice coil inductance: the in-and-out motion of the voice coil over the pole piece varies the amount of iron that is instantaneously enclosed by the voice coil. Since the voice coil acts as an iron core inductor, the instantaneous inductance of the voice coil changes. Demodulation caps and rings act as shorted turn secondary transformer, reducing the inductance so that its modulation is minimized.

Magnetic Circuit Topology

The most diffused topology of a loudspeaker's magnetic circuit is the one with a ring magnet external to the voice coil and soft iron parts are a top and a back plate that close the circuit [8].
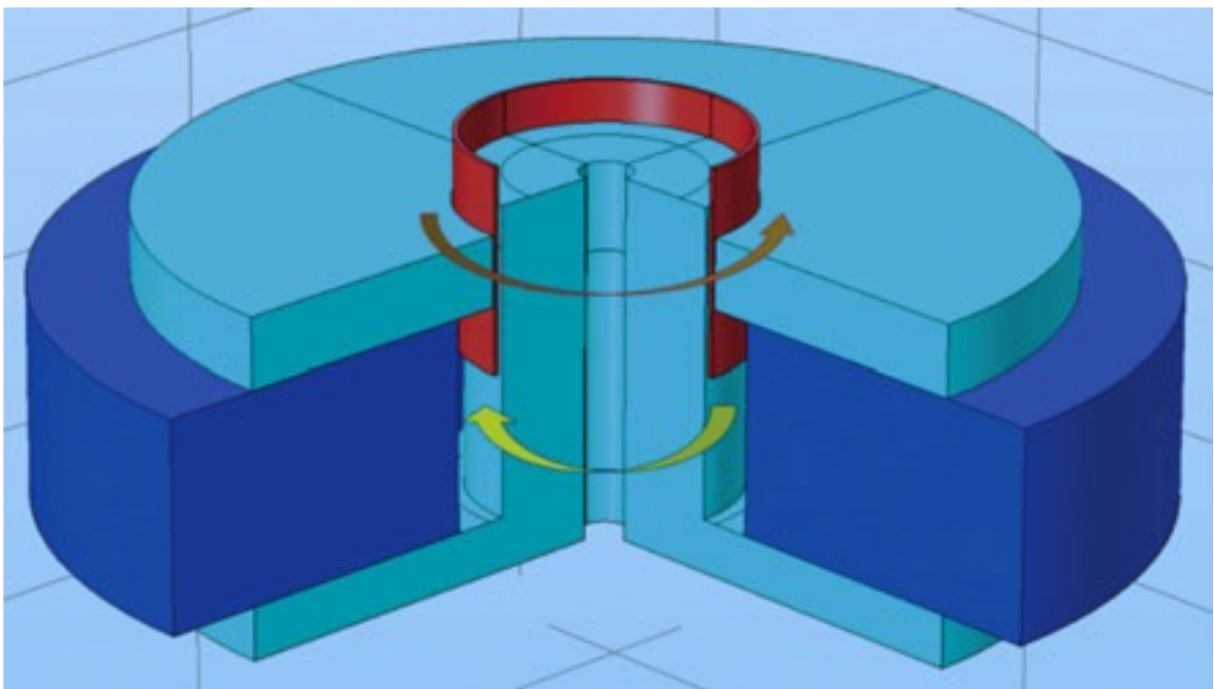

Figure 1.13: Magnetic Circuit Topology [8]

In the figure, we can see how soft iron parts are the light blue ones, while the magnet is the deep blue one.

In this case, the current has an anticlockwise flow, red painted, and this involves the presence also of some inducted currents, or *Focault Currents* which flow in the opposite direction, yellow painted in the image.

When the magnet is a disk (or a ring) inside the coil, magnetic efficiency is higher because there is a lot of soft iron around the magnet, which creates a high-permeability path for the lines of flux, so only a few of them escape the circuit. For the same reasons, stray flux is very low, so this topology is also self-shielding, in case magnetic shielding is desired. However, the maximum flux density in the air gap is limited, as the maximum surface of the disk is limited by the diameter of the moving coil (and for ferrite and neodymium, increasing the thickness of a magnet is not as effective as increasing the area in order to increase the energy available in the air gap). This is even more true if a ventilation hole is necessary to decompress the air behind the dust cap, which necessarily also limits the available magnetic energy of the magnet. The only practical option for high-SPL woofers or subwoofers that require decompression but also a magnetically efficient motor, is to use very large moving coils that allow for a large enough surface for an internal ring magnet that also has a large ventilation hole.

1.3.3. Thiele-Small Parameters

In the early seventies, several technical papers were presented to the AES (Audio Engineering Society) that resulted in the development of what we know today as 'Thiele-Small Parameters'. These papers were authored by A.N.Thiele and Richard H. Small. Thiele was the senior engineer of design and development for the Australian Broadcasting Commission and was responsible at the time for the Federal Engineering Laboratory, as well as for analyzing the design of equipment and systems for sound and vision broadcasting. Small was, at the time, a Commonwealth Post-graduate Research Student in the School of Electrical Engineering at the University of Sydney. Thiele and Small devoted considerable effort to show how the following parameters define the relationship between a speaker and a particular enclosure. However, they can be invaluable in making choices because they tell you far more about the transducer's real performance than the basic benchmarks of size, maximum power rating or average sensitivity. Thiele-Small parameters are an important determination factor of the efficiency and linearity of the speaker, and are mainly divided in three categories, *fundamental,small signal and large signal* parameters, that are briefly described [22]:

Fundamental Parameters

- S_d: Equivalent piston area of the driver diaphragm, in square metres.

- M_{ms}: Mass of the driver diaphragm and voice-coil assembly, including acoustic load, in kilograms. The mass of the driver diaphragm and voice-coil assembly alone is known as M_{md}

- C_{ms}: Compliance of the driver's suspension, in *(m·N)*(the reciprocal of its 'stiffness').

- R_{ms}: The mechanical resistance of the driver's suspension, calculated in $[\frac{Nxs}{m}]$.

- L_{es}: Voice coil inductance, in henries (H).

- R_e: DC resistance of the voice coil, in Ohms(Ω).

- *Bl*: The product of magnetic flux density in the voice-coil gap and the length of wire in the magnetic field, in Tesla-metres *(T·m)* [26].

Small-Signal Parameters

These values can be determined by measuring the input impedance of the driver, near the resonance frequency, at small input levels for which the mechanical behavior of the driver is effectively linear (i.e., proportional to its input). These values are more easily measured than the fundamental ones above [5].

- f_s: Resonance frequency of driver, measured in hertz (Hz). The frequency at which the combination of the energy stored in the moving mass and suspension compliance is maximum, and results in maximum cone velocity. A more compliant suspension or a larger moving mass will cause a lower resonance frequency, and vice versa. Usually it is less efficient to produce output at frequencies below f_s and input signals significantly below $f_s$can cause large excursions, mechanically endangering the driver.

- Q_{ts}: A unitless measurement, characterizing the combined electric and mechanical damping of the driver. In electronics, Q is the inverse of the damping ratio. The value of Q_{ts} s proportional to the energy stored, divided by the energy dissipated, and is defined at resonance.

- Q_{ms}: A unitless measurement, characterizing the mechanical damping of the driver, that is, the losses in the suspension (surround and spider).

- Q_{es}: A unitless measurement, describing the electrical damping of the loudspeaker. As the coil of wire moves through the magnetic field, it generates a current which opposes the motion of the coil. This so-called "Back-EMF" (proportional to *Bl x velocity*) decreases the total current through the coil near the resonance frequency, reducing cone movement and increasing impedance.

- V_{as}: Measured in litres or cubic metres, it is an inverse measure of the 'stiffness' of the suspension with the driver mounted in free air. It represents the volume of air that has the same stiffness as the driver's suspension when acted on by a piston of the same area (S_d) of the cone. Larger values mean lower stiffness, and generally require larger enclosures.

Large-Signal Parameters

: These parameters are useful for predicting the approximate output of a driver at high input levels, though they are harder, sometimes extremely hard or impossible, to accurately measure. In addition, power compression, thermal, and mechanical effects due to high signal levels (e.g., high electric current and voltage, extended mechanical motion, and so on) all change driver behavior, often increasing distortion of several kinds.

- X_{max}: Maximum linear peak (or sometimes peak-to-peak) excursion (in mm) of the cone. The motion of a driver cone becomes non-linear with large excursions, especially those in excess of this parameter.

- X_{mech}: Maximum physical excursion of the driver before physical damage. With a sufficiently large electrical input, the excursion will cause damage to the voice coil or another moving part of the driver. In addition, arrangements for voice coil cooling will themselves change behaviors with large cone excursions.

- P_e: Thermal power handling capacity of the driver, in Watts(W). This value is difficult to characterize and is often overestimated, by manufacturers and others. As the voice coil heats, it changes dimension to some extent, and changes electrical resistance to a considerable extent. The latter changes the electrical relationships between the voice coil and passive crossover components, changing the slope and crossover points designed into the speaker system.

- V_d: Peak displacement volume, calculated by [5] :

$$V_d = S_d \cdot X_{max} \tag{1.6}$$

Focus on BL Factor

The force factor $Bl(x)$ describes the coupling between mechanical and electrical side of lumped parameter model of an electro-dynamical transducer as shown in figure 1.14. This parameter is the integral of the flux density B versus voice coil wire length l [18].
The force factor $Bl(x)$ is not a constant but depends on the displacement x of the voice

coil. Clearly, if the coil windings leave the gap the force factor decreases. The nonlinear function is static (no frequency dependency) and can be represented as a nonlinear graph, table or power series expansion. The shape of the *Bl(x)* curve depends on the geometry of the coil-gap configuration and the field generated by the magnet.
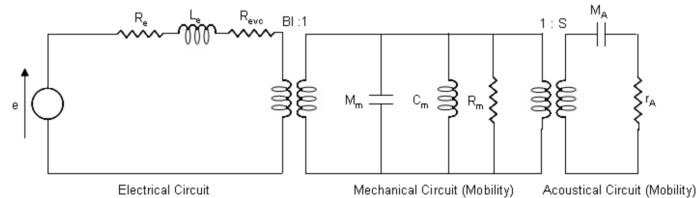

Figure 1.14: Electro-Mechano-Acoustic Model of a loudspeaker [12]

The force factor *Bl(x)* has two nonlinear effects:

- As a coupling factor between electrical and mechanical domain any variation of *Bl(x)* will affect the electro-dynamic driving force *F=Bl(x)i*. This mechanism is also called parametric excitation of a resonating system. High values of displacement x and current i are required to produce significant distortion.

- The second effect of *Bl(x)* is the displacement dependency of the back EMF generated by the movement of the coil in permanent field.

It's easy to demonstrate how a non-constant flux density with respect to displacement will also result in a non-constant force factor, even though the shape of the *Bl(x)* curve will naturally be different from the flux density curve, and therefore distorted.
We can differentiate two types of *Bl(x)* curve, depending on whether the applied current is DC or AC:

- Static is when we only consider DC signals in the computation of the *Bl* curve. In fact, if we apply a DC current of 1A to a coil at a position x in the magnetostatic field, the resulting static force will be *Bl(x)* Newton.

- When AC signals are involved, the force factor behavior will be more complicated due to eddy currents and flux modulation phenomena, and the shape of the *Bl(x)* curve will change slightly.

Some of the previously mentioned Thiele-Small parameters depend on the force factor Bl, and they too will depend on displacement. Q_{es} is inversely proportional to the square of *Bl* and will increase significantly as *Bl* decreases, just like sensitivity, which is proportional to the square of *Bl*. At the design level, it becomes essential to consider the size of the air gap and the dimensions of the moving coil in the loudspeaker.

1.3.4.   FEM

The Finite Element Method (FEM), or also Finite Element Analysis (FEA) is a numerical technique for solving problems which are described by partial differential equations. A domain of interest is represented as an assembly of finite elements, in which the discretized physical problem is solved for. This numerical approach is commonly used by the engineers to predict the behaviour and performances of a generic product for almost every application, without the cost and time of prototyping. In the loudspeaker industry, FEM software are used to study separately and jointly the acoustical, mechanical and electromagnetic features of the transducer [7]. Many authors have started to use FEM calculations in their works, including calculation of Bl factor over displacement curve [8, 18], or involved in optimization simulations [19, 20]. This method is really useful because helps the engineer to setup different parameters and studies without using materials or the need to build prototypes, avoiding extra costs.

2 | Thesis Goal

The goal of this work was the optimization of the magnetic circuit of three commercialized woofer, with changing diameter size. The first circuit is a three inches woofer, with a ferrite magnet, the second one is a ten inches woofer, also with a ferrite magnet and the last one is a fifteen inches woofer, with a neodymium magnet.

(a) 3 inches Woofer

(b) 10 inches woofer

(c) 15 inches woofer

Figure 2.1: Three woofers with different diameters

The process was done in a pre-design phase, with COMSOL Multiphysics, in detail with the built-in Optimization Module, and consisted in the optimization of the top plate and back plate of the loudspeakers' model with a Density Model, an algorithm of topology optimization used by the Optimization Module. The main focus was especially on the analysis and performance described by the Bl curve, with a strong attention on the magnetostatic analysis results and the starting position of the voice coil. The ultimate goal was to obtain an achievable prototype with the following characteristics:

- Obtaining a higher *Bl* value in x=0.

- Obtaining a better symmetry of the *Bl* curve. The symmetry of the Bl curve refers to whether the curve is symmetric around the origin (i.e., the point where the force factor is zero and the diaphragm displacement is zero). A symmetric Bl curve means that the force required to move the diaphragm in one direction is the same as the force required to move it in the opposite direction.

- With the previous results, having a reduced volume of plates, obtaining a better

sustainability and less amount of mass used with a lighter design of the products.

Every step of the process including the explanation of the algorithm used will be described in the next chapters.

3 | State of Art

3.1. Introduction

The main goal on the magnetic circuit optimization on loudspeakers, is to obtain a given flux density in the air gap, maximizing it, while constraining the volume of magnetic material used to the lowest quantity possible. This can be obtained analytically, but simplifying initial conditions obtaining the desired result only under certain assumptions [20]. This problem was definitely solved by the use of numerical methods.

3.2. Analytical Studies

Taking into account a magnetic circuit as shown in Figure 3.1, to reduce the number of free geometrical parameters some initial conditions have been posed.

- Air gap dimensions are fixed

- Magnetic material volume is fixed

- The operating point of the permanent magnet has to be where the energy product is maximum, in $(BH)_{max}$

With this conditions defined a priori, the optimized configuration is the one where the *utility factor*, has its maximum value. The utility factor is defined as [20]:

$$k_u = \frac{\sigma_a}{\sigma_a + \sigma_l} \tag{3.1}$$

Where σ_a is the magnetic flux in the air gap while σ_l is the leakage flux. The value of the utility factor is in the interval [0,1]. Also for the calculation of magnetic scalar potential some conditions defined a priori were set.

- The magnetic permeability of the soft iron materials is set to infinite. This leads to the potential of the iron core and back plate to be *V=0* and the potential of front plate is $V \neq 0$.

- The potential in the magnetic ring changes linearly in axial direction while remains constant in radial direction, this leads the magnetic field to be homogeneous.

Leakage fluxes have been calculated in three different regions of the magnetic circuit, represented as I, II, III in Figure 3.1.
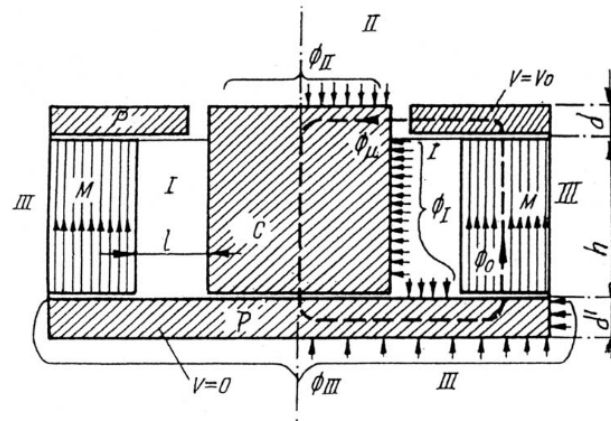
Figure 3.1: Magnetic Circuit of a Loudspeaker [20]

3.3.   Optimization with FEM Calculations

The first attempt to compute magnetic fields with numerical methods was done in the earlier 60's, using finite difference methods. Important information was given on the distribution of leakage fluxes and flux density in permanent magnets, with many plots supporting experiments. After 1980, many software were developed to compute 2D and 3D models with high precision. The main drawback of finite-element methods in comparison with analytical ones is that the system considered is computable only with given properties and materials. The system considered is presented in Figure 3.2.
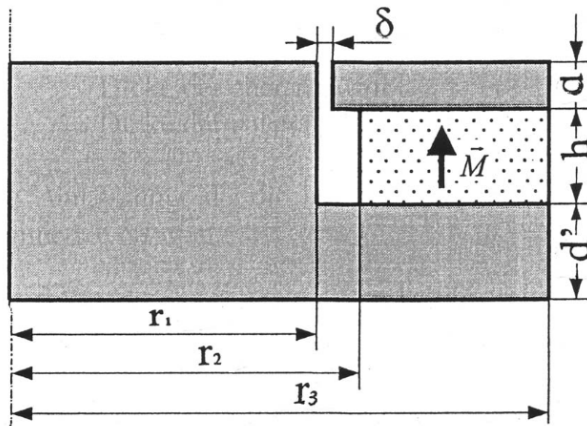
Figure 3.2: Loudspeaker System [20]

Seven dimensions can clearly be seen:

- r_1 iron core radius

- r_2 permanent magnet inner radius

- r_3 permanent magnet outer radius

- δ air gap length

- h height of the magnet

- d thickness of front plate

- d' thickness of back plate

As was previously considered in the analytical experiments, some constraints defined a priori should be taken into account. These constraints come both from acoustical and magnetic considerations, but also from construction requirements. The first constraint is to exclude from the optimization process the thickness of the back plate d', choosing a large value so that soft iron parts of the back plate do not saturate, with $d' = 2d$. Another free parameter taken away can be obtained using only relative dimensions, choosing as reference value δ, resulting in five free parameters [20]:

$$\frac{r_1}{\delta}, \frac{r_2}{\delta}, \frac{r_3}{\delta}, \frac{h}{\delta}, \frac{d}{\delta} \tag{3.2}$$

An acoustical constraint mentioned before is the given geometry of the air gap, determined by the shape of the voice coil, this leads to r_1, r_2 and δ defined. Now, $\frac{r_2}{\delta}$ is constrained by acoustical and manufacturing considerations, and determines the magnitude of the

space between the iron core and the inner surface of the magnetic ring, leaving two free parameters, $\frac{r_3}{\delta}$ and $\frac{d}{\delta}$. The aim of the optimization is to find the value of the parameters defined above, so that, with a given volume of the air gap, [20]

$$V_\delta = \pi[(r_1 + \delta)^2 - r_1^2] \cdot d = \pi \cdot (2r_1 + \delta)\delta \cdot d \tag{3.3}$$

and with a given volume of magnetic material,

$$V_M = \pi(r_3^2 - r_2^2) \cdot h \tag{3.4}$$

the flux density value in the air gap is maximum. From the ratio $\frac{V_m}{V_\delta}$, is obtained a relationship between h and δ, defined as [20]:

$$\frac{h}{\delta} = \frac{V_m}{V_\delta} \cdot \frac{\left(\frac{2r_1}{\delta}\right) + 1}{\left(\frac{r_3}{\delta}\right)^2 - \left(\frac{r_2}{\delta}\right)^2} \cdot \frac{d}{\delta} \tag{3.5}$$

3.4.   Further Considerations

In this section we are going to make some considerations regarding magnetic circuits components in the optimization process.

3.4.1.   Effect of BH Curve on flux density

Generally, neodymium magnets have larger flux density than ferrite ones, and this means that the initial condition on magnetic permeability $\mu_r = \infty$ works for ferrite magnets but are not reliable for Nd-Fe-B ones, also the assumption of linearity of BH curve is wrong, leading sometimes to unrealistic values of density flux. Also has been demonstrated how, reducing the parameter $\frac{r_2}{\delta}$, a much bigger flux density in the air gap is obtained. Obviously, manifacturing considerations have to be taken into account when opting for this kind of solutions.

3.4.2.   Optimal Operating Point of the magnet

A lot of works regarding magnetic circuits in loudspeakers claim that the largest density flux considering initial configuration of the circuit is obtained in the point of maximum energy product BH_{max}. With B the magnetic flux density, and H the magnetic flux

intensity. This consideration starts from Ampere's Law [20],

$$\oint \vec{H} \cdot d\vec{s} = \Theta \tag{3.6}$$

with two assumptions:

- The magnetic field in the magnet and air gap is homogeneous

- $\mu_r = \infty$ so $H_{Fe}=0$

The relationship between the intensity of magnetic field in the magnet and in the air gap is describes as:

$$H_\delta \cdot \delta = H_M \cdot h \tag{3.7}$$

And from the continuity of the air flux,

$$B_\delta \cdot A_\delta = k_u \cdot B_M \cdot A_M \tag{3.8}$$

With k_u the utility factor seen in (3.1). Multiplying (3.7) and (3.8), the result is [20]:

$$B_\delta \cdot H_\delta \cdot \delta \cdot A_\delta = k_u \cdot B_M \cdot A_M \cdot H_M \cdot h \tag{3.9}$$

And consequently, making explicit B_δ,

$$B_\delta = \sqrt{k_u(\mu_0 B_M \cdot H_M) \cdot \frac{V_M}{V_h}} \tag{3.10}$$

Resulting in, k_u is maximum when BH is maximum. In fact, the induction B_{mag} and field strength H_{mag} should be close to B_{max} and H_{max} giving the maximum product $Max(B_{mag}H_{mag}) = B_{max}H_{max} = BH_{max}$ [19].
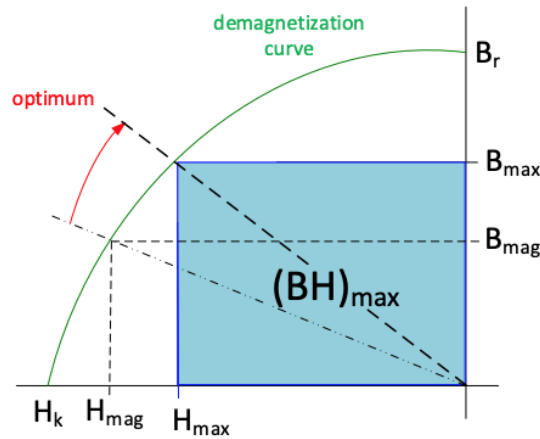
Figure 3.3: Optimum BH Value [19]

But this is not always happening, because the finite elements computation has clearly shown that k_u depends strongly on iron saturation, not simultaneously attain with BH_{max}.

3.4.3.   Shape Dimensions and Pole Plates

In 1970's could not be calculated analytically what was the best design choice to maximize the flux density in the air gap. With numerical methods this is possible, but every choice is up to the designer, because finite elements software doesn't give any hint on the best choice to optimize the performance.

3.4.4.   Air-Gap Topology

Typical configurations that maximize either efficiency or linearity of the electro-dynamical transducer are three [19]:

- The so-called equal-length configuration uses a minimum voice coil overhang to exploit the magnetic fringe field outside the gap, This configuration gives the highest force factor value *Bl(x=0)* at the voice coil rest position, which is beneficial for maximizing the effective force factor *Bl* when reproducing common audio signals. Unfortunately, this configuration generates significant harmonic and intermodulation distortion and other undesired nonlinear symptoms (DCdisplacement, instabilities ecc.) for voice coil displacement x

- The overhang configuration uses spare windings below and above the gap, waiting to be used when the voice coil is moved. This generates a plateau in the Bl(x) characteristic in Figure 3.4, giving more linearity and less nonlinear distortion for

moderate excursion.
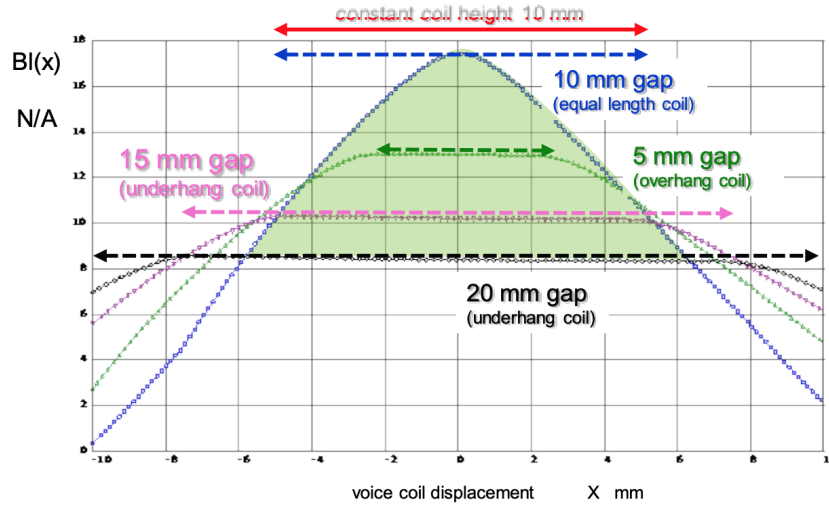
Figure 3.4: Bl(x) in underhang, overhang and equal length configuration [19]

- The underhang configuration in Figure 4 uses wider pole plates and a short coil to generate a linear plateau in the nonlinear *Bl(x)* characteristics and creates more linearity

3.4.5.   Voice Coil Height

The voice coil height h_c limits the maximum displacement X_{max} in an equal-length configuration. If nonlinear control can be applied to the loudspeaker and the nonlinear distortion can be cancelled actively, the maximum displacement can be increased to half of the voice coil height *($X_{max} = h_c/2$)*, where the force factor decreases to half of the *Bl* found at the rest position [19]

$$Bl(x = \pm \frac{h_c}{2}) \approx 0.5Bl(x = 0) \tag{3.11}$$

In a real loudspeaker the Bl figure results from the contribution of the length of each coil turn multiplied by the local B value. If more turns are added to the voice coil, or equivalently increasing its winding height from h to (h + δh), and expressing with $K = \frac{\delta h}{h}$, we obtain, evaluating motor strength, that [28]

$$B_s > B_a \frac{\sqrt{(1 + K)} - 1}{K} \tag{3.12}$$

or

$$B_s < B_a \frac{-1 - \sqrt{(1 + K)}}{K} \tag{3.13}$$

Where B_a is expressed as the ratio between the Bl and the winding length of the coil and B_s Bs is a mean B, averaged over the space occupied by the $\overline{\delta h}$ portion of the coil, and this leads to a greater motor strength depending on coil height.

3.4.6. Air Gap Depth

The optimal value h_g can be found by finding a gap geometry at which the induction at both ends of the voice coil [19]

$$B(x = \pm 0.5h_c, h_g) = 0.7B_{max} \tag{3.14}$$

With h_c is the coil height and h_g is the gap depth, is 70% of the maximum induction B_{max} in the gap. For a smaller value of the gap depth h_g, the windings at both ends of the voice coil would generate a lower contribution to the squared Bl value while increasing the electrical resistance Re, giving a lower motor efficiency factor Bl^2/R_e.
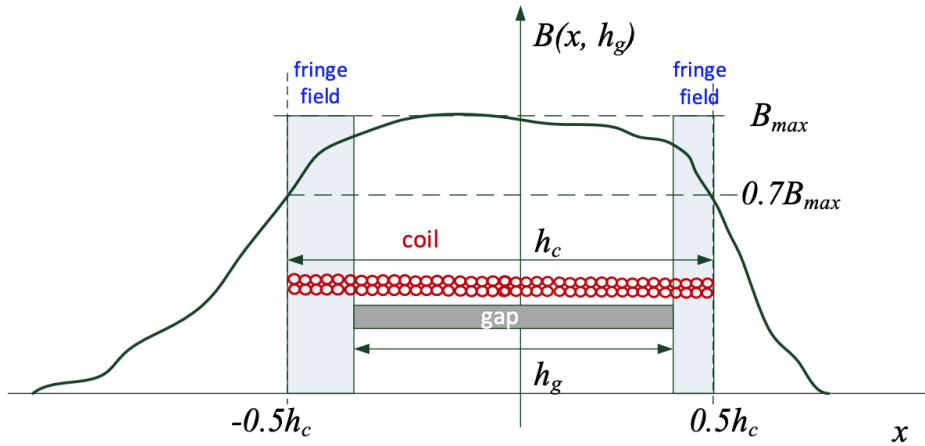
Figure 3.5: Air Gap Depth [19]

3.4.7. Symmetric Field

The vibration of the voice coil in positive and negative direction is determined by the Lorentz Force, explained in equation (1.1). The final aim is to convert the electrical energy in acoustical energy with the lowest amount of distorsions possible. This leads to the request of to be symmetric with respect to the direction of movement of the voice coil. In fact, the difference between the leakage flux below the air gap and above it has

to be minimized, and to reach this goal there are two main design choices that could be chosen [20]:

- Increasing the height of the soft iron core, and in this way the leakage flux above the air gap increases, obtaining a good shape of the flux inside the magnetic field.
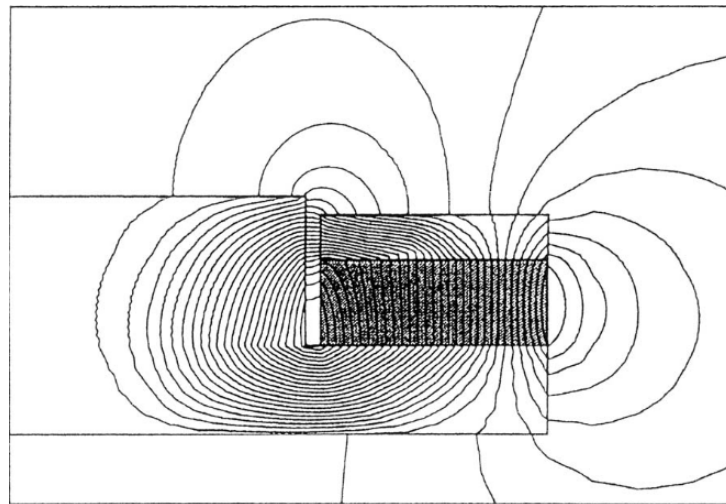
Figure 3.6: Height of the soft iron core increased [20]

- Incline the shape of the iron core near the air gap, unless is less effective than the previous choice
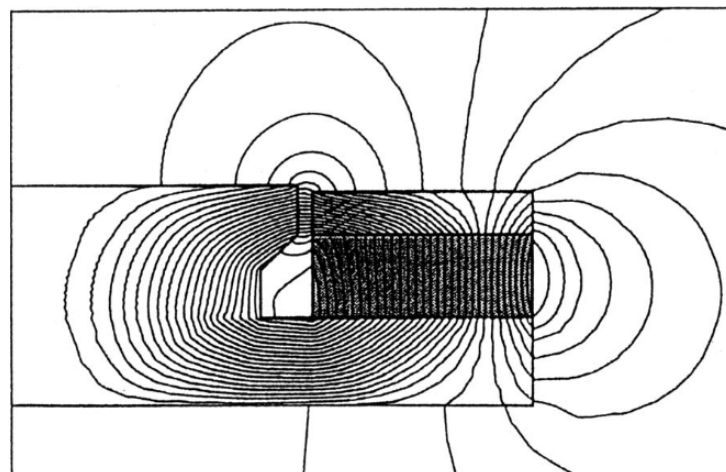
Figure 3.7: Iron Core Inclined [20]

Most designs have a core flush with the top of the front plate. This physically asymmetric design exhibits magnetic asymmetry as well. Extending the core piece so that it sticks out past the front plate makes the gap flux density distribution more symmetric. Asymmetric

flux distribution leads to higher distortion because the drive force to the voice coil is uneven. Notice that the peak flux density is what the computer actually predicts; the total flux predicted is still close to the measured amount if you look at the complete distribution in and out of the gap. [15]

3.4.8. Reducing leakage flux between pole plates

Modern loudspeaker usually use pole plates where the outer diameter is smaller than the magnetic ring one. This measure is adopted to increase the density flux in the air gap, but this also leads to important achievement in terms of material used, containing also the manifacturing cost.
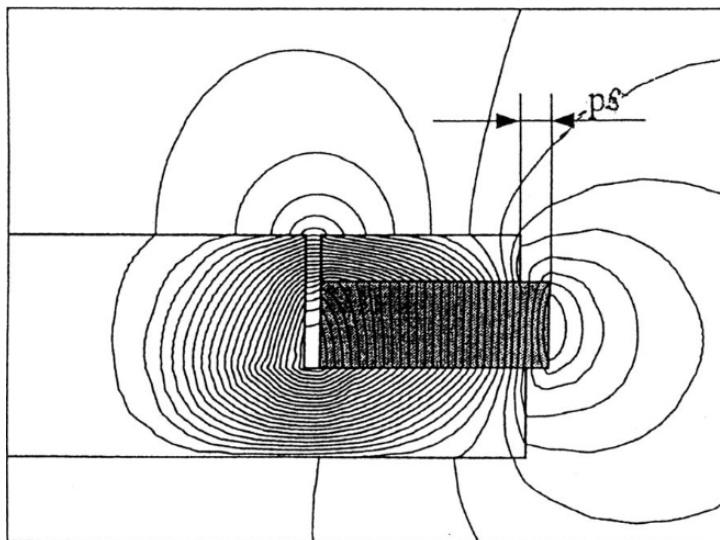
Figure 3.8: Pole Plates with reduced diameter [20]

Another option is to give a conical shape to pole plates, reducing also volume while increasing the leakage flux. This kind of solution can be higher in terms of cost, because a particular geometry is more expensive in terms of manufacturing costs.
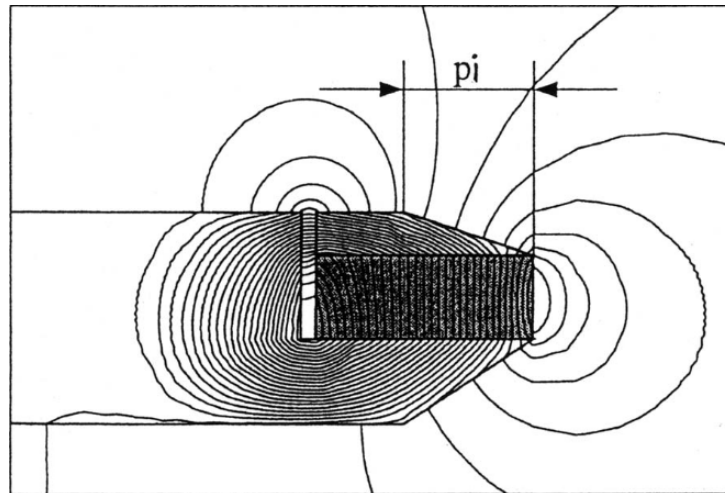
Figure 3.9: Conical Shape [20]

Two common design geometries exist: magnet-around-coil 3.11 and magnet-in-coil 3.10
In-coil designs exhibit less leakage than around-coil designs as there are fewer leakage
paths available. Hence, incoil designs tend to be magnetically shielded. Low gap flux
densities intersect a lot of conductor length since the voice coils have a large diameter
(often three or four inches) so the Bl product can stay reasonable. Reluctance losses
should be slightly lower for in-coil geometries as well due to shorter flux path length.
Core geometry also affects magnet performance [15].
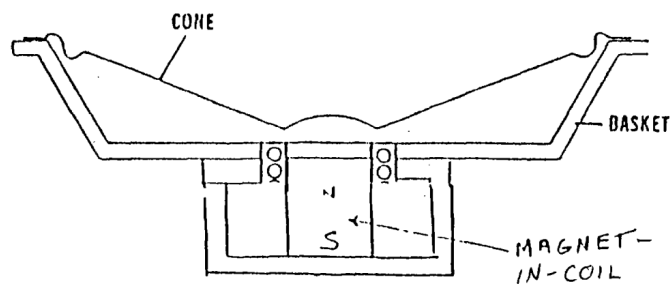
Figure 3.10: In Coil Configuration [15]
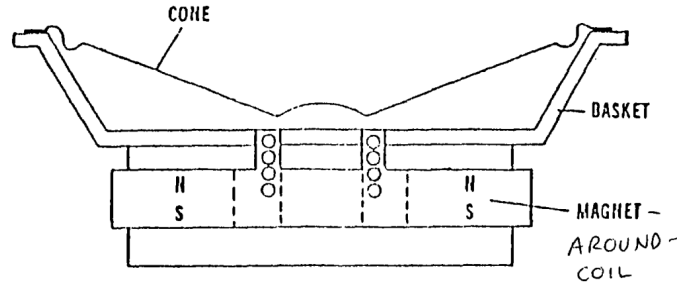
Figure 3.11: Around Coil Configuration [15]

3.4.9. Iron Parts Design

The iron parts of the system should be loaded magnetically as high as possible, to obtain that, considering the shape in Figure 3.9, there are two possibilities:

- Constraining back plate shape, to keep it thin.

- Provide the iron core with a cylindrical hole

Both these solutions are to obtain a better flux density with the least volume of iron possible. To design a set of plates using the minimum amount of material, we wish to keep the material cross-section to the bare minimum necessary to carry the flux at that point. Setting aside leakage and production feasibility some considerations on the "ideal" plate shape can be done [15].

There is a disparity between two methods of calculating flux. Multiplying B, the magnet flux, by the surface area of the magnet gives a total flux value greater than multiplying the gap flux times the gap area. Losses cause the difference. To determine the needed cross-section, a half-inch bore through the core center still left enough material to carry all the flux.

For the plates, the flux can be assumed to be flowing radially from the gap, thus giving the formula for the plate sectional cross area [15].

$$A_{plate} = \Pi \cdot P_d \cdot P_t \tag{3.15}$$

Where P_d and P_t are respectively the plate diameter and the plate thickness at the considered diameter.

4 | Materials & Methods

In this section is analyzed every step of the implementation process, from the starting geometries to the endpoint. Characteristics considered in the numerical models, to evaluate magnetic circuit performance and improvements obtained thanks to topology optimization are:

- Displacement dependent force factor *Bl(x)*

- *Bl(x)* curve symmetry

- Optimal plates shape to maximize flux density and symmetry of the *Bl(x)* curve with an evaluation of plates volume

Every numerical analysis was done using COMSOL®Multiphysics as the FEM Software [11].

4.1. Prototypes

Nominal models are prototypes produced by Faital that were used as starting models, whose Bl curves have been measured and validated by subsequent thesis studies. These prototypes are:

- *Woofer 1*: The first prototype is a 3-inches woofer with a ferrite magnet, with a copper cap on the central pole, the model can be seen in Figure 4.1.

- *Woofer 2*: The second prototype is a 10-inches woofer with a ferrite magnet and a steel basket. The coil in this prototype is in an overhung configuration ,the model can be seen in Figure 4.2.

- *Woofer 3*: The third prototype is a 15-inches woofer with both an aluminium demodulation ring and a aluminium basket; unless the two previous prototype, it has a NdFeB magnet. The coil in this prototype is in an overhung configuration, the model can be seen in Figure 4.3.

A better scheme of prototypes material is written in table 4.1:

	Component	Material
Woofer 1	- voice coil - magnet - polar plates - demodulation - basket	- CCAW - ferrite - stainless steel - copper cap - stainless steel
Woofer 2	- voice coil - magnet - polar plates - basket	- aluminium - ferrite - stainless steel - stainless steel
Woofer 3	- voice coil - magnet - polar plates - demodulation - basket	- copper - NdFeB (N35H) - stainless steel - aluminium - aluminium

Table 4.1: Woofer Materials
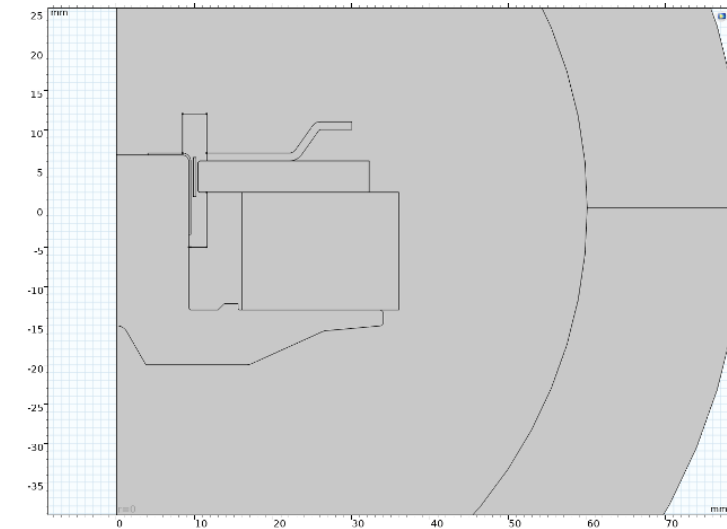
Figure 4.1: Woofer 1
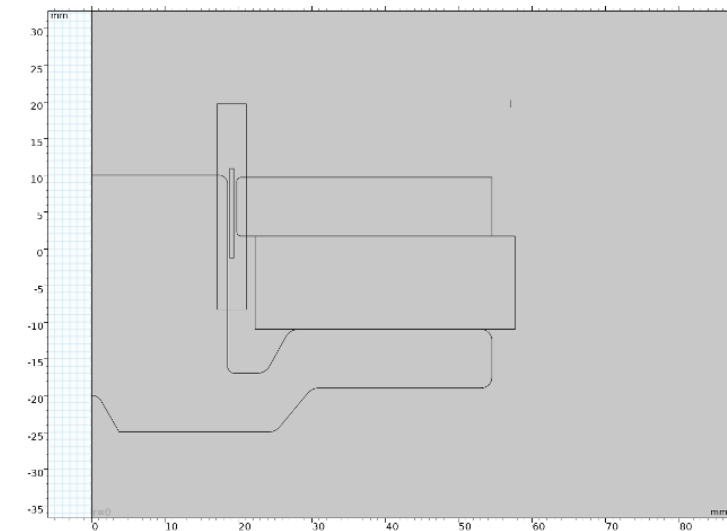
Figure 4.2: Woofer 2
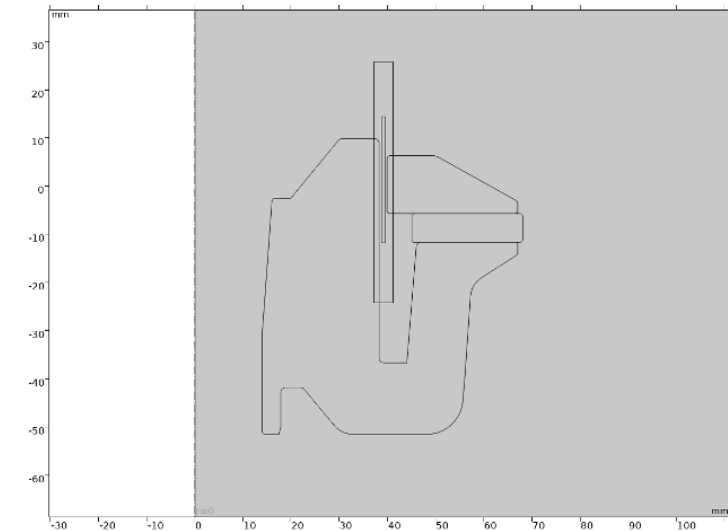
Figure 4.3: Woofer 3

4.2. COMSOL Environment

4.2.1. Introduction to COMSOL Multiphysics Ⓡ

Comsol Multiphysics Ⓡ is a commercial finite element analysis software package used for modeling and simulating various physical systems and phenomena. It is a powerful multiphysics simulation software that allows engineers, scientists, and researchers to simulate and analyze the behavior of complex systems involving multiple physical domains, such as heat transfer, fluid dynamics, electromagnetics, structural mechanics, acoustics and chemical reactions. Comsol Multiphysics provides a user-friendly interface and allows users to easily build and solve complex physical models. It also supports various solvers and numerical methods, including finite element analysis, boundary element method, and finite volume method, among others [11]. In this thesis, the final released version of COMSOL 6.1 has been used, and in particular, Comsol Multiphysics Ⓡ uses the FEA (Finite Element Analysis) with the possibility to use an adaptive meshing, error control over various numerical solvers and the possibility to run various types of studies, also cluster computing with batch and parametric sweeps. Partial differential equations (PDEs) form the basis for the laws of science and provide the foundation for modelling a wide range of scientific and engineering phenomena. The basic desktop interface is shown in Figure 4.4
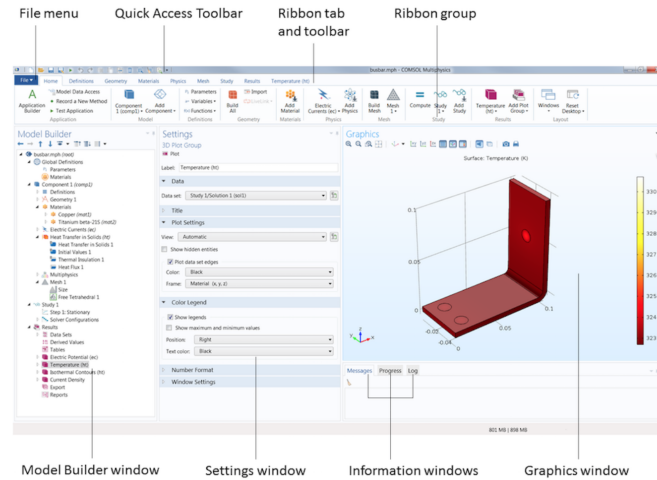
Figure 4.4: COMSOL Ⓡ Interface [16]

4.2.2. FEM Models

In the COMSOL environment, for this thesis work numerical models are set up in a 2D axysimmetric model. Numerical models used are the three models represented in Figure 4.1, 4.2 and 4.3, and the reason why was chosen a 2D axysimmetric model is because magnetic circuit geometry is axialsymmetric, boundary conditions respect axial symmetry and axialsymmetric solutions of the problem are expected, also was preferred to a 3D model to avoid unnecessary computational cost. Every model represented was considered just with motor components, avoiding baskets and demodulation rings, even where present, they were not considered in the computational process. The reason for that was that in an optimization design process for top and back plate, basket and rings contribution was negligible, and avoided a heavier computational requirement, also, the main motivation was that the optimizer had to be left free to act without modifying the optimal design of plates due to the presence of the ring and the basket. Each geometry was then incorporated in a semicircle representing the surrounding air. The outer layer is designed to represent the *infinite domains*. Infinite domains are a layer of virtual domains that surrounds the geometry and to which is applied an infinite coordinate scaling stretched towards infinity. Materials cited in **??** were then applied to components, but they will be explained in detail in the next section. Finally, the geometric domains were discretized in triangular elements composing the *mesh*, where over it, PDEs representing the problem were solved.

4.3. Analyses

4.3.1. Magnetostatic Analysis

From the magnetostatic analysis many useful information about the ferromagnetic components and density flux are retrieved. These information are mainly about:

- Ferromagnetic materials behavior, evaluating the saturation of the magnetic circuit

- The operating point of the permanent magnetic material, on the demagnetization curve compared to the point of maximum energy product B_{Hmax}

- The evaluation of the density flux, looking at different characteristics such as magnitude, shape of the flux lines and symmetry.

Symmetry is an important descriptor of the *Bl(x)* curve, in fact if the Bl curve of the speaker is symmetrical, then the force generated by the coil will be balanced in both directions of cone movement, which can lead to more accurate and linear sound reproduction and it's defined through the simmetry index S.I calculated as [7]:

$$S.I = (1 - \sqrt{\frac{1}{N} \cdot \sum_{j=1}^{N} (2 \cdot \frac{Bl(x_j) - Bl(-x_j)}{Bl(x_j) + Bl(-x_j)})} \cdot 100\% \tag{4.1}$$

Where N is the number of displacement points (x_j) evaluated, and express a percentage value for symmetry. In this work, the symmetry value using (4.1) has been calculated using an Excel sheet, using *Bl(x)* curve values taken from COMSOL. The fundamental laws of any magnetic field problem are Maxwell Equations:

$$
\begin{cases}
\nabla \cdot \boldsymbol{D} = \rho, & (4.2a) \\
\nabla \times \boldsymbol{E} + \dfrac{\partial \boldsymbol{B}}{\partial t} = \boldsymbol{0}, & (4.2b) \\
\nabla \cdot \boldsymbol{B} = 0, & (4.2c) \\
\nabla \times \boldsymbol{H} - \dfrac{\partial \boldsymbol{D}}{\partial t} = \boldsymbol{J}. & (4.2d)
\end{cases}
$$

Describing respectively the Gauss Electric Law (4.2), Faraday law (4.2b), Gauss magnetic law (4.2c), Maxwell-Ampère Law (4.2d), accompanied by the constitutive laws:

$$
\begin{cases}
\boldsymbol{D} = \epsilon_0 \boldsymbol{E} + \vec{P}, & \text{(4.3a)} \\
\boldsymbol{B} = \mu_0 (\vec{H} + \vec{M}), & \text{(4.3b)} \\
\boldsymbol{J} = \sigma \vec{E}, & \text{(4.3c)}
\end{cases}
$$

Where the quantities involved in both systems are:

- $\vec{E}$: Electric field intensity

- $\vec{D}$: Electric displacement field

- $\vec{J}$: Current Density

- $\vec{\rho}$: Electric charge density

- $\vec{P}$: Polarization Vector

- $\vec{\epsilon}$: vacuum permittivity, equal to $8.85 * 10^{-}12 \ Fm^{-}1$

In case of linear, homogeneous, isotropic materials, constitutive laws can be written, in case of fields and charges are time-invariant, which means that the time derivatives of E, B, D, and H are zero, as:

$$
\begin{cases}
\nabla x H = \boldsymbol{J}, & \text{(4.4a)} \\
\boldsymbol{B} = \nabla x A, & \text{(4.4b)} \\
\boldsymbol{J} = \sigma \vec{E} + \sigma \vec{v} X B + J_e, & \text{(4.4c)}
\end{cases}
$$

Recalling the fact that fields and charges are time-invariant, which means that the time derivatives of E, B, D, and H are zero, (4.2d) is simplified to (4.4a). From the third equation, we know that B is divergence-free, which means that its divergence is zero $\nabla x B = 0$. This implies that B can be expressed as the curl of a vector potential A, as seen in (4.4b). When non-linear components are involved, like steel components for our consideration, the relationship between $\vec{B}$ and $\vec{H}$ becomes [7]:

$$
\tilde{B} = f(\tilde{H}) \tag{4.5}
$$

And the current density is expressed as:

$$
J = \sigma \tilde{E} + \tilde{J}_e \tag{4.6}
$$

Where $\vec{J_e}$ is an externally generated current. We also assume that the current density can be decomposed into conduction and convection components: $\sigma_v x B + \sigma_e E$ obtaining (4.4c). If we use the definition of magnetic potential $\vec{B} = \nabla \times \vec{A}$ and Equation (4.3b), we can derive the magnetostatic equation [7]:

$$\nabla \times (\frac{1}{\mu_0}\nabla \times \tilde{A} - \tilde{M}) = \tilde{J} \qquad (4.7)$$

4.4. Sources Materials

4.4.1. Air

The surrounding medium that constitutes the domain around the models is *air*, having relative permeability μ_r and relative permittivity ϵ_r equal to 1. Also the conductivity value of air is really small. After the definition of the air material, air domains properties are used also in the *Ampere's Law* node in the *Magnetic Fields* interface. In Figure 4.5 there is an overview of COMSOL domains defined for all three models.
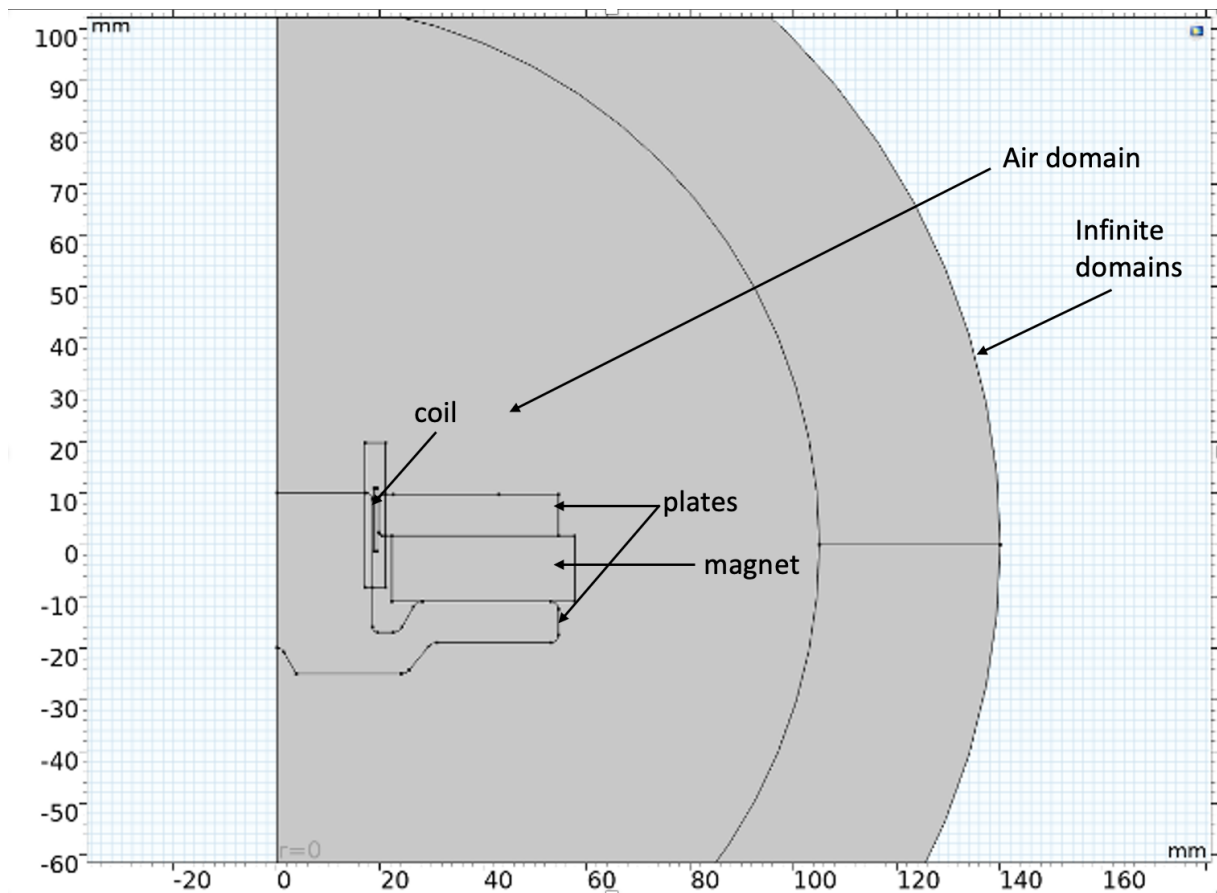
Figure 4.5: Domains in COMSOL Interface

4.4.2. Magnets

Magnets' materials were ferrite for Woofer 1 and Woofer 2 and neodymium for Woofer 3. Permanent magnets are then modeled in COMSOL thanks to the *Magnet* node of the *Ampere's Law*, where a different $\vec{Br}$ is defined for both materials:

- $[\vec{Br}] = 0.4\text{T}$ for ferrite

- $[\vec{Br}] = 1.19\text{T}$ for neodymium N35H

Where $\vec{Br}$ is the remanent flux density, so the flux density where there is no magnetic field. The previous values have been measured from the hysteresisgraph measurement [7], and The $\vec{Br}$ is vertically and homogeneously aligned toward the top for all three geometries. This is considered valid if the working point of the magnet is far from the knee of its BH curve. The constitutive equation for Magnets in Ampere's Law nodes is:

$$\mu_0 \mu_{rec} H + \tilde{Br} = B \tag{4.8}$$

Where μ_{rec} is the recoil permeability and takes 1.05 as a value for both ferrite and neodymium.

4.4.3. Top and Back Plates

Top and back plates were the steel components of the model. These domains are modelled in COMSOL using an *Ampere's Law* node, and due to the fact that the density flux is different, is necessary to use an hysteresis model. This model's constitutive equation is explained with:

$$\tilde{B} = f(||H||)\frac{\tilde{H}}{||H||} \tag{4.9}$$

Where is the magnetic flux density and $\vec{H}$ is the magnetic field. This model relies on the magnetization part of the hysteresis curve (magnetic characteristic).
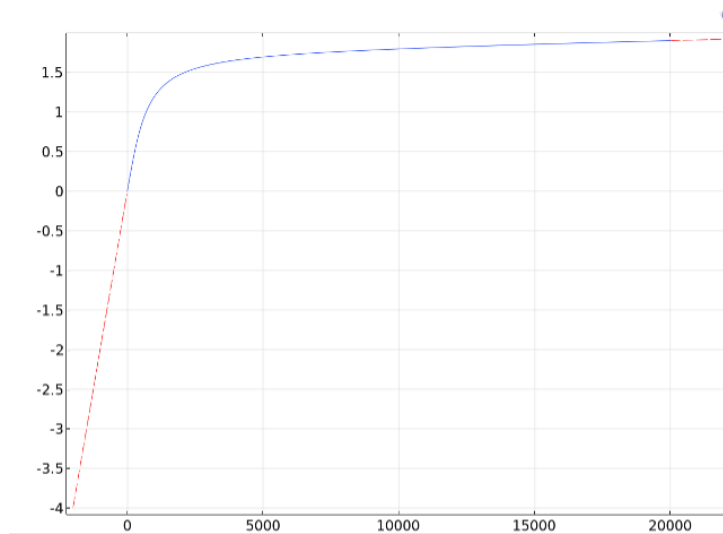
Figure 4.6: BH curve for back plate
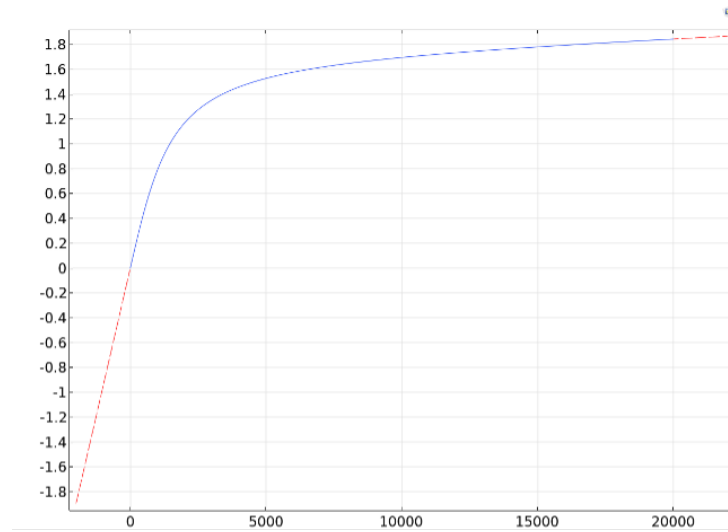
Figure 4.7: BH curve for top plate

4.4.4. Coil

In all the three models, coil material is copper or aluminum, where each conductivity is taken from literature and is respectively $\sigma_c = 55.0x10^6 \ Sm^{-1}$ and $\sigma_a = 37.5x10^6 \ Sm^{-1}$. Regarding the Ampere's Law node in COMSOL, there is a *Coil* feature that allows the user to model the coil with parameters as number of turns, that are 60 for Woofer 1, 110 for Woofer 2 and 130 for Woofer 3 and the wire shape and size, both taken from technical documents.

4.4.5. Mesh Elements

The main challenge choosing the mesh with Woofer 1, Woofer 2 and Woofer 3 was to choose a *maximum element size* lower, so a finer mesh, in region of interests, so the voice coil, plates and magnet while using a thicker mesh element size in air regions and infinite domain region, to avoid unnecessary computational cost. The total amount of domain elements and boundary elements for every model is reported in table 4.2

	Domain Elements	**Boundary Elements**
Woofer 1	10803	909
Woofer 2	11396	844
Woofer 3	9297	779

Table 4.2: Mesh Elements
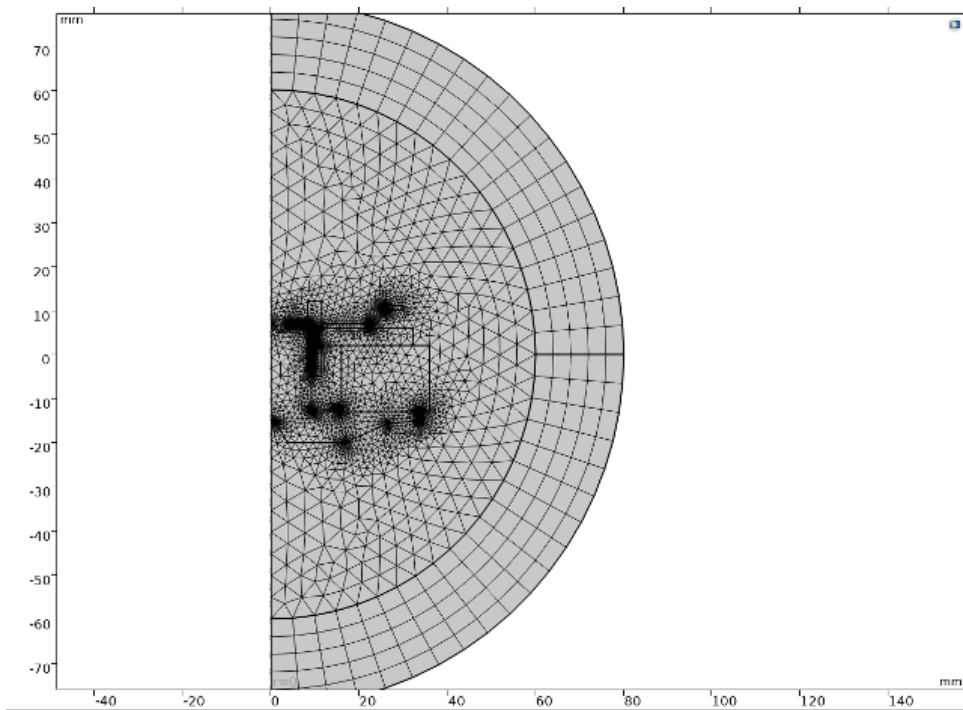
Figure 4.8: Mesh for Woofer 1
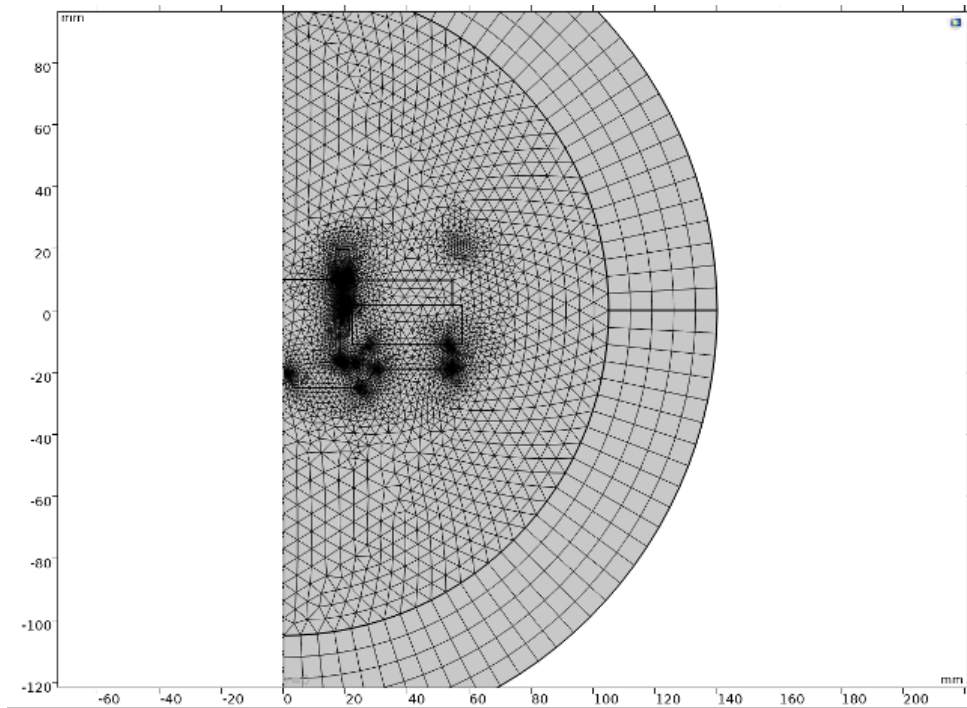
Figure 4.9: Mesh for Woofer 2
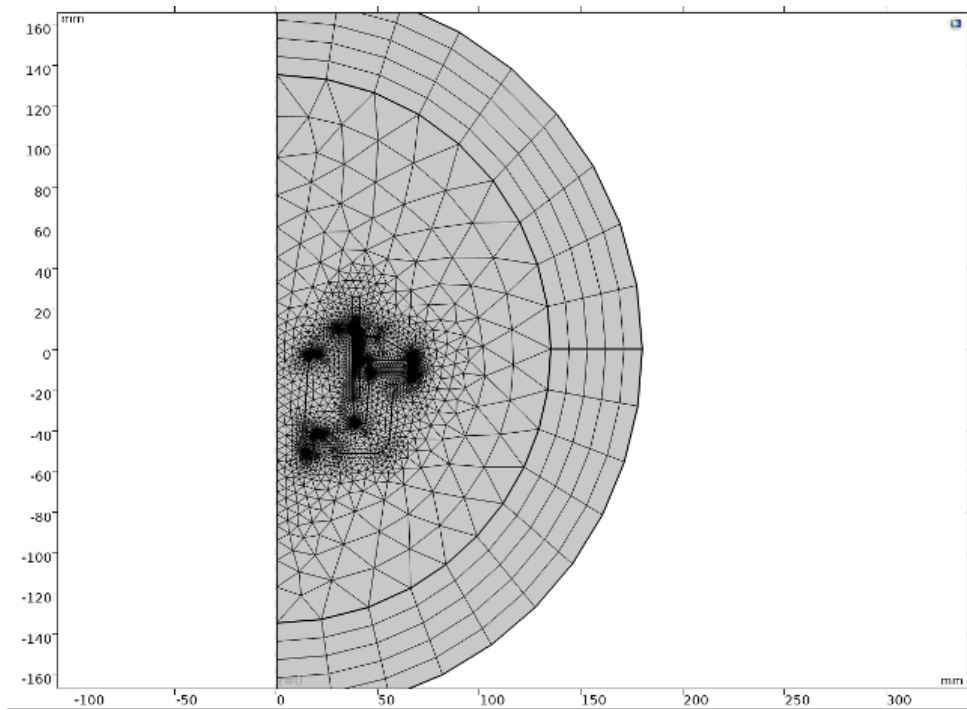
Figure 4.10: Mesh for Woofer 3

4.4.6. Study Settings for Nominal Models

Considering all the information in previous sections, the magneto-static analysis described in Section 4.3.1, is carried out by the *Stationary Study* in COMSOL Study Interface. This study made possible to evaluate all the ferromagnetic properties of the circuit, and the computation of the Bl curve over displacement. To do that, first the *Bl* variable was defined as the Lorentz Force recalling definition in (1.1), then the corresponding integration area was computed on the voice coil; Using a *parametric sweep* on the voice coil position, the Bl factor was evaluated with different coil displacements, and the study was executed considering a DC current of 1mA, to avoid flux modulation. In the table 4.3 are reported all the analyses done with respective computation time for every woofer type.

	Analysis	Computation Time
Woofer 1	Magnetostatic(from -3 mm to 3 mm, step 0.1 mm)	4 min 27
Woofer 2	Magnetostatic(from -7 mm to 7 mm, step 0.1 mm)	2 min 15
Woofer 3	Magnetostatic(from -12 mm to 12 mm, step 0.1 mm)	12 min 54

Table 4.3: Analyses with computation time

4.5. Topology Optimization

4.5.1. Introduction

Topology optimization in COMSOL refers to a computational technique that identifies the optimal layout of material within a given design space to achieve specific performance objectives while minimizing material usage and cost. It is a process of iteratively modifying the geometry of a physical system to minimize a specific performance metric, such as stress, deformation, or heat transfer, while adhering to design constraints. The process of topology optimization in COMSOL involves creating a model of the physical system using the software's geometry modeling tools, defining the boundary conditions and material

properties, and specifying the performance objectives and design constraints. A finite element analysis is then performed to simulate the behavior of the physical system and provide data on the distribution of the performance metric throughout the design space [11]. The topology optimization algorithm then modifies the geometry of the physical system to minimize the performance metric while adhering to the design constraints. The algorithm evaluates multiple designs, modifying the geometry in small increments each time, and selects the optimal design that meets the performance objectives and design constraints. The result of topology optimization in COMSOL is a design that is tailored to meet specific performance objectives while minimizing the use of materials and reducing the overall cost of the system. It allows designers to explore a wide range of design options and identify optimal solutions that would be difficult or impossible to achieve using traditional design methods. Generally, the algorithm steps for topology optimization include [27]:

- *Create a model*: Create a model of the physical system using the software's geometry modeling tools. Define the boundary conditions and material properties and specify the performance objectives and design constraints.

- *Perform finite element analysis*: Perform a finite element analysis to simulate the behavior of the physical system and obtain data on the distribution of the performance metric throughout the design space.

- *Modify the geometry*: The topology optimization algorithm modifies the geometry of the physical system to minimize the performance metric while adhering to the design constraints. The algorithm evaluates multiple designs, modifying the geometry in small increments each time, and selects the optimal design that meets the performance objectives and design constraints.

- *Iteration of the process*: Iterate the process of finite element analysis and geometry modification until an optimal design is obtained.

- *Results Evaluation*: Evaluate the results of the topology optimization algorithm to determine the effectiveness of the design in meeting the specified performance objectives and design constraints.

4.5.2. Density Model Method

COMSOL Multiphysics provides several topology optimization methods, including the density method, the level set method, and the phase field method. These methods differ in how they represent the material distribution within the design space and how they

optimize the design. In this work, the *Density Model* has been used. The density model optimization method is a widely used topology optimization technique in COMSOL Multiphysics. This method involves representing the design space as a collection of small elements, each of which can be assigned a continuous density value between zero and one. A density value of one indicates that the element is made of solid material, while a density value of zero indicates that the element is void. The density values of the elements are used as design variables in the optimization process, and the objective is to find the optimal distribution of these values that maximizes or minimizes a given performance metric. In fact, the density model implements a control variable θ_c, bounded between 0 and 1 where, generally, 1 is assigned to solid domain (steel in this thesis work) and 0 to fluid domains (air). The density model feature supports regularization with a Helmholtz Equation defined by (4.10) [17]:

$$\Theta_f = \Theta_c + R_{min}^2 \nabla^2 \Theta_f \tag{4.10}$$

Where θ_c was previously defined, and θ_f is the filtered variable where the filter radius is let by default to the mesh edge size. The main issue related Helmholtz filter is the grayscale, which is reduced by applying a smooth step function, defined as *projection* in topology optimization, that reduces this phenomenon but increases computational cost and makes convergence more difficult for the optimizer. The density topology feature supports projection based on the hyperbolic tangent function and describes the *material volume factor*, θ, in Equation (4.11):

$$\Theta_p = \frac{tanh(\beta(\theta_f - \theta_\beta)) + tanh(\beta(\theta_\beta))}{tanh(\beta(1 - \theta_\beta)) + tanh(\beta(\theta_\beta))} \tag{4.11}$$

Where θ_β is the projection point, and β controls the amount of projection. Another method to reduce grayscale, which can appear in any case if the optimization problem favours it, is to use interpolation functions. The density model interface supports two interpolation schemes, the SIMP (solid isotropic material with penalization) and the RAMP (rational approximation of material properties method). The interpolated variable is called *penalized material volume factor* and is used for interpolating the material parameters, while the interpolation scheme used in this case is the SIMP. The resulting expression is written in (4.12):

$$\Theta_p = \Theta_{min} + (1 - \Theta_{min})\Theta^{pSIMP} \tag{4.12}$$

Where Θ_p is the interpolation variable, and the p^{SIMP} exponent is used to make the grayscale less favorable. In this thesis work, the density model was applied to domains of top and back plate, in a topology optimization definition node.

Figure 4.11: Density Model Interface [17] [1]

---

[1]In this COMSOL interface are clearly visible all equations previously described, the type of filter (Helmholtz) and domain where the density model is applied, in this case, domain 3,4 and 10 refer to plates' domains

4.5.3. Geometry Update

As can be seen in Figure 4.11, the initial geometries defined in Figure 4.1, Figure 4.2 and Figure 4.3 are slightly changed. This choice was done in the pre-optimization phase so that, to allow the optimization solver to freely modify the starting geometry as desired, the starting geometry for the optimizer is not the same as the nominal models. In fact, the initial shape of both plates was changed to a simpler squared one, and made slightly bigger. In Figure 4.1 the dimension of the back plate was increased, also in Figure 4.2, while in Figure 4.3 both plates' dimension was increased. In Figure 4.15, can be seen an example of plates dimension increased in comparison with the nominal geometry, in this case for Woofer 3.
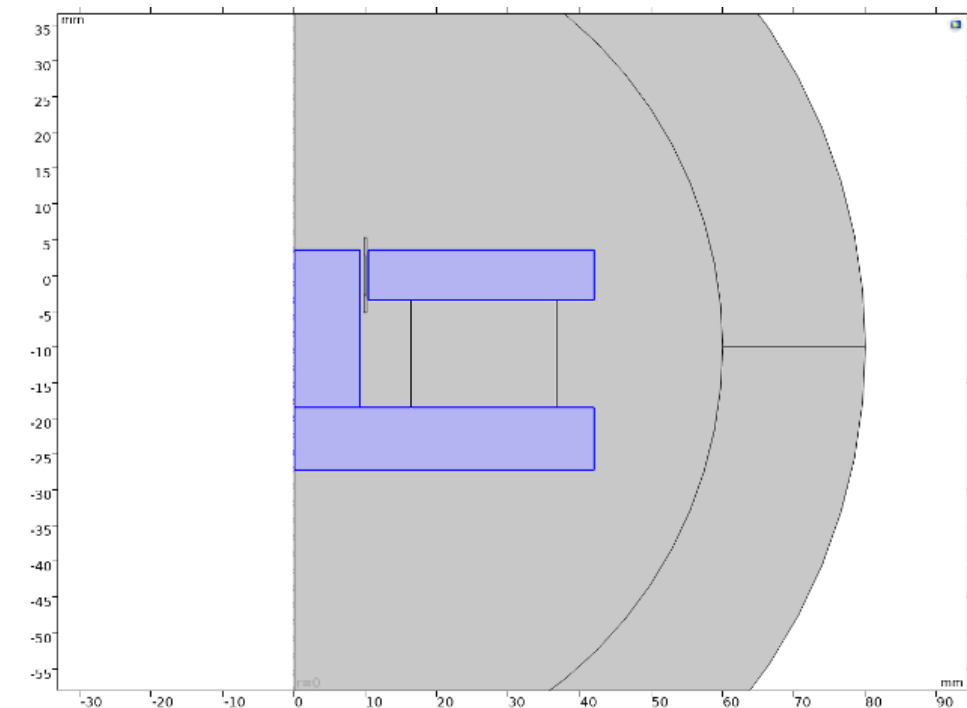
Figure 4.12: Geometry Update Woofer 1
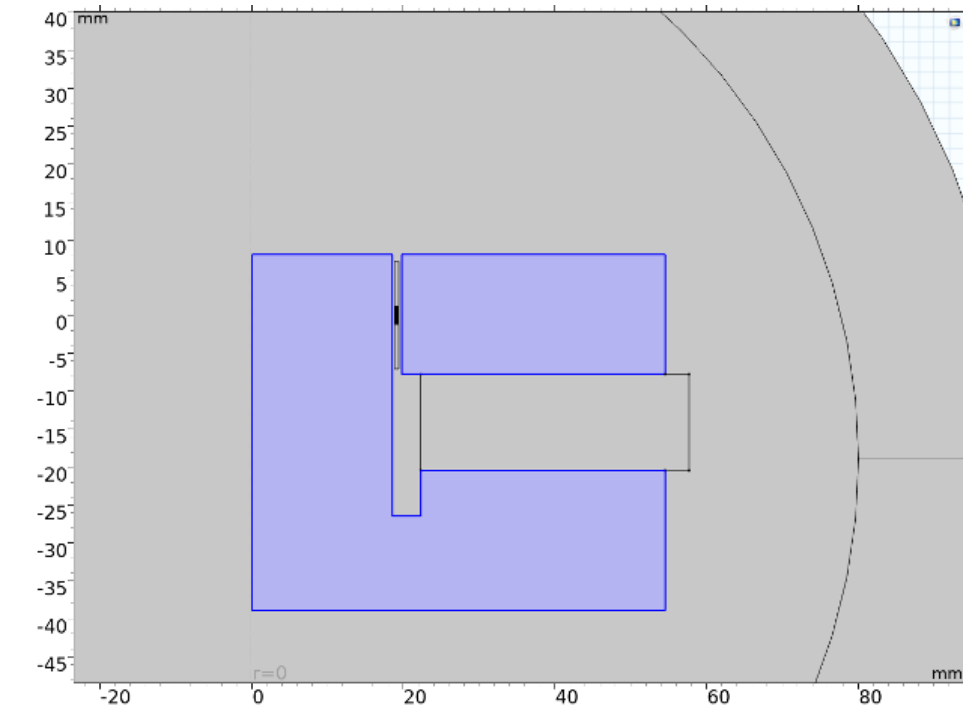
Figure 4.13: Geometry Update Woofer 2
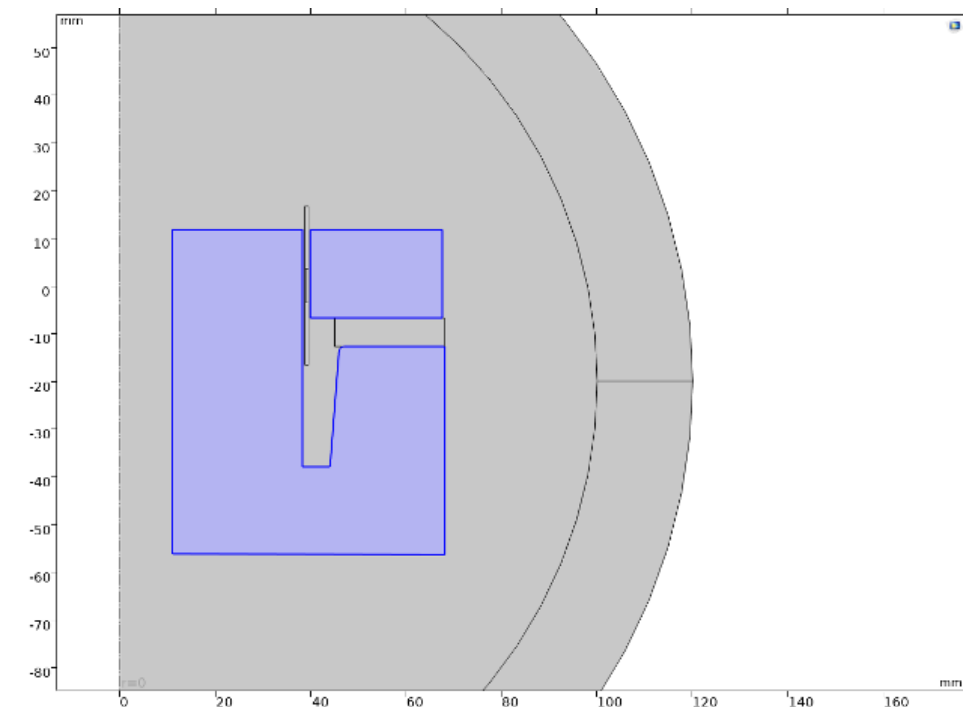
Figure 4.14: Geometry Update Woofer 3
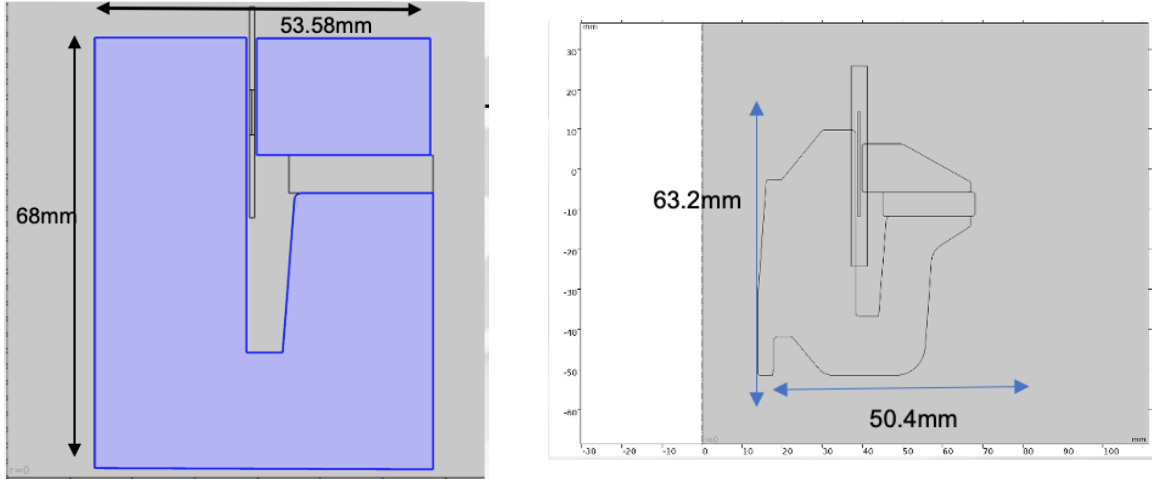
Figure 4.15: Comparison measurements nominal and geometry update

4.5.4. Magnetic Fields Update

Top and Back Plate

From the initial situation seen in section 4.4, also in the *Magnetic Field* interface there are some differences. In fact, the aim of this thesis work is to optimize plates topology, and to do that, adding two Ampere's Law nodes for top and back plate and starting from the magnetization model equation already cited in (4.4b), the relative permeability μ_r is defined as:

$$\mu_r = 1 + dtopo1.\theta_p * (mu_r(mf.Br, mf.Bz) - 1) \tag{4.13}$$

Where, in the expression, $dtopo1.\theta_p$ is the variable that represents the fraction of the domain occupied by the magnetic material, and $(\mu_r(mf.Br, mf.Bz))$ is a function that calculates the relative permeability of the material based on the values of the magnetic field components in the simulation, taking two arguments, *Br* and *Bz*, corresponding respectively to the components of the magnetic field vector in radial and axial directions. If $(mu_r(mf.Br, mf.Bz - 1))$ is computed, what is obtained is the deviation of the relative permeability from the value in free space, corresponding to 1, while multiplying the expression for $dtopo1.\theta_p$, this deviation is scaled by the fraction of the domain occupied by the magnetic material. The overall permeability of the material in the simulation is then obtained adding 1 to the scaled deviation. From (4.13), the mu_r function is defined as:

$$mu_r = \frac{\sqrt{(Bx^2 + By^2 + \epsilon[T^2])}}{\frac{comp\#.mat\#.BHCurve.BHCurve1_{inv}(\sqrt{(Bx^2+By^2+\epsilon[T^2])})}{\mu_0}} \tag{4.14}$$

In this expression, Bx and By are the components of the magnetic field vector in the x and y directions, respectively, while $\epsilon[T^2]$ is a small value which utility is to avoid divisions by 0. In the first denominator, the expression $comp\#.mat\#.BHCurve.BHCurve1_{inv}$ is a function in COMSOL that calculates the inverse of the BH curve of the magnetic material. Taking the inverse of the BH curve allows you to calculate the magnetic field strength as a function of the magnetic flux density. This is useful in determining the permeability of a magnetic material, which is defined as the ratio of the magnetic flux density to the magnetic field strength. Finally, μ_0 is a constant in COMSOL that represents the magnetic constant or the permeability of free space. Two functions were defined, called mu_r and mu_r2, explained in the exact same way as (4.14), but having the initial materials possibly slight differences in the BH curve, the mat variable in the denominator takes top plate and back plate respective values. Summing up, the penalized volume factor $dtopo1.\theta_p$ will be applied to the objective function used by the topology optimization algorithm, combining the performance criteria with a penalty term that discourages excessive use of material defining relative material properties for the selected domains.

4.5.5.   Study Setup

Initial Conditions

There were some initial conditions decided a priori before computing the *Stationary Study* step for optimization. In fact, the first condition was about the maximum *Bl* value at displacement equal to 0 and to do that, a new parameter was added called *Bl target*. The role of this parameter is to have a target for every model corresponding to $\sim +5\%$ of the *Bl* calculated for the nominal models, its role will be better explained in the next section 4.5.5. There were two geometric costraints added:

- The magnet size fixed, this was simply for the fact that the main focus was on the optimization of plates instead of plates and permanent magnet.

- For manifacturing reasons, also the air gap size was fixed.

The last initial condition, that will be better explained in section 4.5.5, was that the linear displacement of the coil was defined.

Probes and Parametric Sweep

Also with topology optimization, the stationary study is carried out by the *Study Interface*, adding a topology optimization node with three objective functions explained in the next section. As already seen in 4.4.6, a parametric sweep is carried out also in the optimization

study, computing the *Bl* curve in function of coil displacement x. Anyway, there are some differences in the study setup for the parametric sweep: in fact, to evaluate coil positions, instead of parametrizing coil displacement, *probes* from the *Definition Node* in COMSOL have been used.
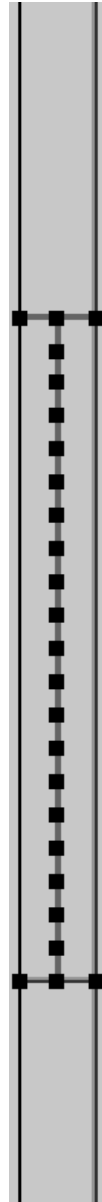
Figure 4.16: Probes for optimization

In COMSOL Multiphysics, domain point probes and boundary point probes provide the value of some field quantity at a point in the domain or on a boundary [9]. Point probes defined were mainly three, for all three models:

- *Point 1*: Is the point relative to the center position of the coil, to evaluate *Bl* when

the displacement is 0, the representation can be seen in Figure 4.17.

- *Point 2*: Is an array of points, corresponding to all voice coil point probes for x>0, positive displacement of the coil, the representation can be seen in Figure 4.18

- *Point 3*: Is an array of points, corresponding to all voice coil point probes for x<0, negative displacement of the coil, the representation can be seen in Figure 4.19
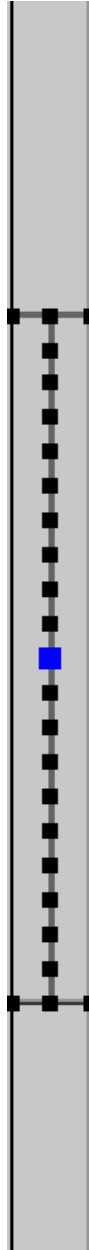
Figure 4.17: Point 1
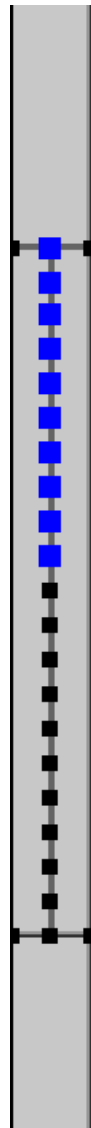
Figure 4.18: Point 2
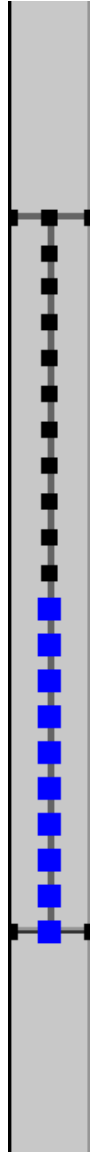
Figure 4.19: Point 3

To compute the *Bl* curve, a *BL Point* variable has been defined, that computes the integral over the expression $BL_integrand * coillocation_z$, where the first term is the calculation of the magnetic force on the coil, defined by Equation (4.15):

$$\frac{|mf.Br| * N0 * 2 * \pi * r}{w_{coil} * h_{coil}} \tag{4.15}$$

where $|mf.Br|$ represents the magnetic flux density, while N0, w_{coil}, h_{coil} are parameters corresponding to the number of coil turns, coil width and coil height. and the second term is a mathematical condition, that discerns whether the probe point should contribute to

the integral over the voice coil domain or not, defined by Equation (4.16):

$$(z > (dest(z) - \frac{h_{coil}}{2})) * (z < (dest(z) + \frac{h_{coil}}{2})) \qquad (4.16)$$

that evaluates to "1" (true) if the variable z is greater than the value of $dest(z) - h_{coil}/2$ AND less than the value of $dest(z) + h_{coil}/2$. Otherwise, it evaluates to "0" (false). [2] The integral over which is computed the expression is the voice coil domain. Considered all this information, a parametric sweep is then defined in the study interface. Differently from what has been reported in Section 4.4.6, this time, the parametric sweep considered only one parameter:

- *para*: this parameter has been used to define the starting coil position, avoiding any out-of-field effect and centering the *Bl* curve in x=0.

As referred in Section 4.5.5, in the initial conditions the linear displacement of the coil was defined a priori.

Objective Functions

In topology optimization, an objective function is a mathematical expression that quantifies the performance of a design based on certain criteria, defined by the user. The objective function is typically defined in terms of a set of design variables, which describe the distribution of material in the design domain. COMSOL provides three types of minimizations for objective functions:

- *Minimization of the objective function value*

- *Maximization of the negative of the objective function value*

- *Minimization of the negative of the objective function value*

The type chosen for objective function is the *Minimization of the objective function value* type. This type of minimization can act on either a single objective function or the sum of multiple objective functions, depending on the user's optimization problem requirements. In this case, being three objective functions, the solver will try to find a set of design variables that minimizes the sum of all the objective functions in the optimization problem, by iteratively updating $theta_c$ variable, seen already in Section 4.5.2; recalling it, θ_c was the control variable assigning true or false value whether the domain material was air or steel. The algorithm responsible to iteratively update density model's control variable θ_c

---

[2]In COMSOL, the "dest" operator is used to define the destination or target for a particular operation or calculation. In this case $dest(z)$is used to define a region or subdomain in a geometry based on its position along the z-axis relative to the position of another feature [9]

will be described in the next section. The relative importance of each objective function can be adjusted by assigning weighting factors to each of the objective functions, that corresponds to weights *w1*, *w2* and *w3* which will be described in a moment. Seen from another point of view, in this case the solver is trying to minimize the difference from the BL_0 value in (4.17), so having the result as close as possible to the decided target, is trying to minimize the difference from probe points values for x>0 and x<0 maximizing the symmetry of the curve in (4.18) and minimizing the volume in (4.19). Considering goals discussed in 2, objective functions that were chosen for this work, for all three models, are:

$$w1 * (comp\#.point1 - BL_0)^2 \tag{4.17}$$

(4.17) is the objective function for the maximum value of *Bl* in x=0. Explaining it, the objective function is trying to minimize the squared difference between the value of comp#.point1 and the target value BL_0, with the weight *w1* controlling the relative importance of this objective function compared to other objectives in the study. In this case, *w1* is equal to 1, so is given maximum relative importance in comparison to other objectives in the study.

$$w2 * (comp\#.point2 - comp\#.point3)^2 \tag{4.18}$$

(4.18) is the objective function concerning the *Bl* curve symmetry. This objective function is trying to minimize the squared difference between the values of comp#.point2 and comp#.point3, with the weight w2 controlling the relative importance of this objective function compared to other objectives in the study, penalizing larger differences between these two variables more severely than smaller differences. In this case, also *w2* is equal to 1, so is given maximum relative importance in comparison to other objectives in the study. The last objective function is (4.19):

$$w3 * comp\#.dtopo\#.theta_{avg} \tag{4.19}$$

This objective function express the desired volume constraint, in fact $dtopo.\#.theta_{avg}$ is the average material volume factor, multiplied for the weight *w3* that is less significant than the two previous *w1* and *w2*, with value equal to 1/3.

Solver Algorithm
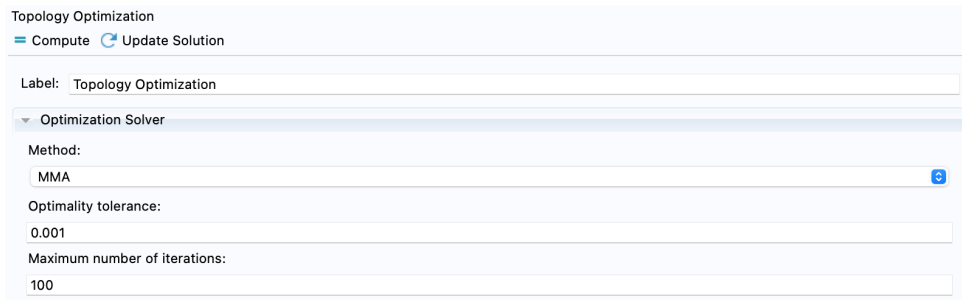
COMSOL provides three optimization solvers algorithms to solve optimization problems, and they are [10]:

- *MMA(Method of Moving Asymptotes)*: is a gradient-based optimization solver that is widely used for topology optimization problems. It uses a set of asymptotes to approximate the behavior of the objective function and constraints in the vicinity of the current design point, and moves these asymptotes towards the optimal solution.

- *SNOPT(Sparse Nonlinear Optimizer)*: is a sequential quadratic programming (SQP) solver that can handle nonlinear optimization problems with smooth constraints and objectives. It uses sparse matrix techniques to efficiently handle large-scale problems, and it can handle both equality and inequality constraints.

- *IPOPT(Interior Point Optimizer)*: is an interior-point optimization solver that can handle large-scale nonlinear optimization problems with smooth constraints and objectives. It uses a barrier function to approximate the constraints and an augmented Lagrangian method to handle the objective function.

In this work, the MMA solver has been chosen, being the faster algorithm for the proposed problem compared to the other two and also, asking to COMSOL developers, this algorithm was suggested over the SNOPT and IPOPT one. The algorithm considers two variables during computation:

- *Optimality Tolerance*: The optimality tolerance parameter in MMA determines the level of accuracy required to consider a design as optimal during the optimization process. During the optimization process, MMA iteratively updates the design variables in order to minimize the objective function subject to the constraints. At each iteration, the solver evaluates an objective value and consequently updates control variables, checking conditions for optimality [3]. If these conditions are met to a certain degree of accuracy, the solver considers the design to be optimal and terminates the optimization process.

- *Number of Iterations*: Iterations are the steps the algorithm compute iteratively to reach the most accurate possible result.

In this work, optimality tolerance has been set to 0.001, which is a small value, increasing complexity and computational demand but also guaranteeing more accuracy in the process, with 100 iterations.

Figure 4.20: MMA Solver Interface

---

[3]This refers to what previously described in Section 4.5.5, when discussing about the control variable update of the Density Model

4.5.6.   Outputs and Filtered Geometries

After having defined all parameters used and the study setup, like has been reported in 4.4.6, the table 4.4 reports all studies done for topology optimization with computational times.

	Study	Computation Time
Woofer 1	Topology Optimization	1 min 57
Woofer 2	Topology Optimization	11 min 26
Woofer 3	Topology Optimization	19 min 19

Table 4.4: Studies with computation time

After having obtained these results, next step is to export the optimized geometry to perform the same analysis step seen in Section 4.4.6, to see if optimized geometry results in terms of *Bl* value in x=0 and *Bl* curve symmetry value correspond to the optimization solver ones. To do that, in the *Results* section of the COMSOL interface, a *Filter* node is added, with the filtering expression defined as:

$$if\,(isnan(dtopo\#.\theta_c)\&\&isnan(dtopo.\theta_c),\,NaN,\,dtopo\#.\theta * dtopo\#.\theta) \qquad (4.20)$$

Where θ_c is the control material volume factor, used as input for the filter. The expression (4.20) evaluates if $dtopo\#.\theta_c$ are not numbers (NaN). If variables are NaN, the expression returns NaN. If one or both of the variables are not NaN, the expression multiplies the values of $dtopo\#.\theta$ and returns the result. The final step for filtering is to impose a lower boundary, over which the filter is applied, that is suggested from literature to be imposed at 0.5. After filtering, the optimized geometry can be exported in a new component or in a new model.

4.6.   Optimized Geometries

Recalling what has been said in 4.5.6, last step is always carried out by the *Study Interface* on optimized exported geometries for all three models. In this study setup, exactly as 4.4.6, the magnetostatic analysis is carried out and also the parametric sweep on voice coil displacement to compute the *Bl* curve. Table 4.5 reports all studies done for topology

optimization with computational times.

	Analysis	Computation Time
Woofer 1	Magnetostatic(from -3 mm to 3 mm, step 0.1 mm)	4 min 22
Woofer 2	Magnetostatic(from -7 mm to 7 mm, step 0.1 mm)	13 min 13
Woofer 3	Magnetostatic(from -12 mm to 12 mm, step 0.1 mm)	32 min 9

Table 4.5: Analyses with computation time

5 | Results

What follows are the graphic comparisons of *Bl* curves and volumes for all three models, between the optimized geometry and the nominal one, that summarize the work goal.

5.1. Woofer 1

5.1.1. Nominal Model

Graphic results are reported, with magnetostatic results,
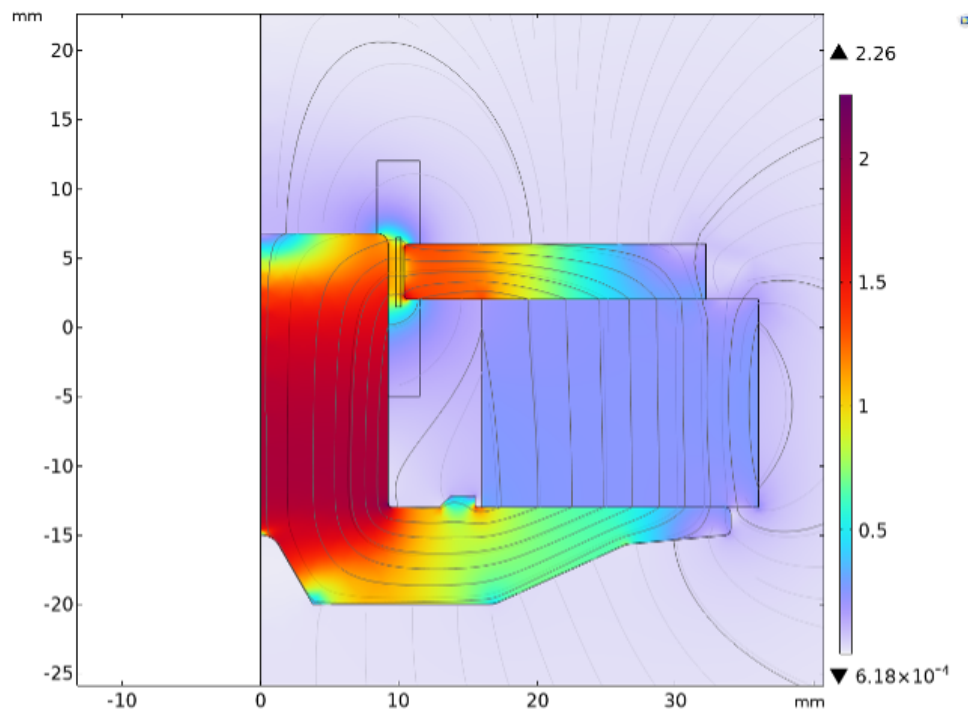
Figure 5.1: Magnetostatic Analysis results for Woofer 1

And *Bl* curve:
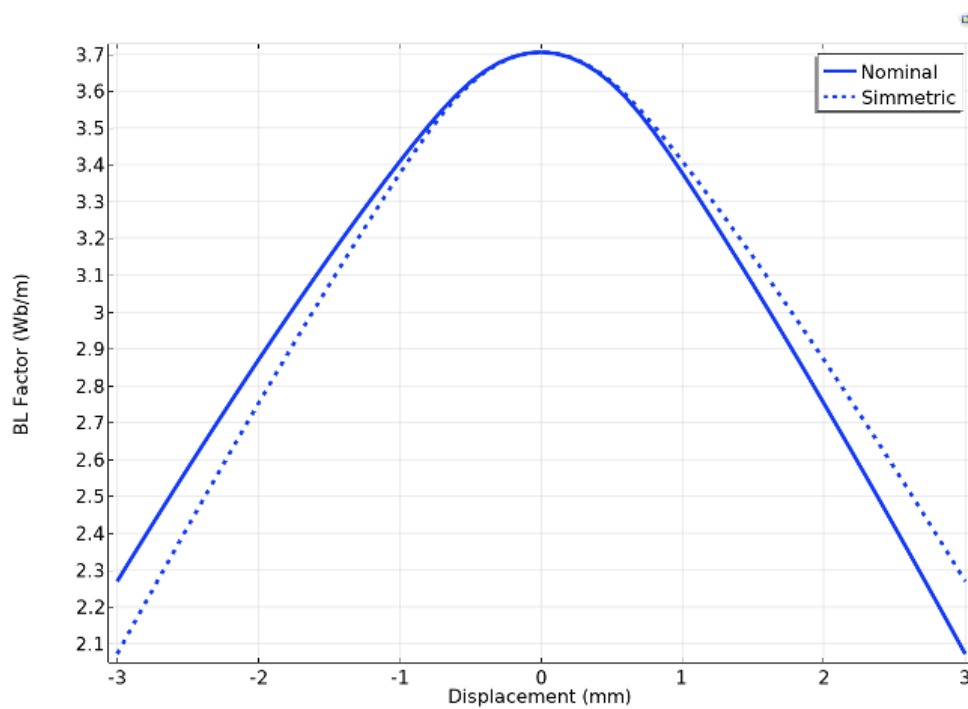
Figure 5.2: Bl factor over displacement curve for Woofer 1

The peak of nominal geometry curve is around 3.7 [Wb/m] with a symmetry index of 97.8 %.

5.1.2.   Filtering and Final Results

Graphic results, after optimizer algorithm work, are displayed in Figure 5.3 :
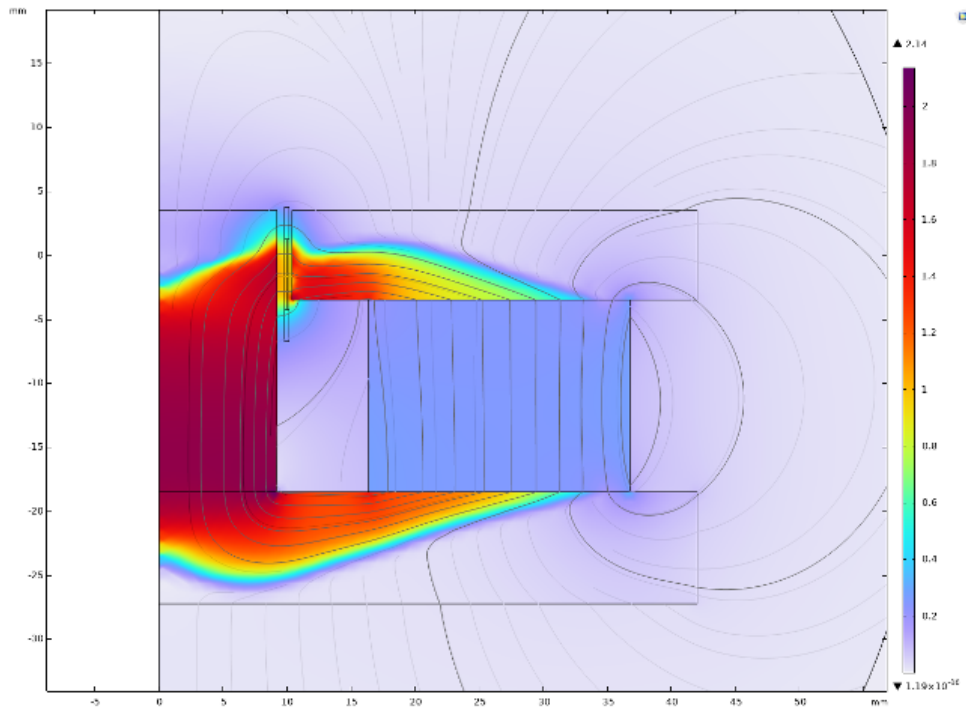
Figure 5.3: Magnetostatic after topology optimization(Woofer 1)

These are filtering results, which algorithm is described in Section 4.5.6:
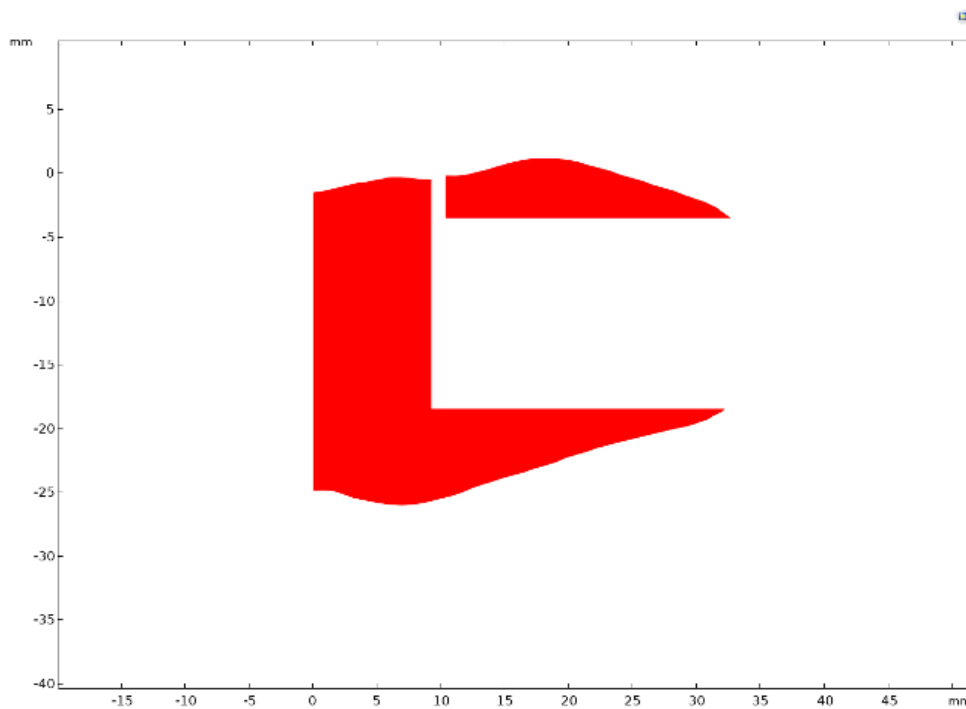
Figure 5.4: Geometry Filtered for Woofer 1

These are the exported optimized geometries for Woofer 1, recalling Section 4.5.6, after having performed a very little improvement on geometry shape:
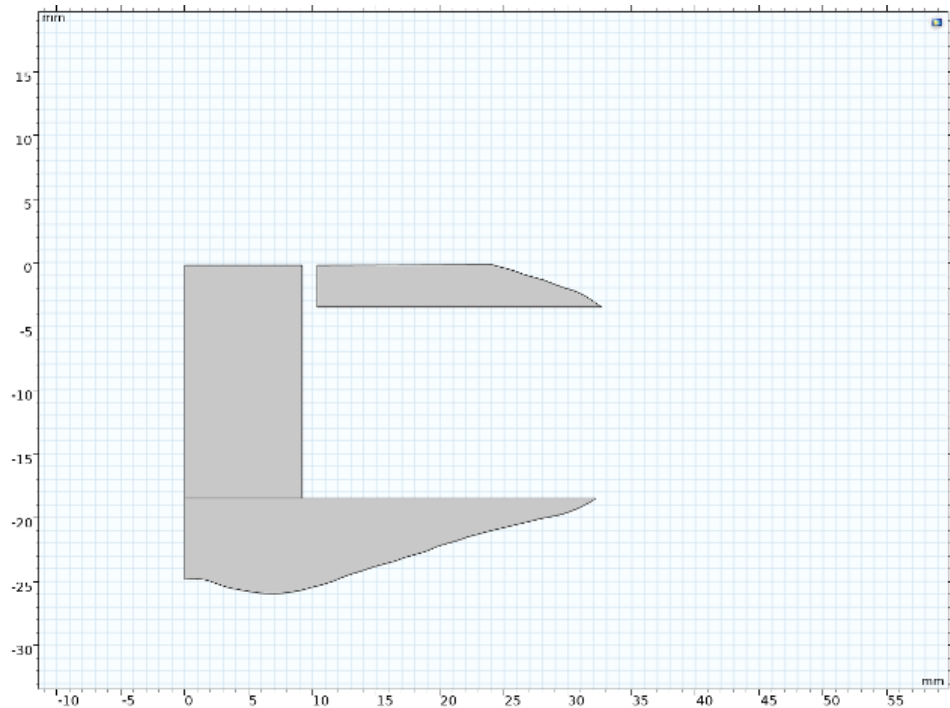
Figure 5.5: Optimized Geometry for Woofer 1

Here are also the graphic results for magnetostatic analyses, recalling Section 4.6:
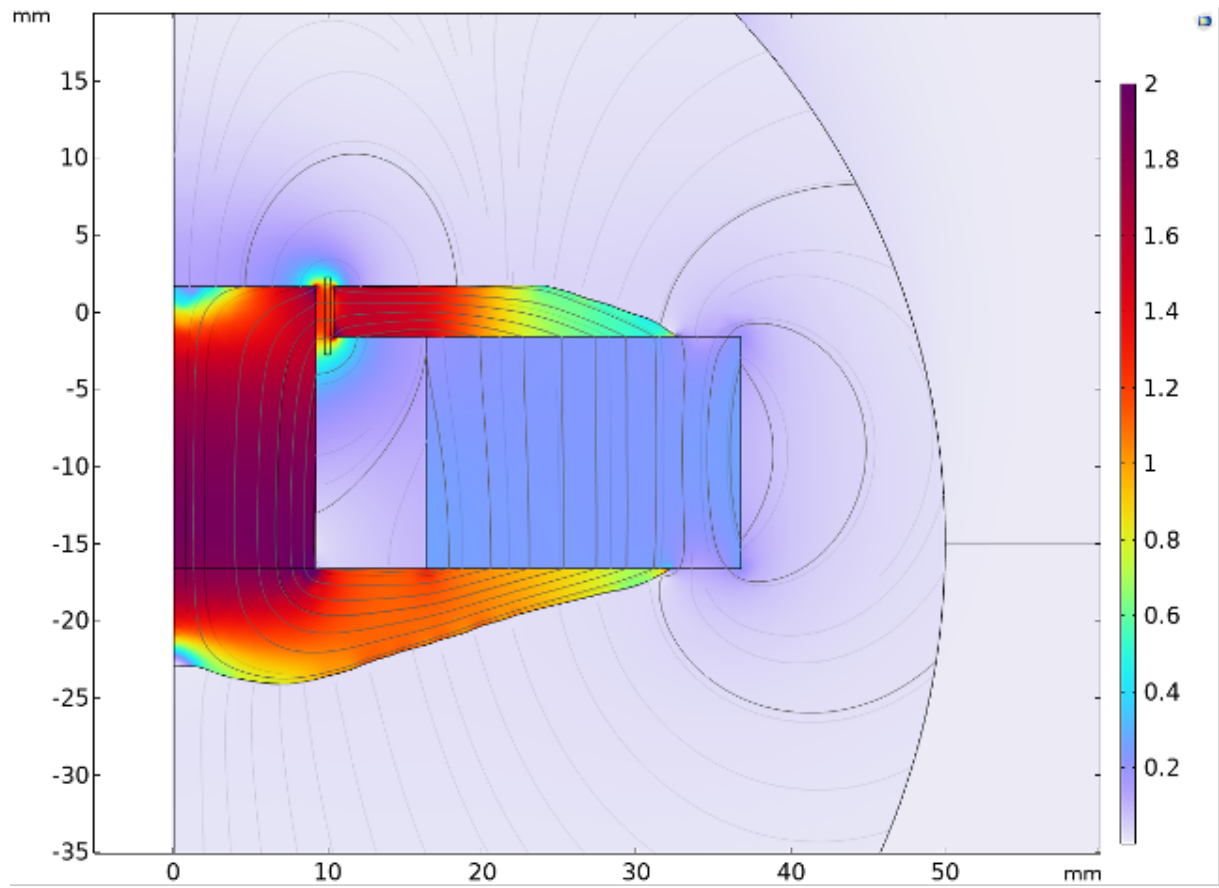
Figure 5.6: Magnetostatic Analysis for optimized geometry of Woofer 1

And *Bl* curve:
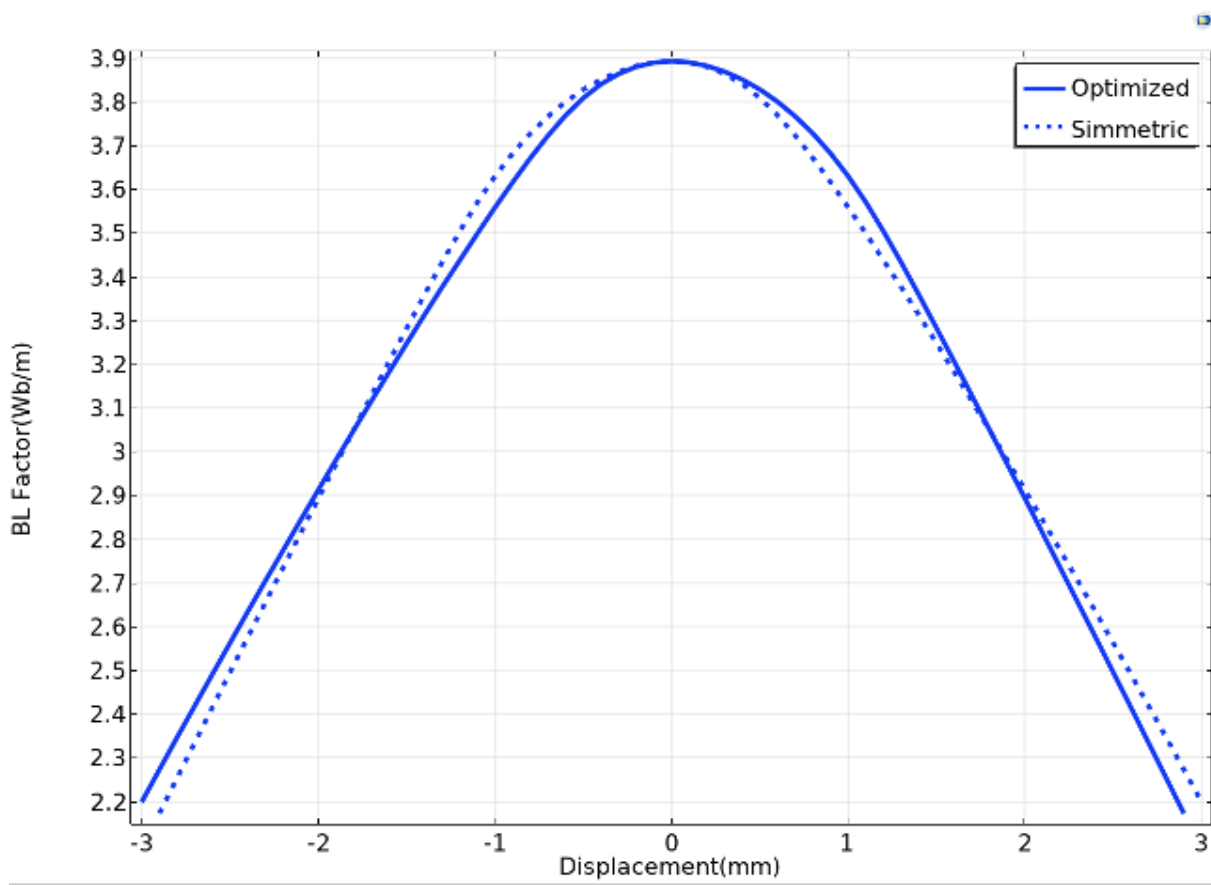
Figure 5.7: Bl curve for optimized geometry of Woofer 1

5.1.3. Optimized Bl and Nominal Bl
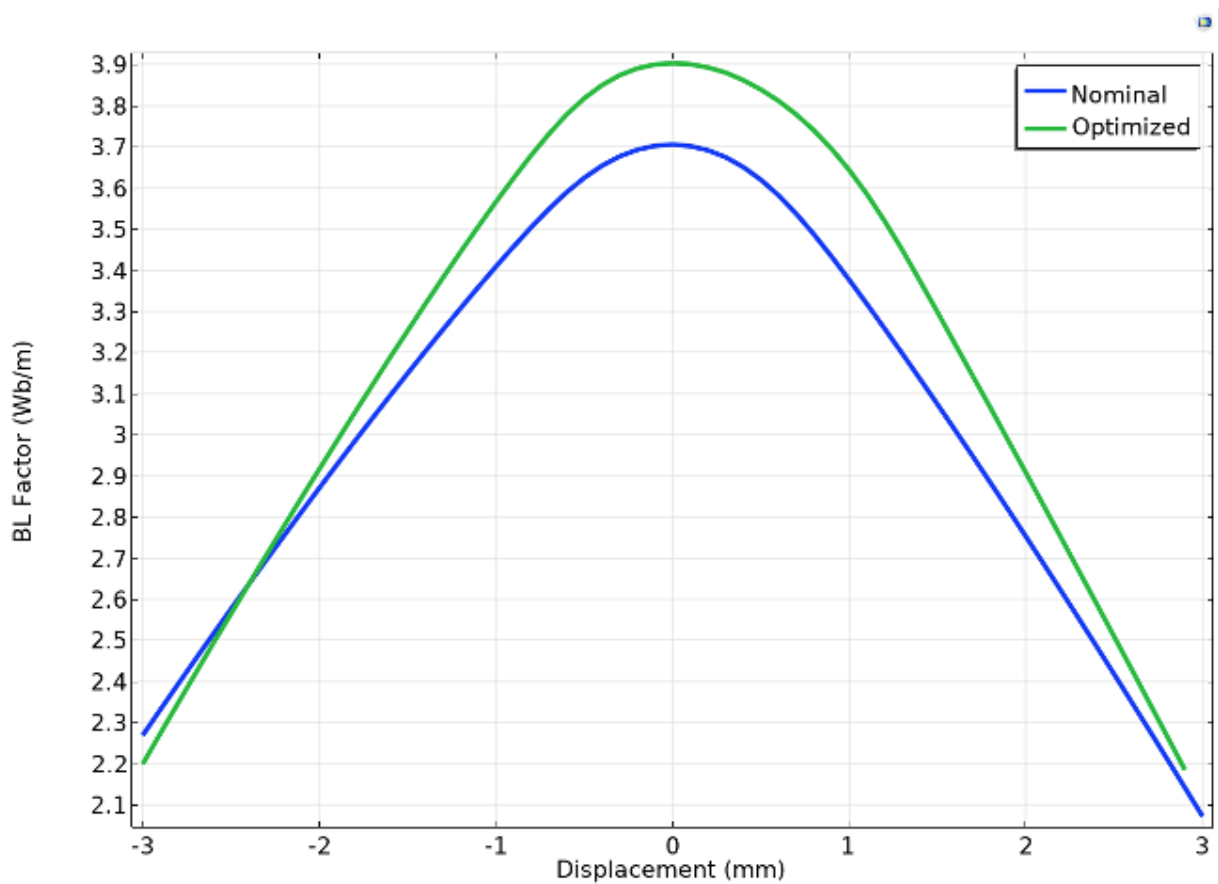
Figure 5.8: Bl comparison for optimized and nominal geometry in Woofer 1

5.1.4. Final and Nominal Volume

The peak of optimized geometry is around 3.9 [Wb/m] with a symmetry index of 98.7 %.
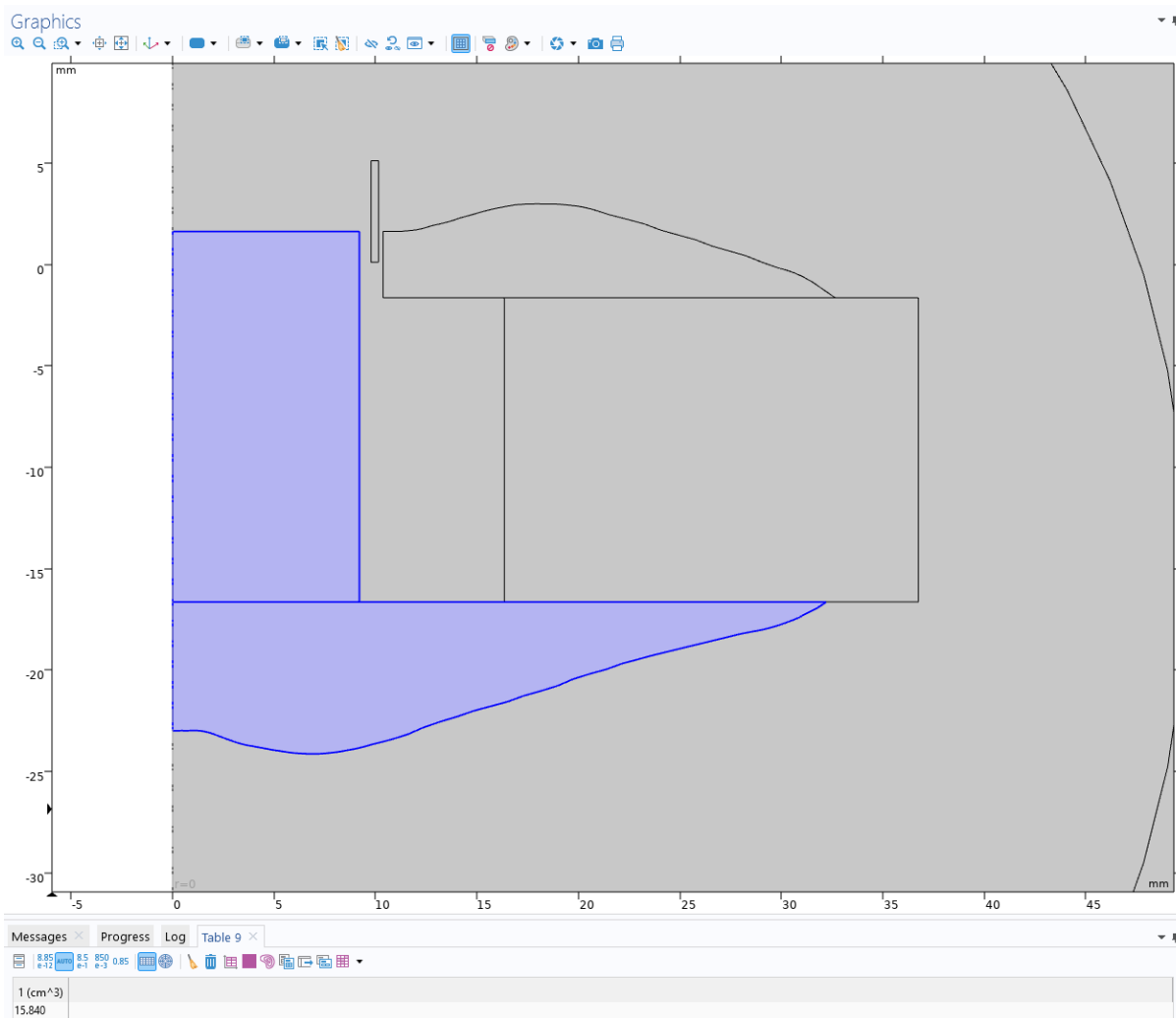
Figure 5.9: Optimized volume for PPI
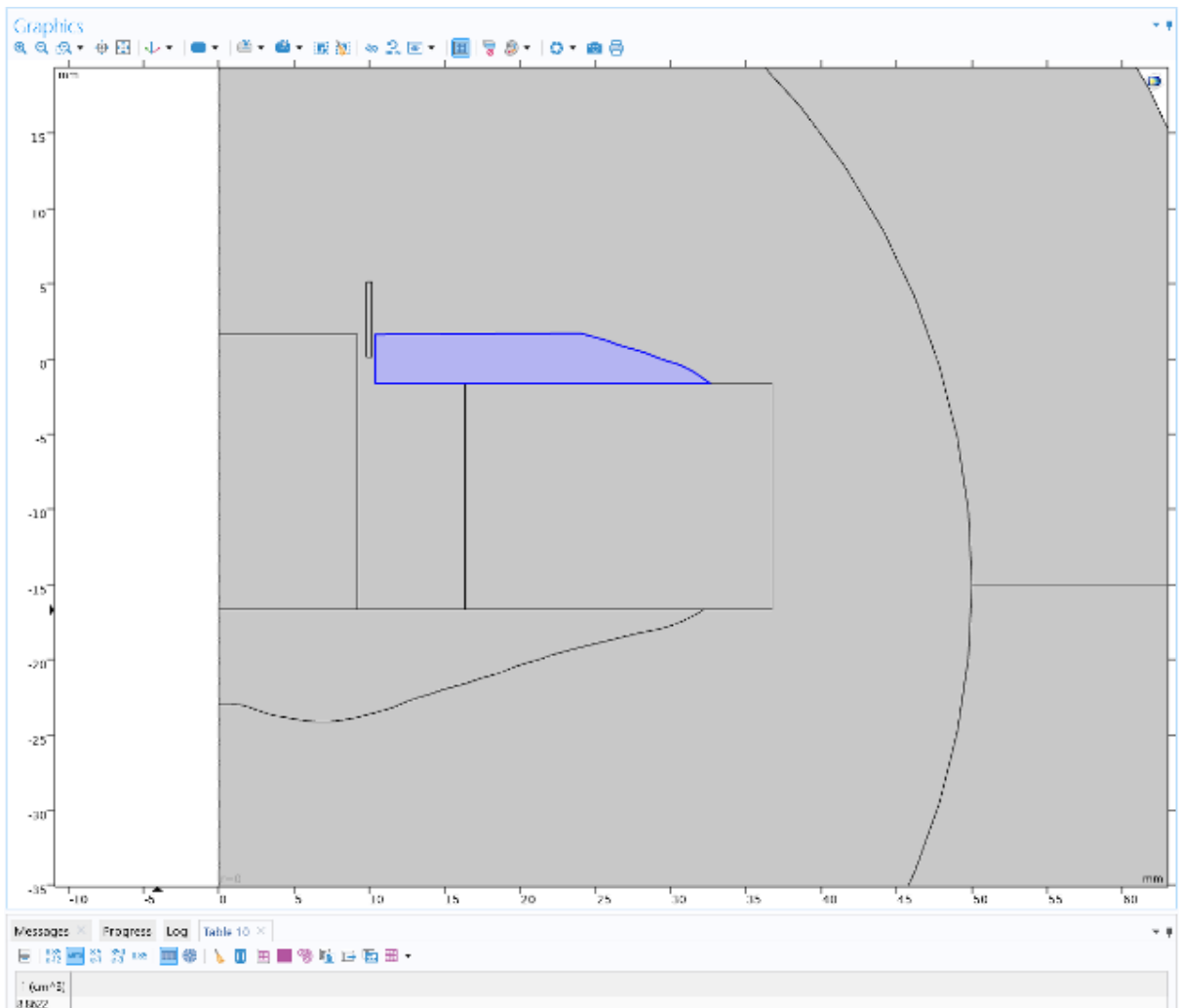
Figure 5.10: Optimized volume for PPS

Optimized volume for the PPI is 15.840 m^3 while for the PPS is 8.86 m^3.

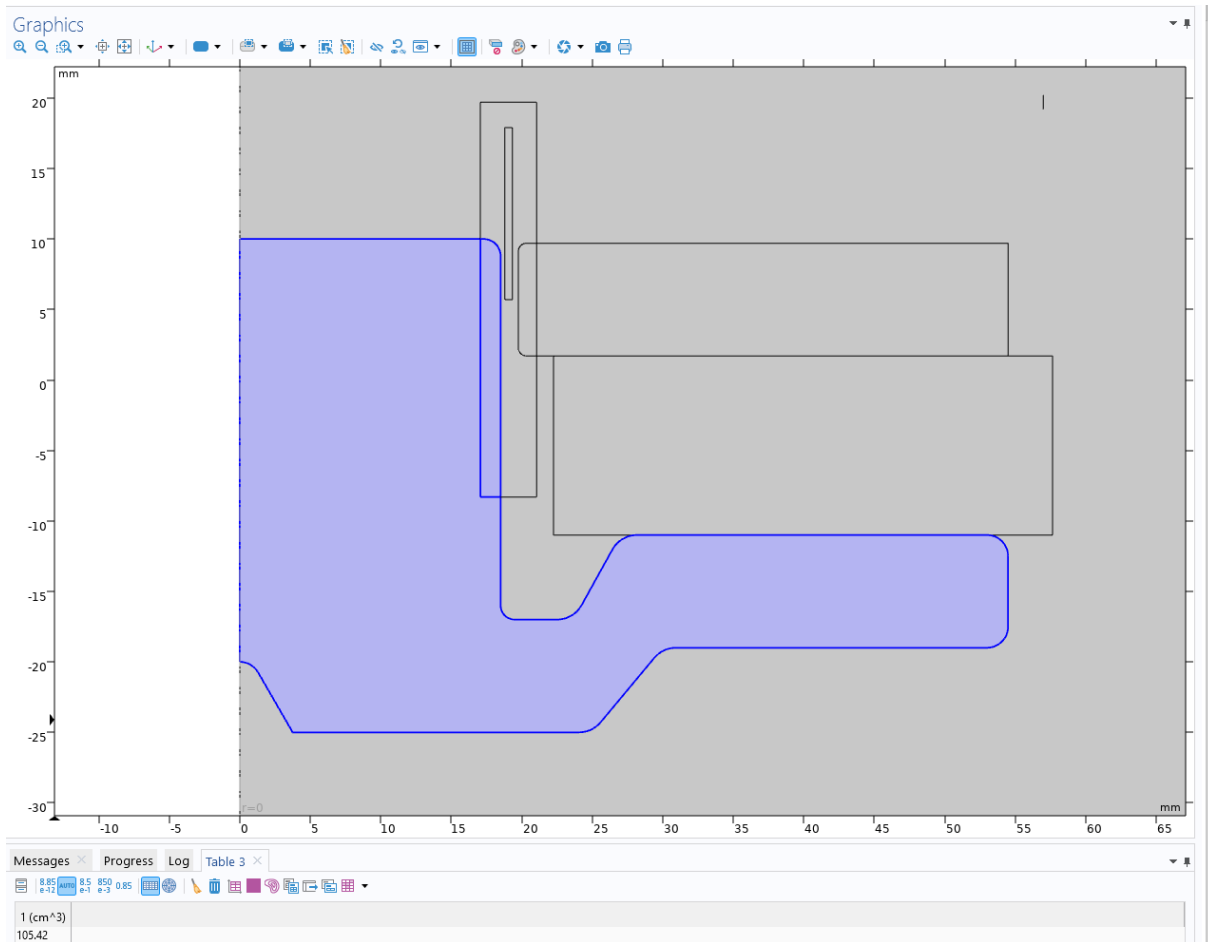These values are reported in Figure 5.9 and 5.10 under the model representation.
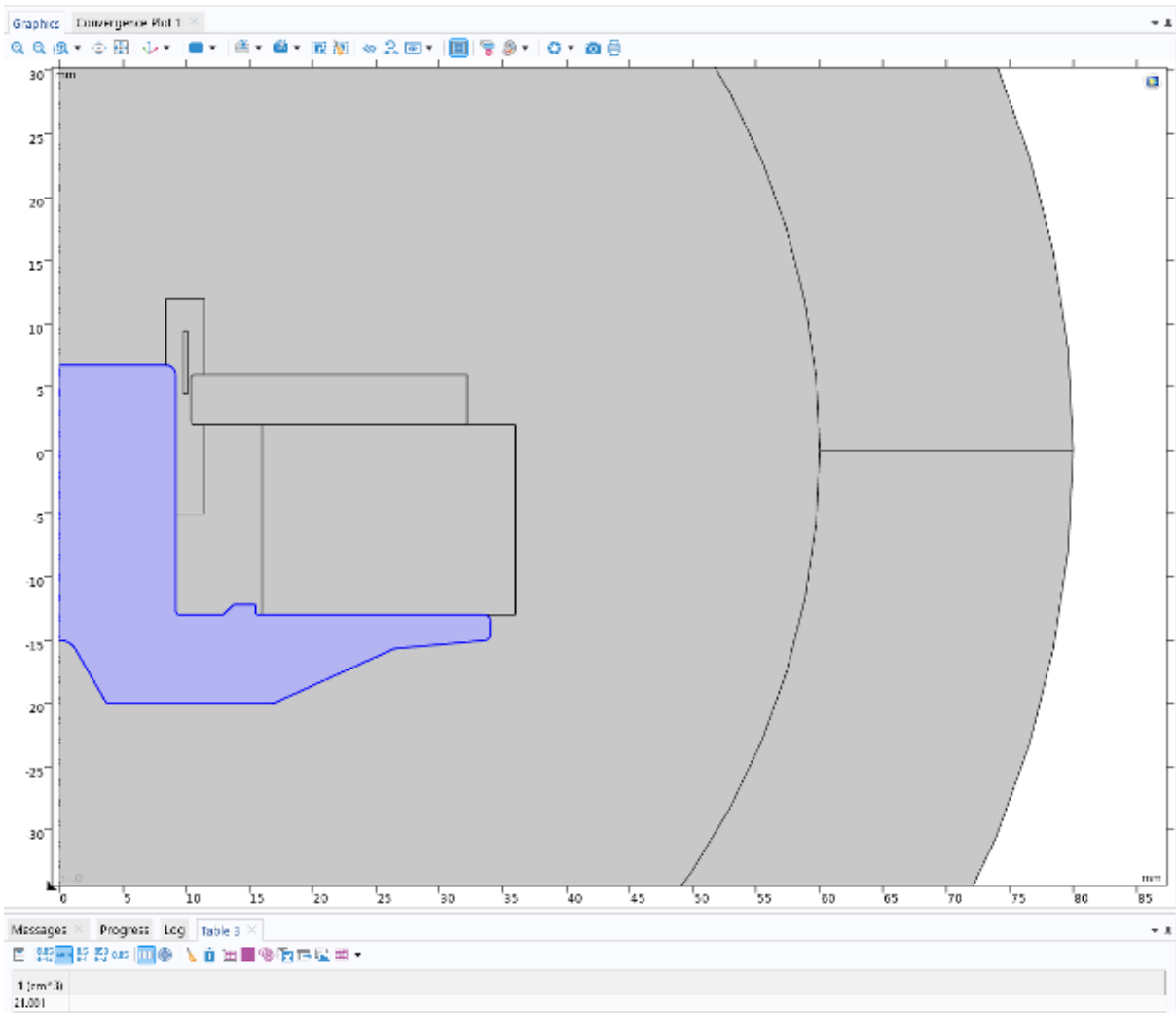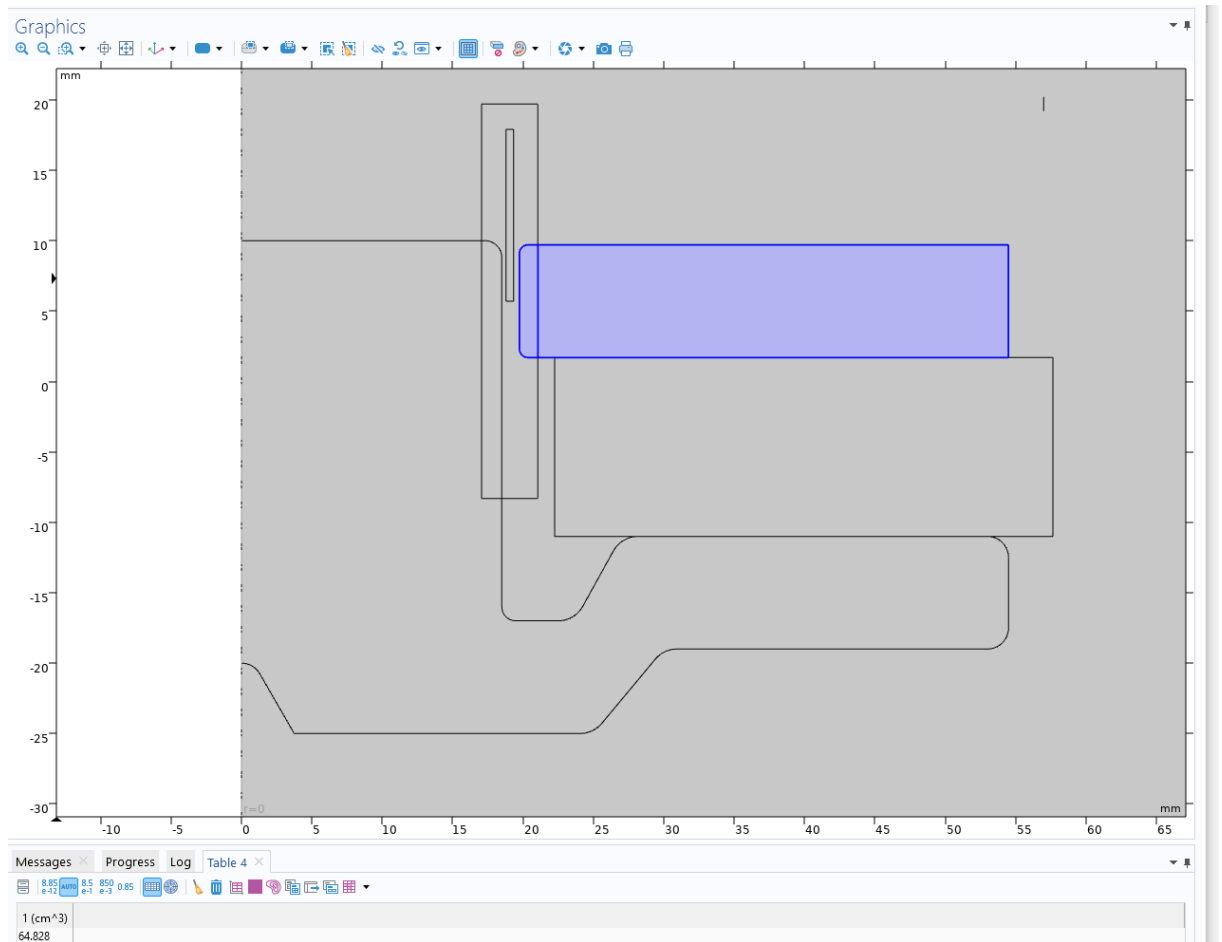
Figure 5.11: Nominal volume for PPI
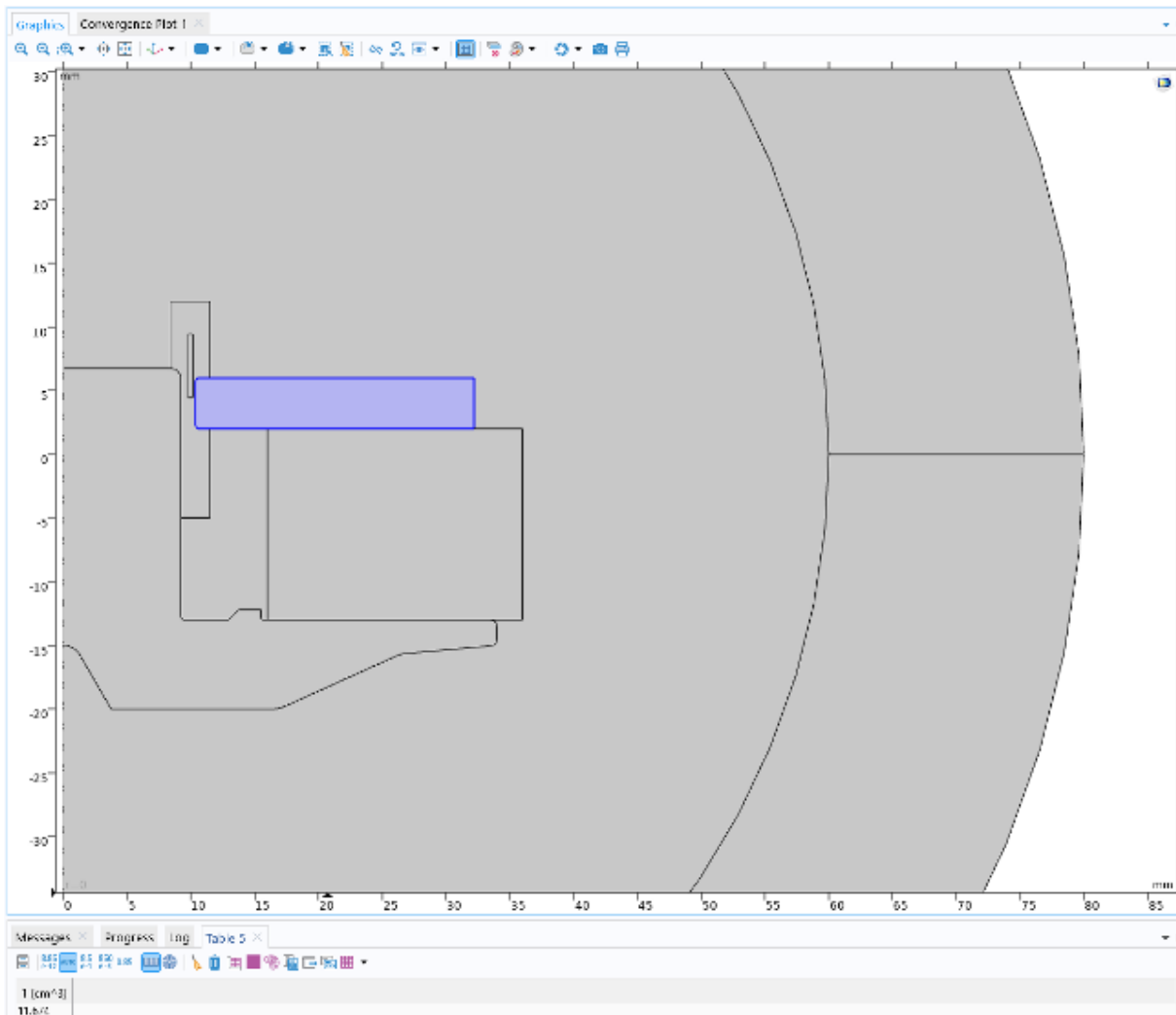
Figure 5.12: Nominal Volume for PPS

Nominal volume for the PPI is 21.001 m^3 while for the PPS is 11.674 m^3.

These values are reported in Figure 5.11 and 5.12 under the model representation.

A graphic representation of the two volumes comparison can be seen in Figure 5.13 :
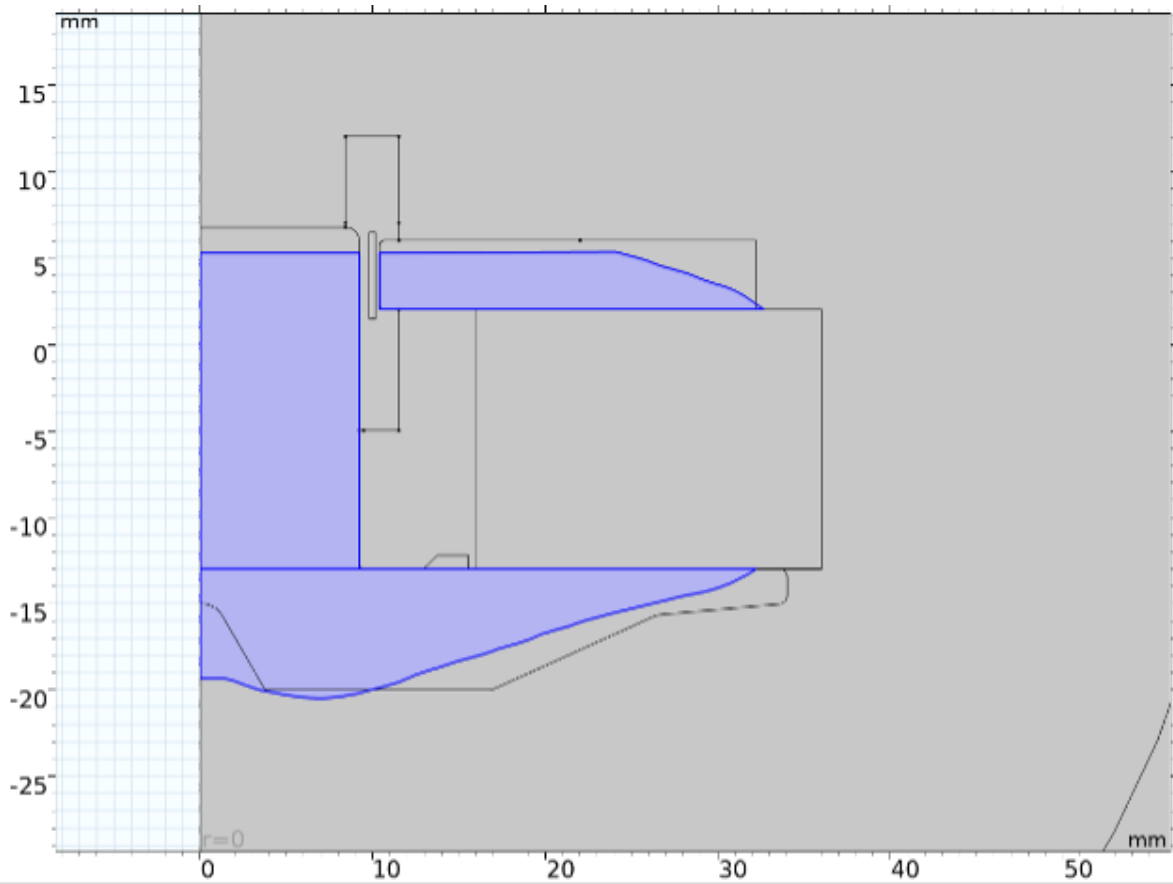
Figure 5.13: Comparison between optimized and nominal volume for FE1

5.2. Woofer 2

5.2.1. Initial Geometry

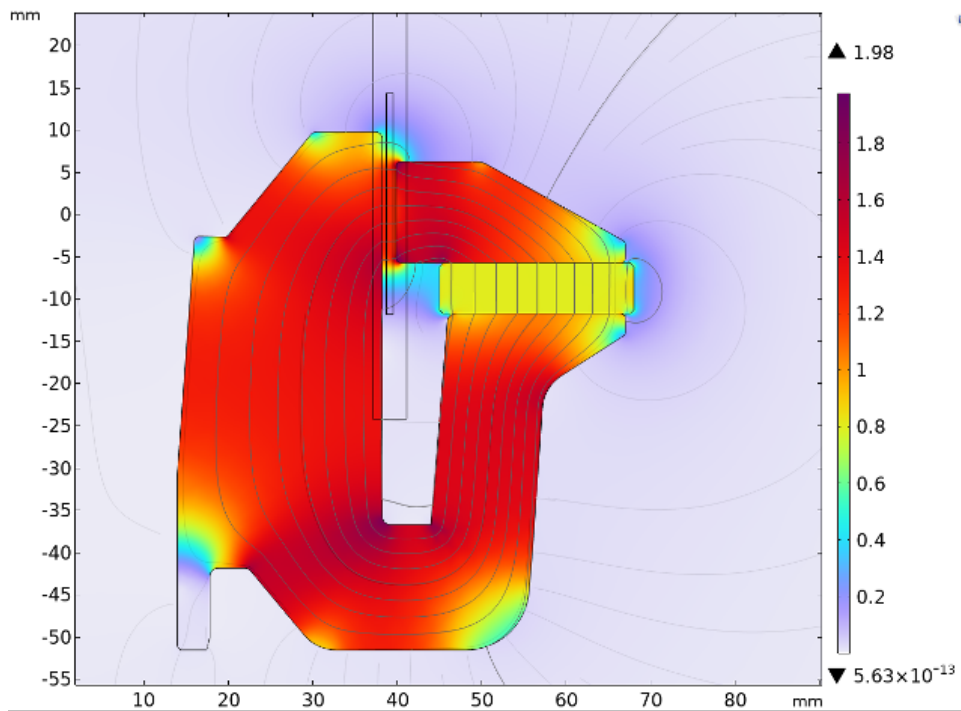Graphic results are reported, with magnetostatic results,
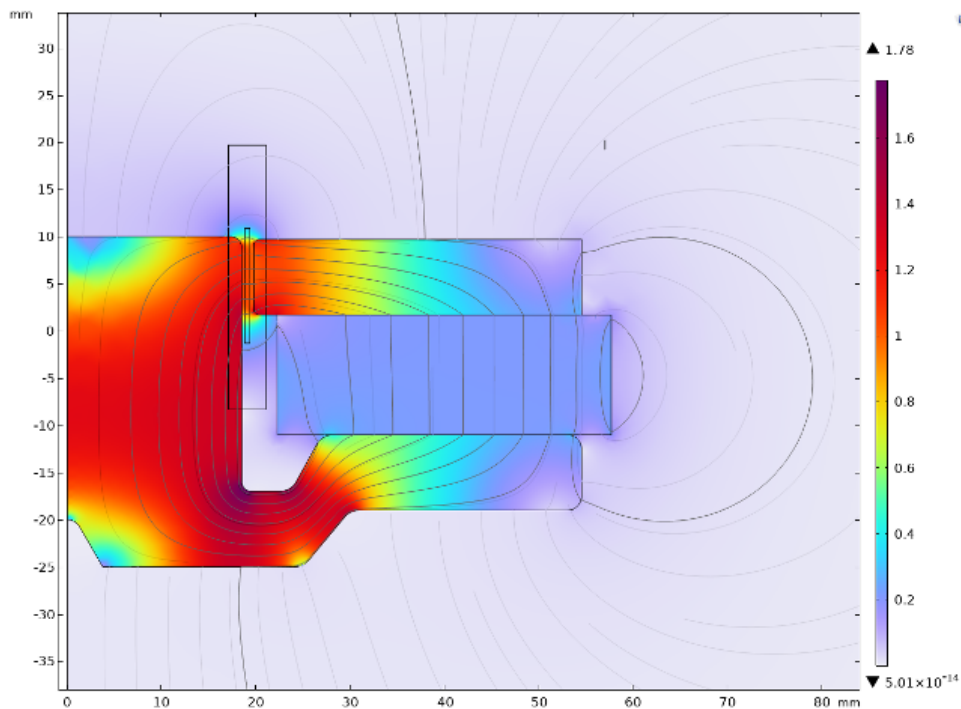
Figure 5.14: Magnetostatic Analysis results for Woofer 2
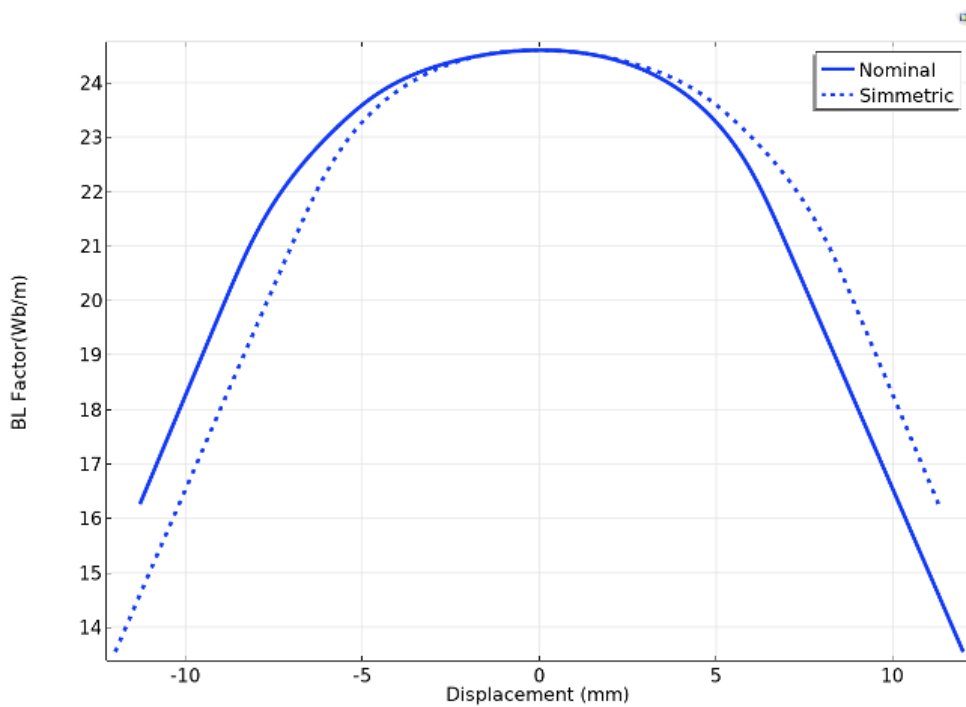
And *Bl* curve:
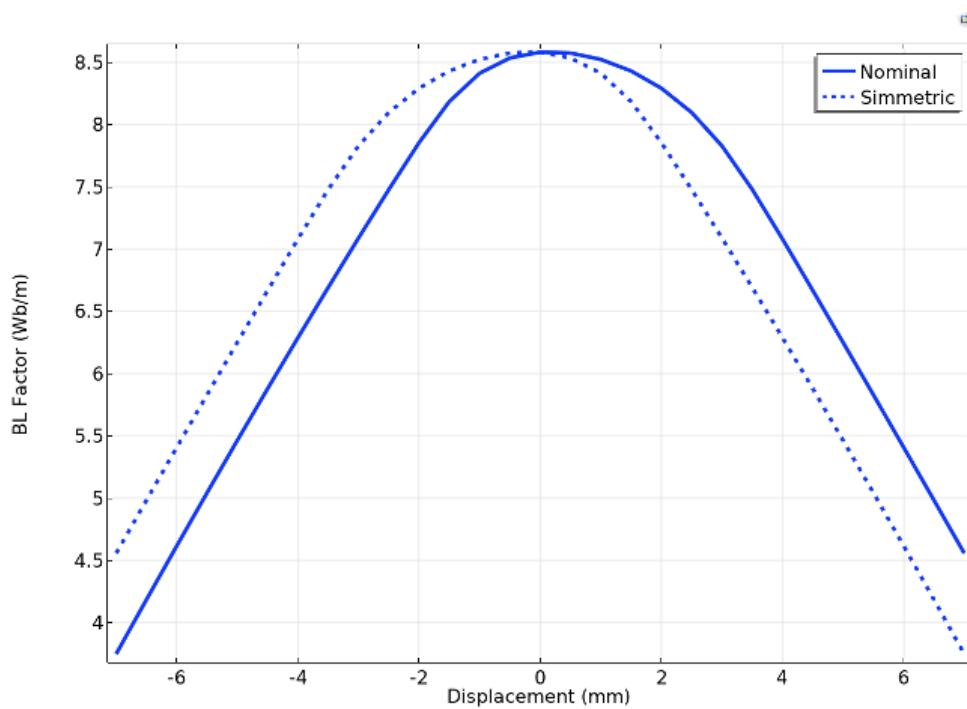
Figure 5.15: Bl factor over displacement curve for Woofer 2

The peak of nominal geometry curve is around 8.6 [Wb/m] with a symmetry index of 94.1 %.

5.2.2.   Filtering and Final Results

Graphic results, after optimizer algorithm work, are displayed in Figure 5.16:
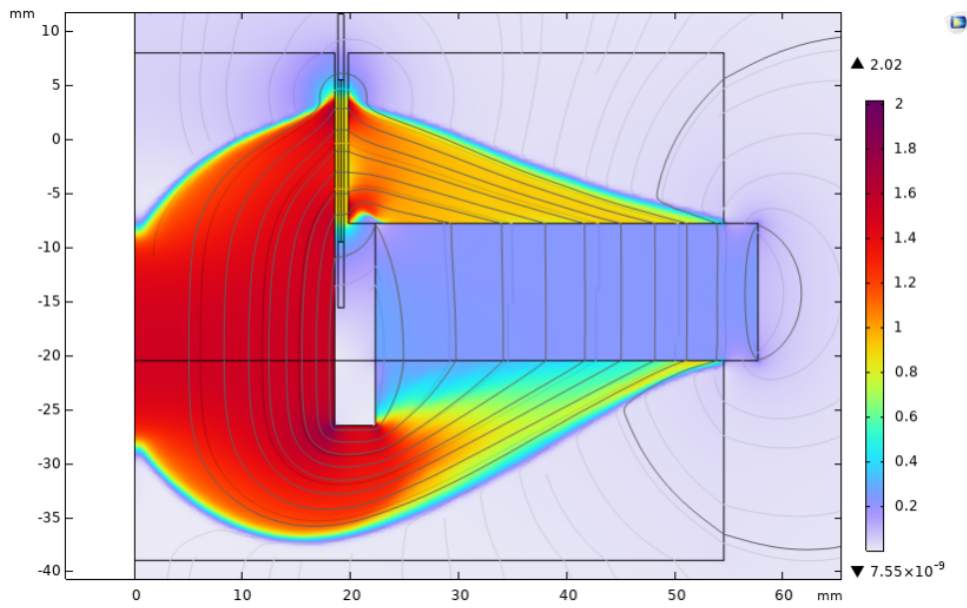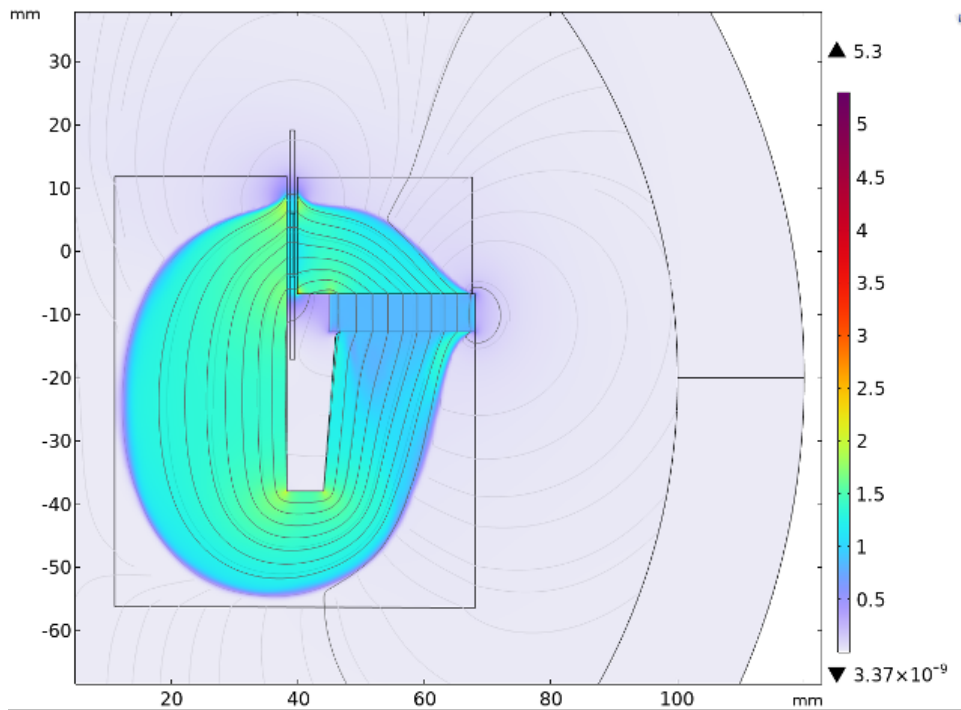
Figure 5.16: Magnetostatic after topology optimization(Woofer 2)

These are filtering results, which algorithm is described in Section 4.5.6:
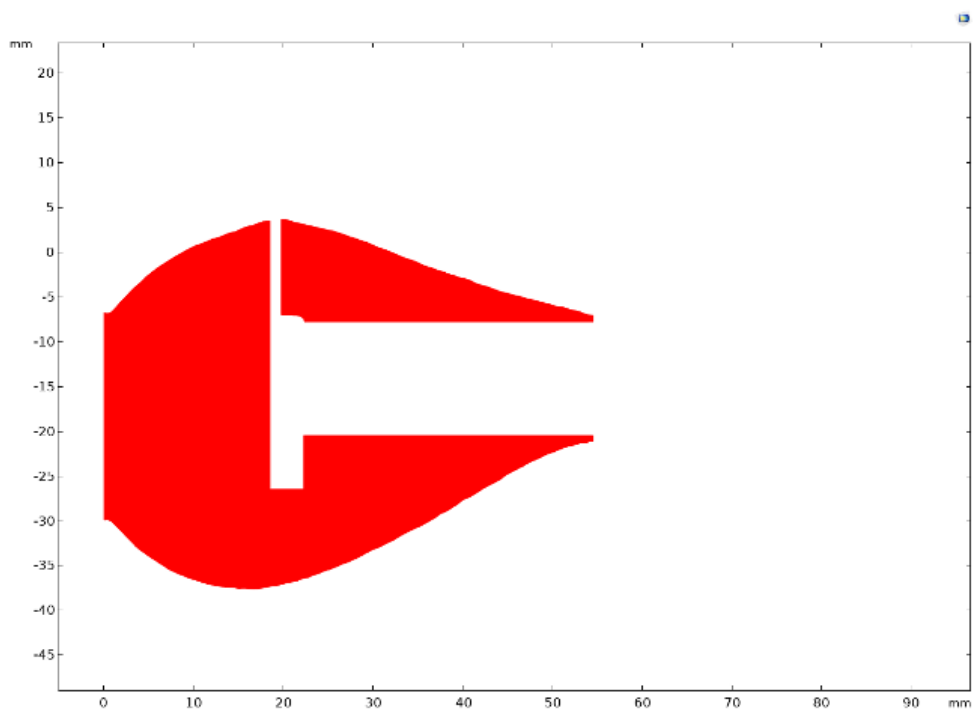
Figure 5.17: Geometry Filtered for Woofer 2

These are the exported optimized geometries for Woofer 2, recalling Section 4.5.6, after having performed a very little improvement on geometry shape:
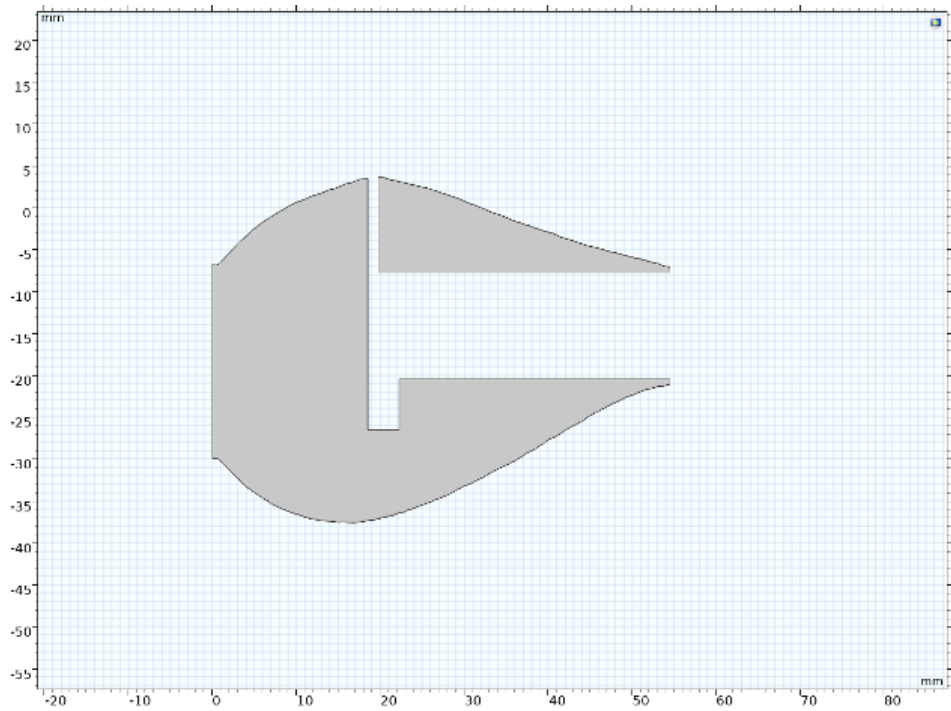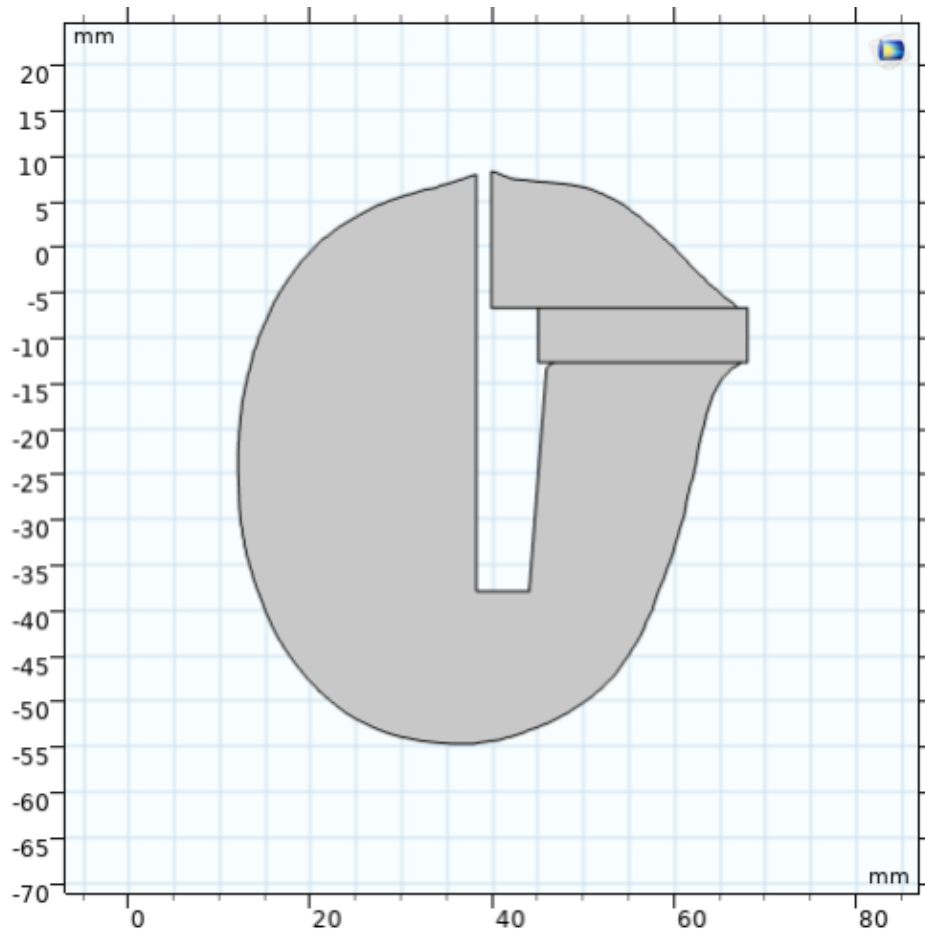
Figure 5.18: Optimized Geometry for Woofer 2

Here are also the graphic results for magnetostatic analyses, recalling Section 4.6:
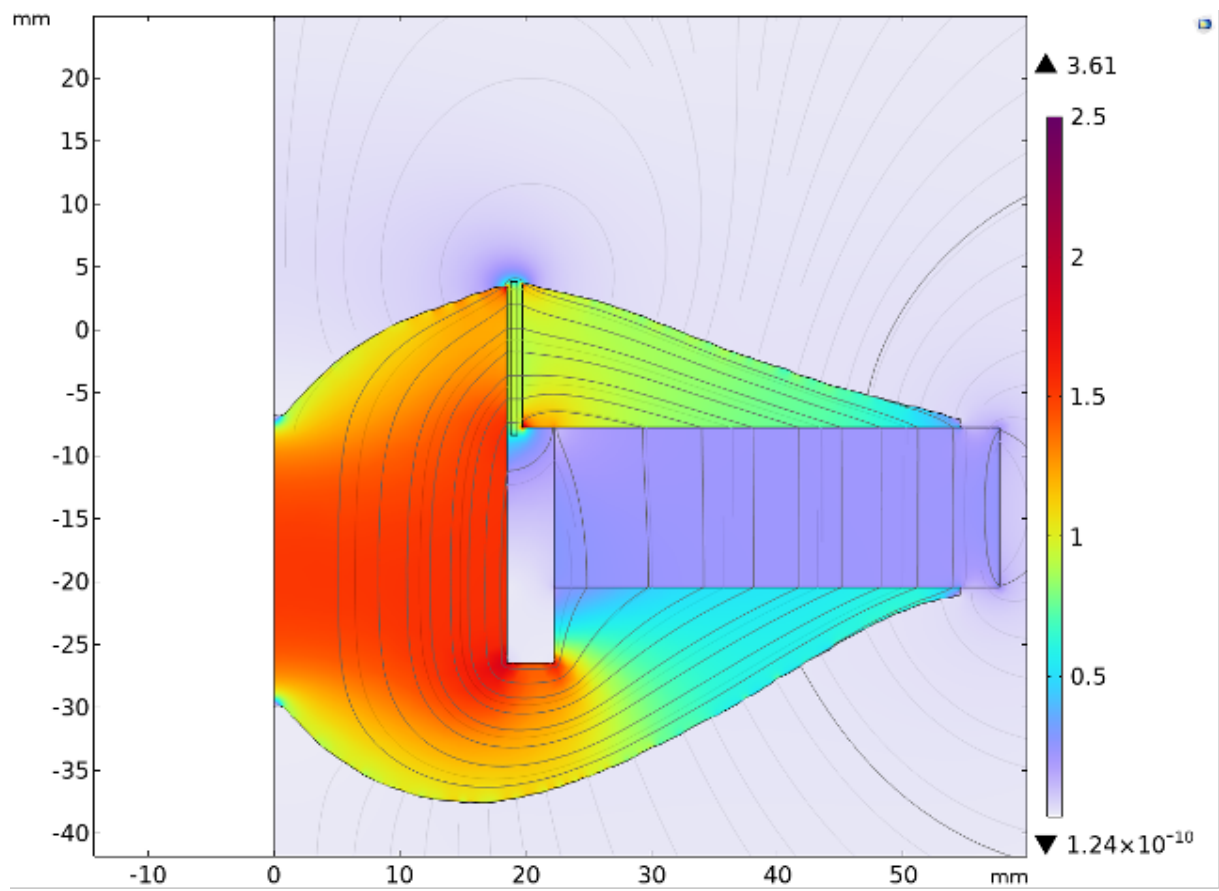
Figure 5.19: Magnetostatic Analysis for optimized geometry of Woofer 2

And *Bl* curve:
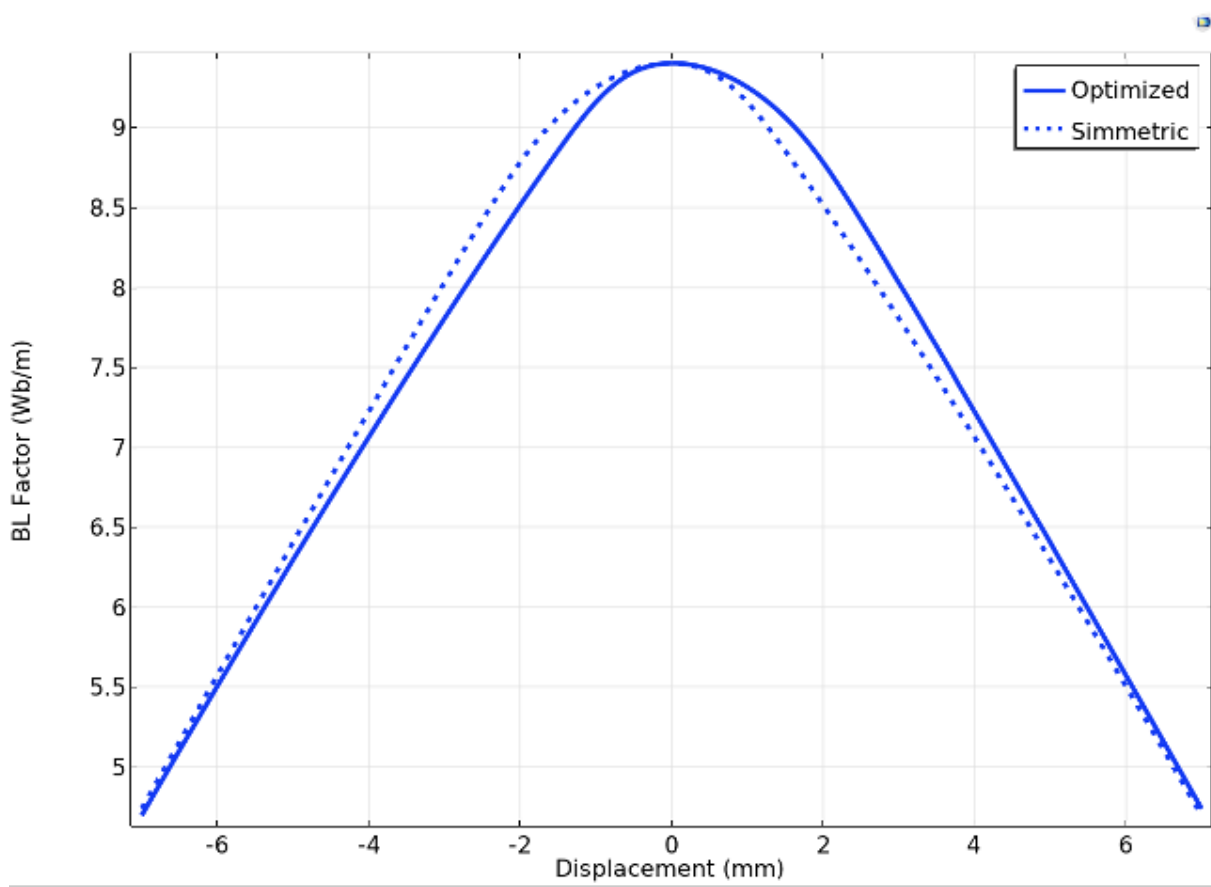
Figure 5.20: Bl curve for optimized geometry of Woofer 2

5.2.3. Optimized Bl and Nominal Bl
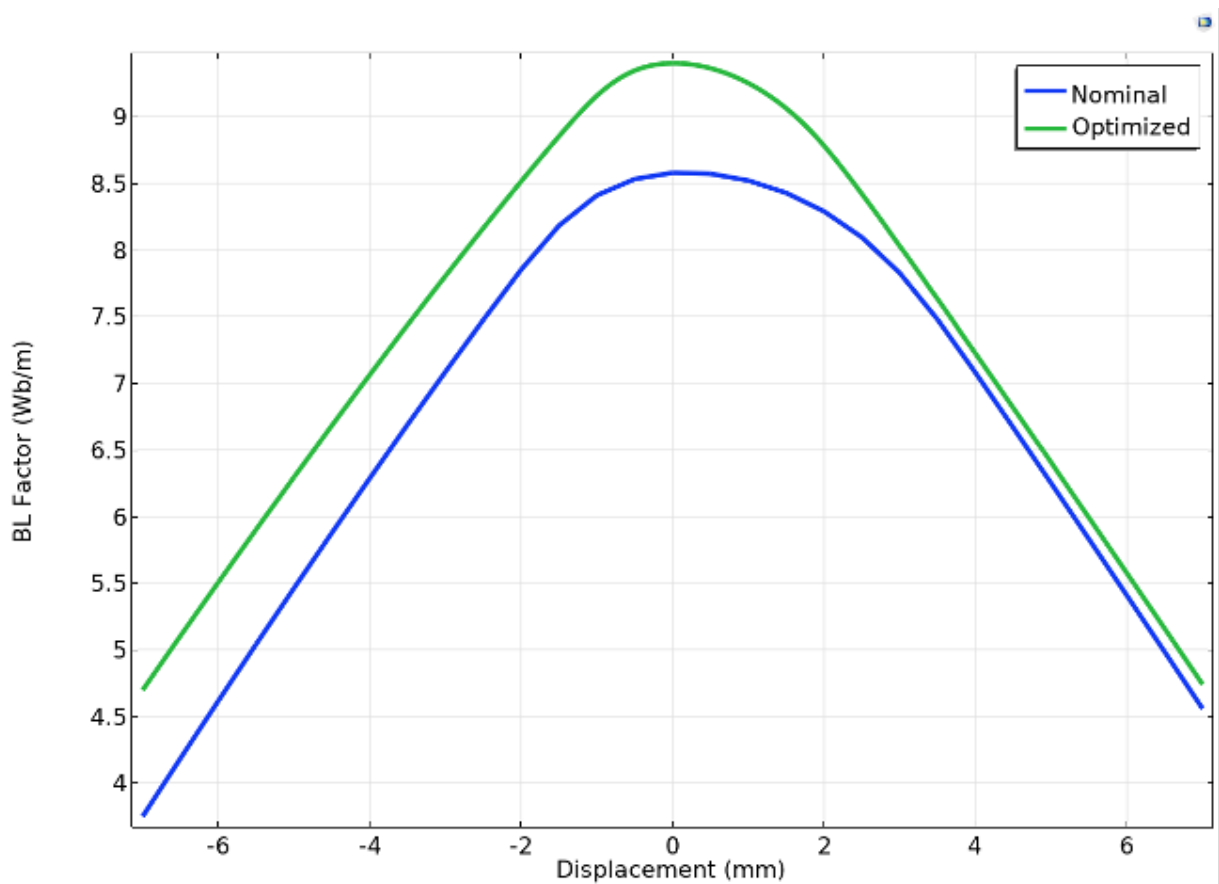
Figure 5.21: Bl comparison for optimized and nominal geometry in Woofer 2

The peak of optimized geometry is around 9.5 [Wb/m] with a symmetry index of 98.9 %.

5.2.4.   Final and Nominal Volume
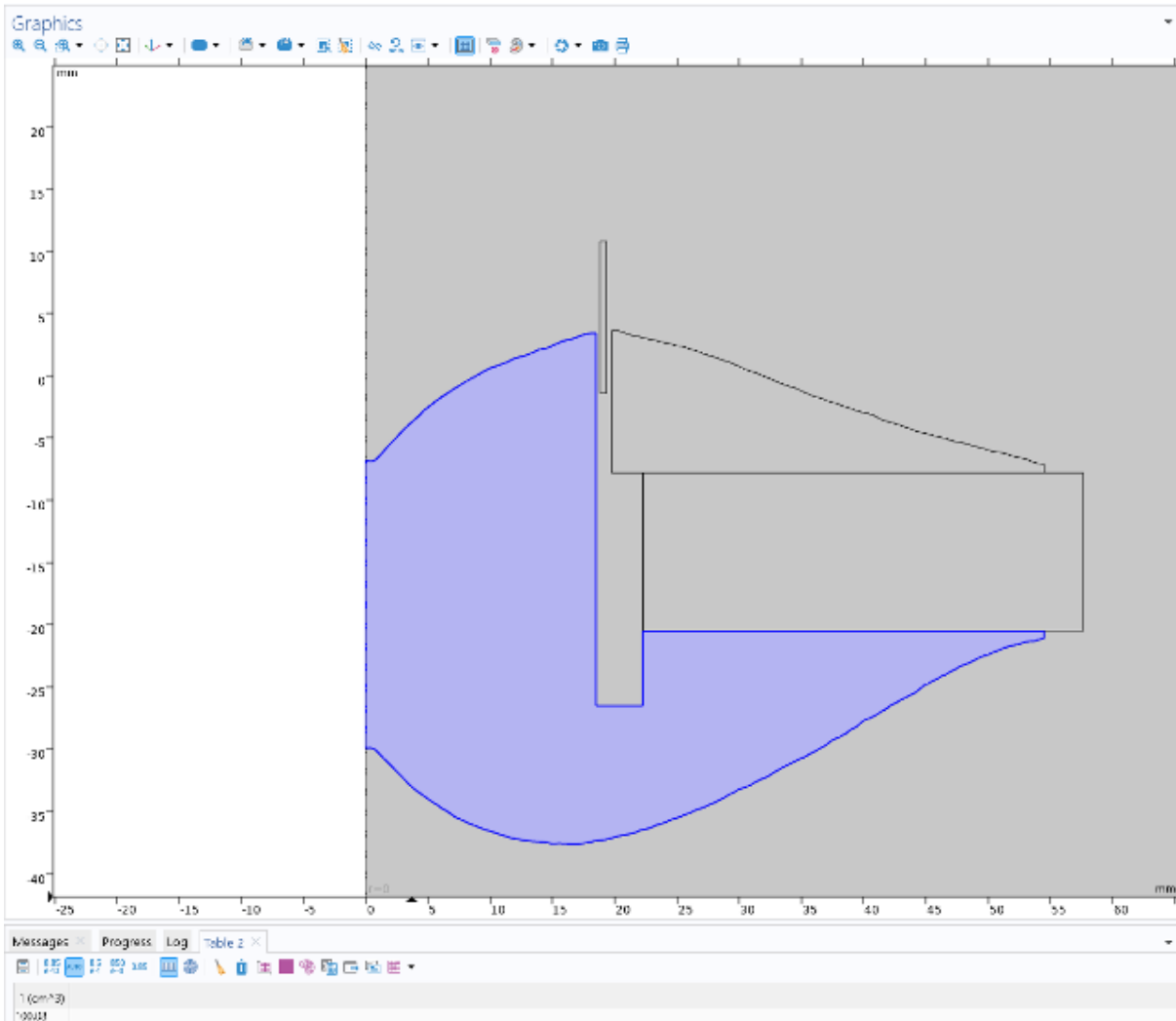
Figure 5.22: Optimized volume for PPI
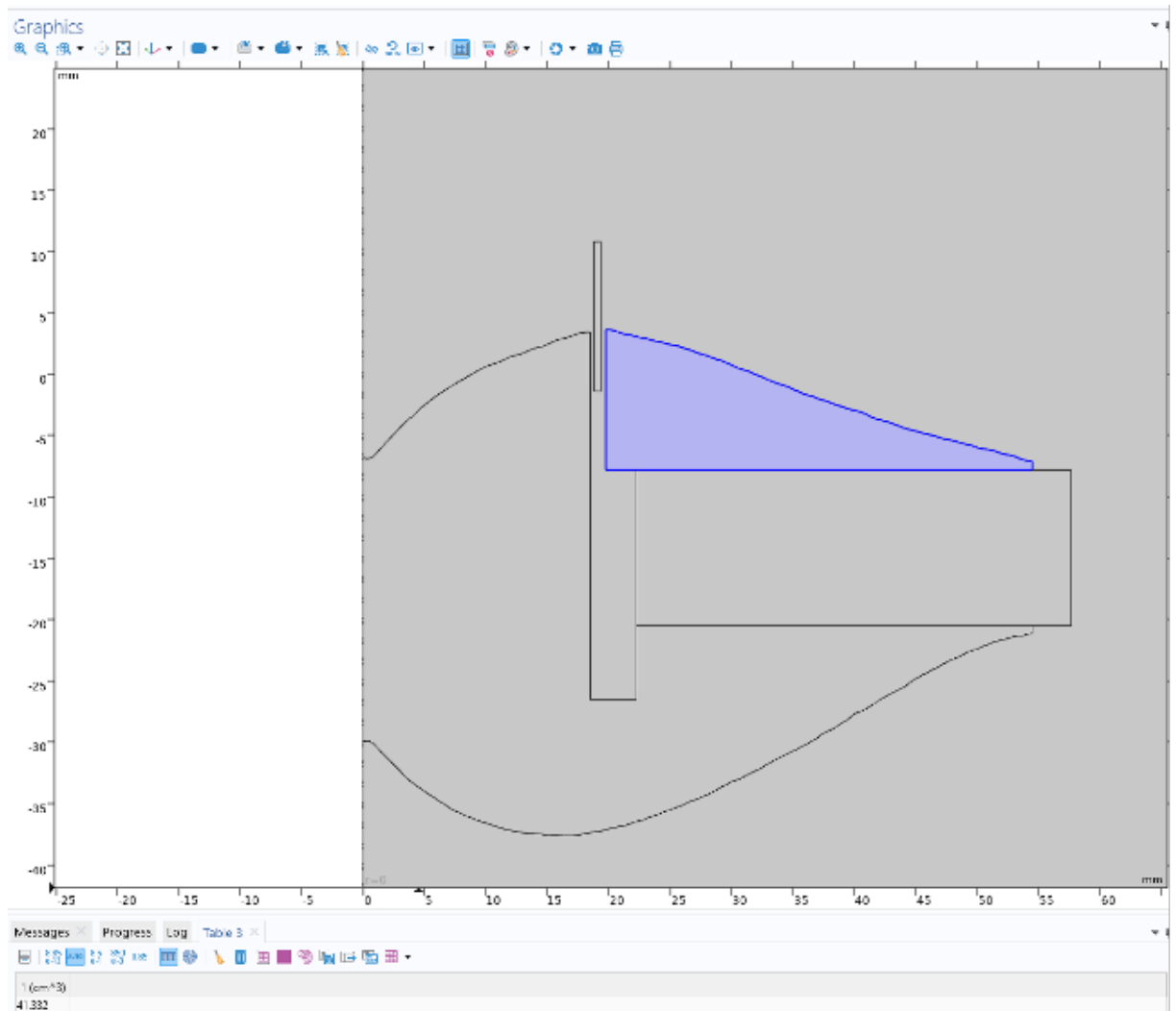
Figure 5.23: Optimized volume for PPS

Optimized volume for the PPI is 100.08 m^3 while for the PPS is 41.32 m^3.

These values are reported in Figure 5.22 and 5.23 under the model representation. m^3.

Figure 5.24: Nominal volume for PPI

Figure 5.25: Nominal Volume for PPS

Nominal volume for the PPI is 105.42 m^3 while for the PPS is 64.82 m^3.

These values are reported in Figure 5.24 and 5.25 under the model representation.

A graphic representation of the two volumes comparison can be seen in Figure 5.26 :
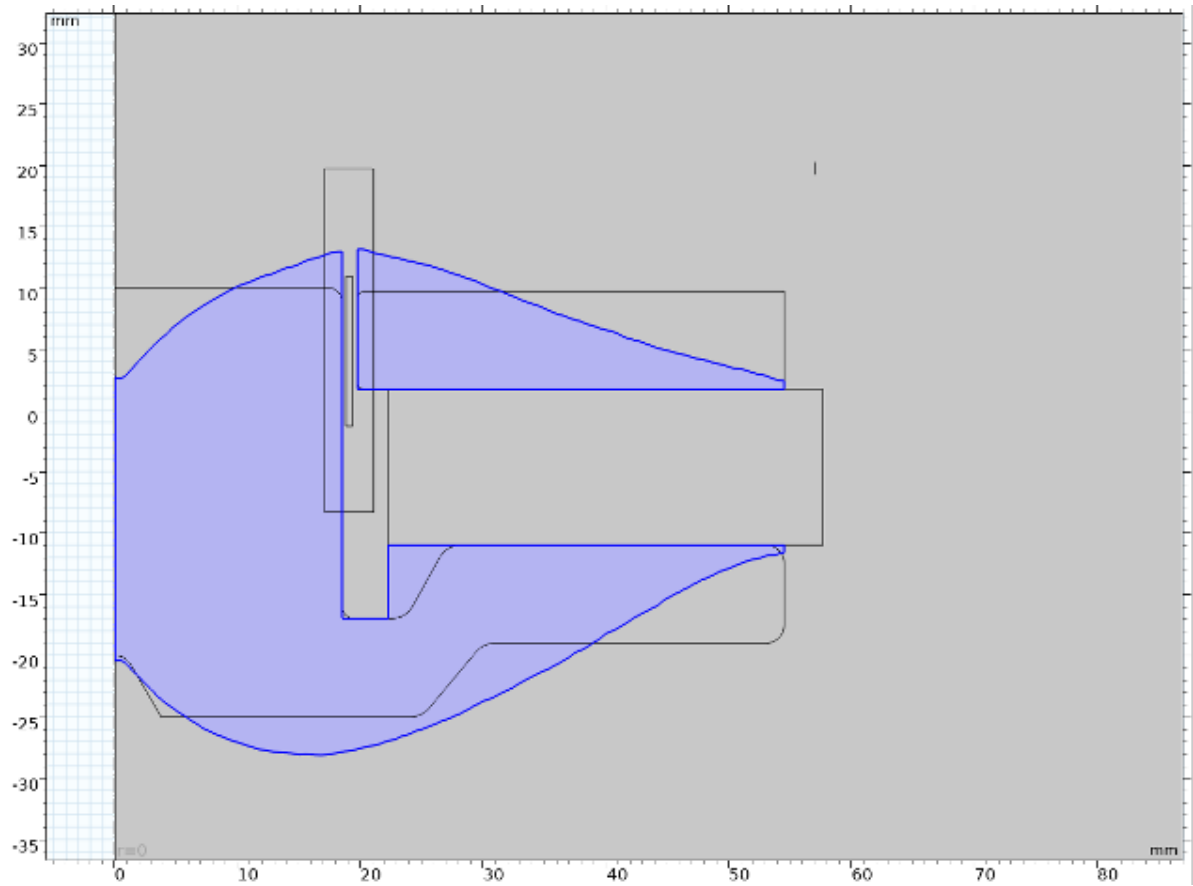
Figure 5.26: Comparison between optimized and nominal volume for FE2

5.3.   Woofer 3

5.3.1.   Initial Geometry

Graphic results are reported, with magnetostatic results,

Figure 5.27: Magnetostatic Analysis results for Woofer 3

And *Bl* curve:

Figure 5.28: Bl factor over displacement curve for Woofer 3

The peak of nominal geometry curve is around 24.5[Wb/m] with a symmetry index of 96.8 %.

5.3.2. Filtering and Final Results

Graphic results, after optimizer algorithm work, are displayed in Figure 5.29 :

Figure 5.29: Magnetostatic after topology optimization(Woofer 3)

These are filtering results, which algorithm is described in Section 4.5.6:
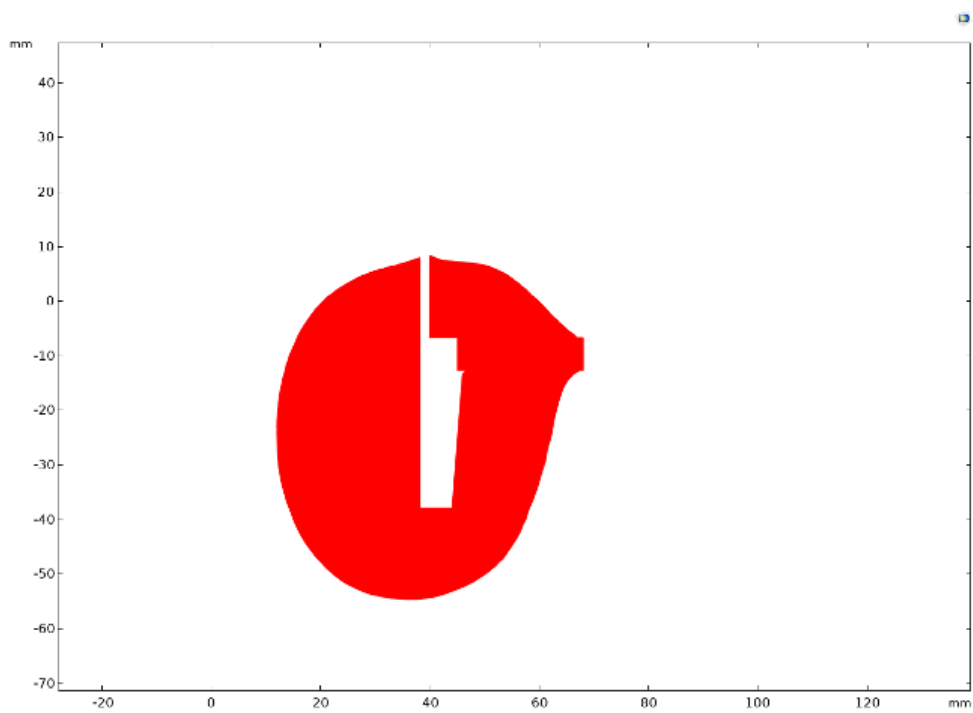
Figure 5.30: Geometry Filtered for Woofer 3

These are the exported optimized geometries for Woofer 3, recalling Section 4.5.6 after having performed a very little improvement on geometry shape:

Figure 5.31: Optimized Geometry for Woofer 3

Here are also the graphic results for magnetostatic analyses, recalling Section 4.6:
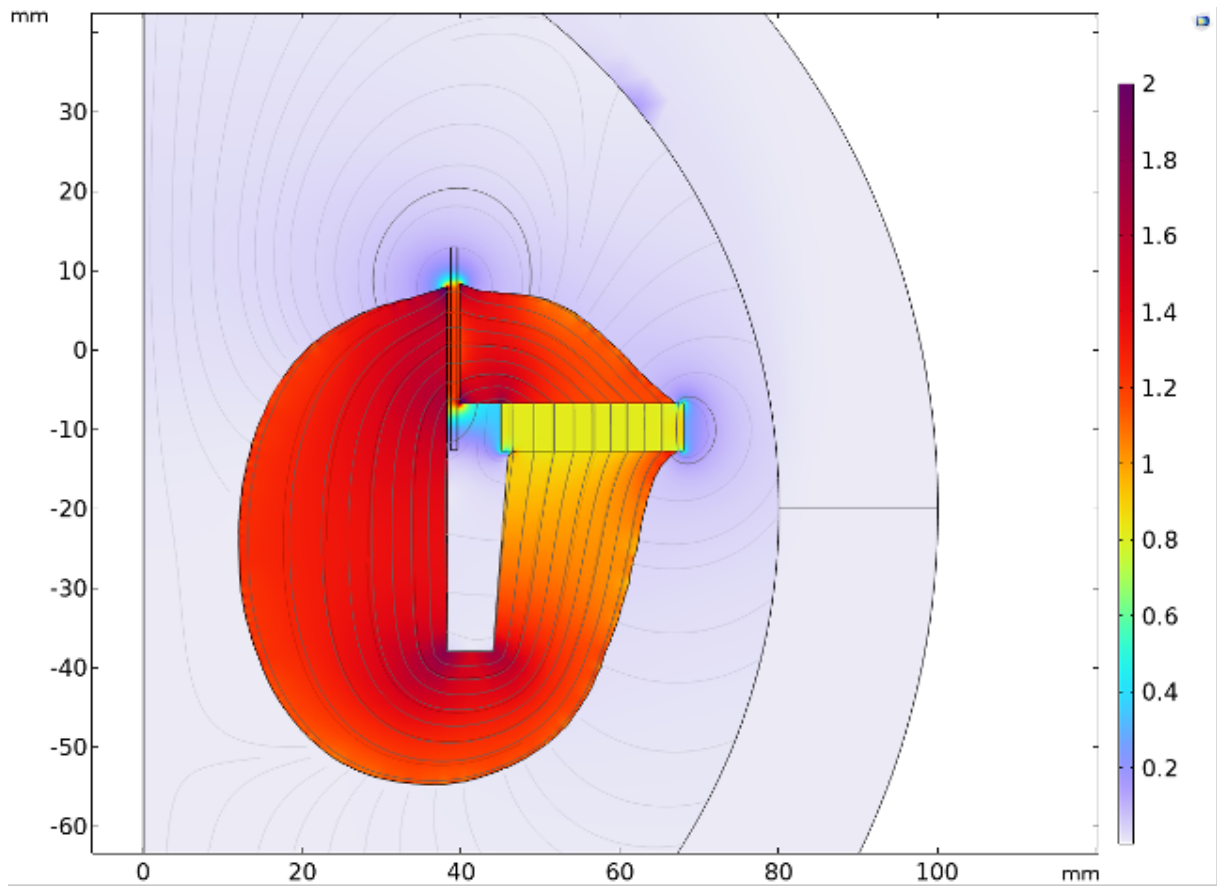
Figure 5.32: Magnetostatic Analysis for optimized geometry of Woofer 3

And *Bl* curve:
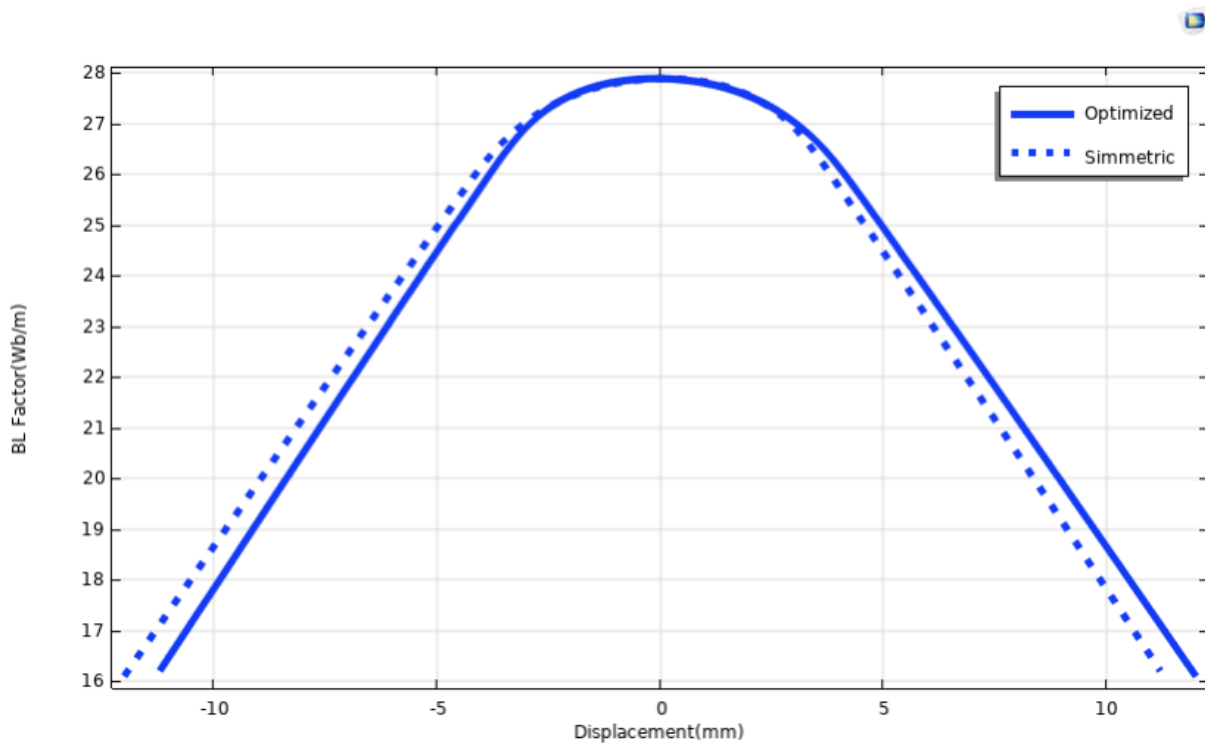
Figure 5.33: Bl curve for optimized geometry of Woofer 3

5.3.3. Optimized Bl and Nominal Bl
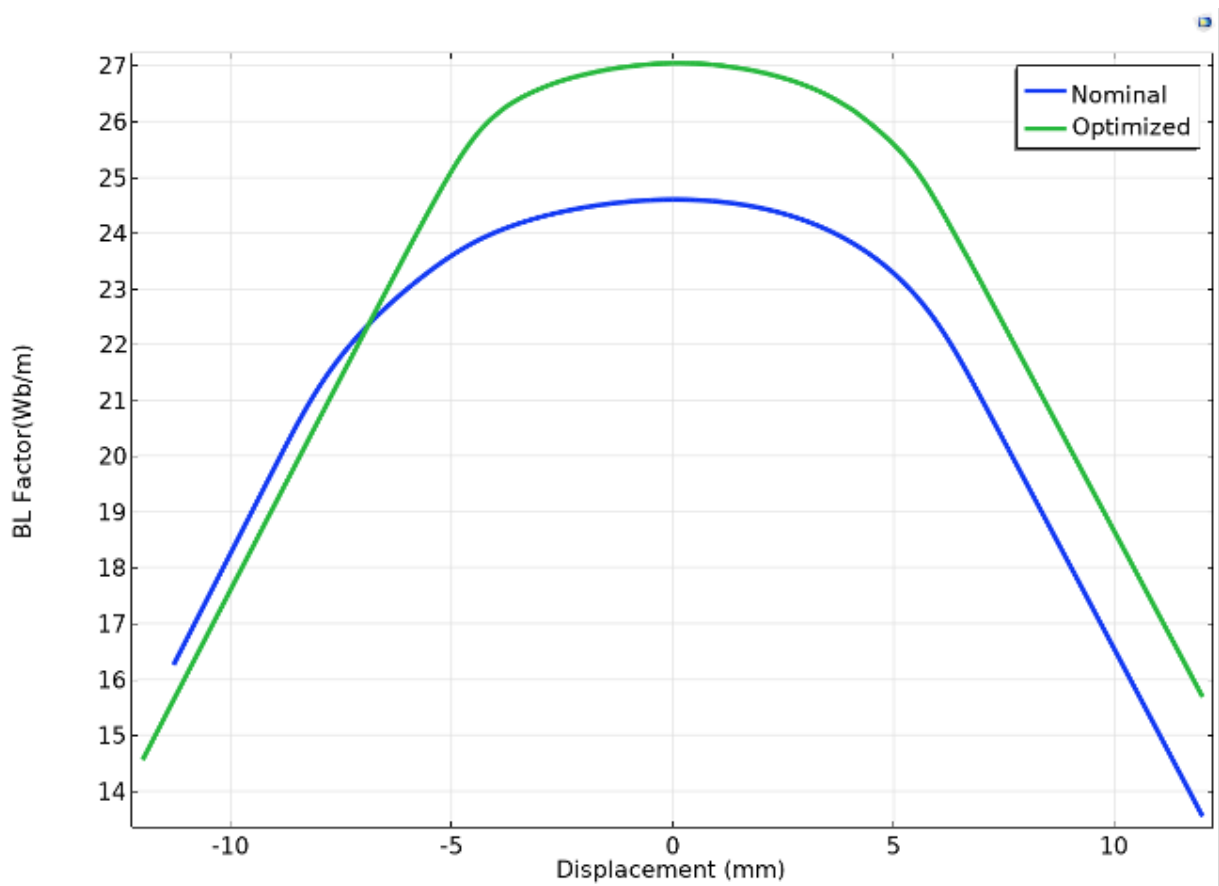
Figure 5.34: Bl comparison for optimized and nominal geometry in Woofer 3

The peak of optimized geometry is around 27 [Wb/m] with a symmetry index of 98.5 %.

5.3.4.   Final and Nominal Volume
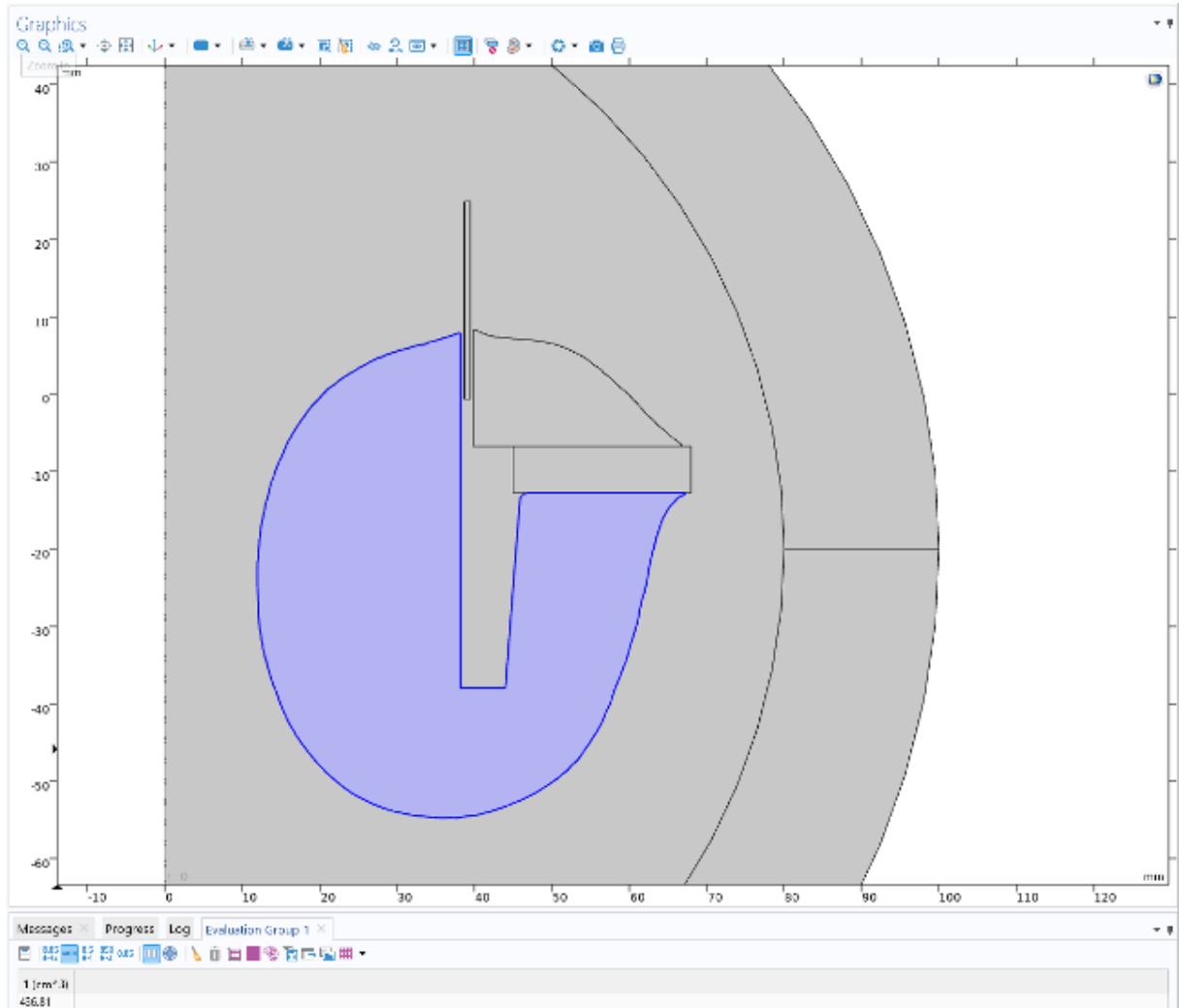
Figure 5.35: Optimized volume for PPI
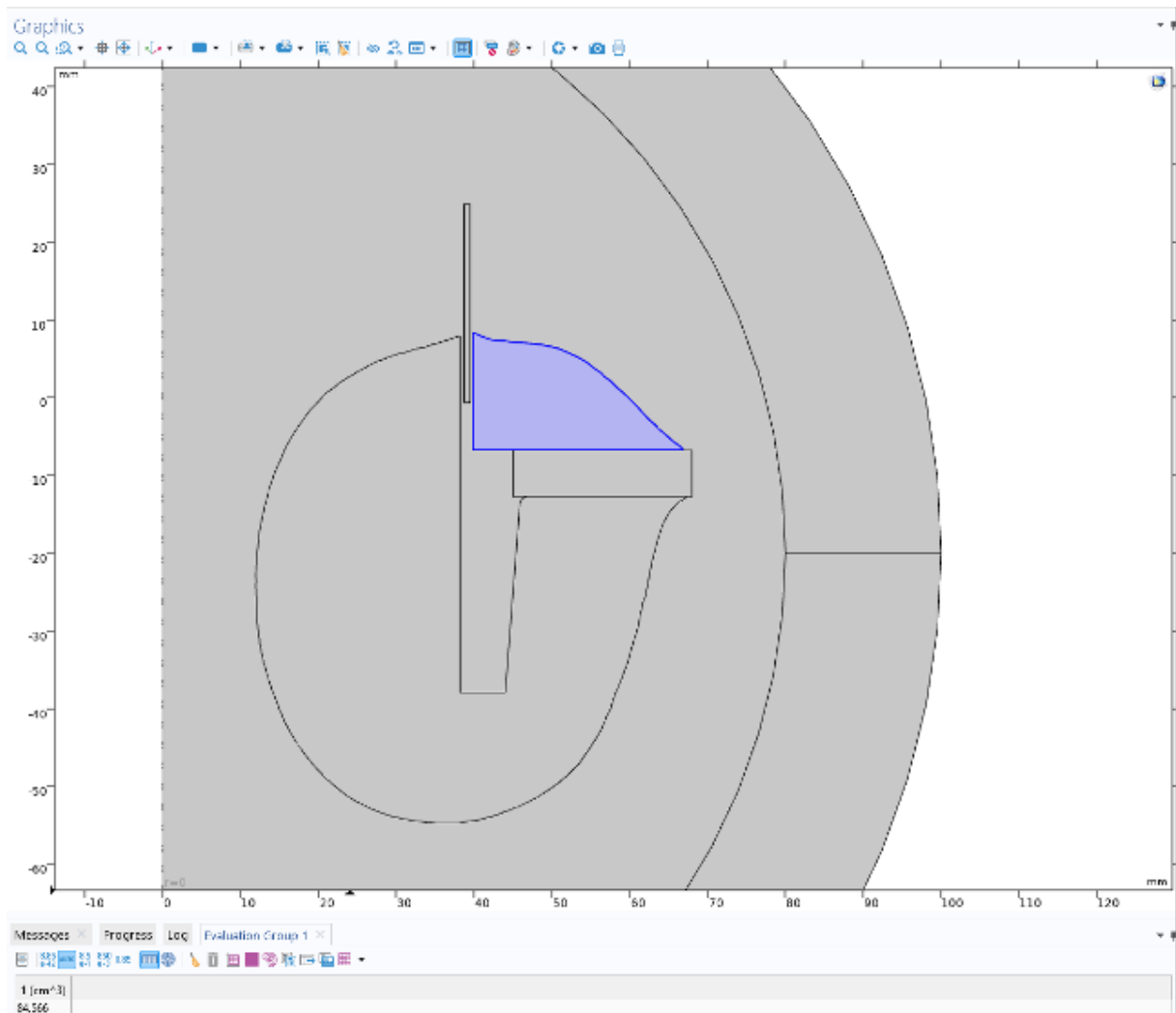
Figure 5.36: Optimized volume for PPS

Optimized volume for the PPI is 436.81 m^3 while for the PPS is 84.55 m^3.
These values are reported in Figure 5.35 and 5.36 under the model representation.
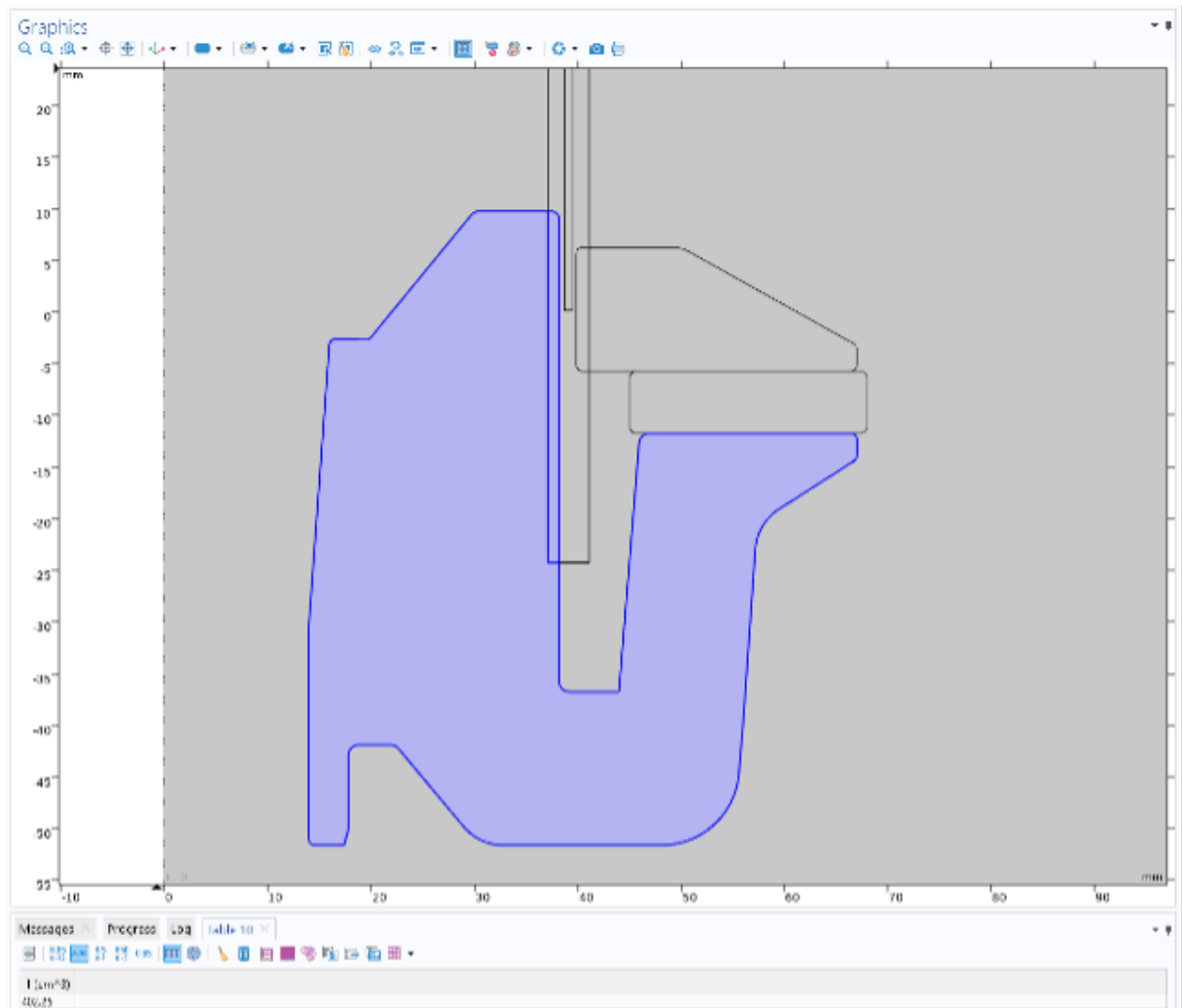
Figure 5.37: Nominal volume for PPI
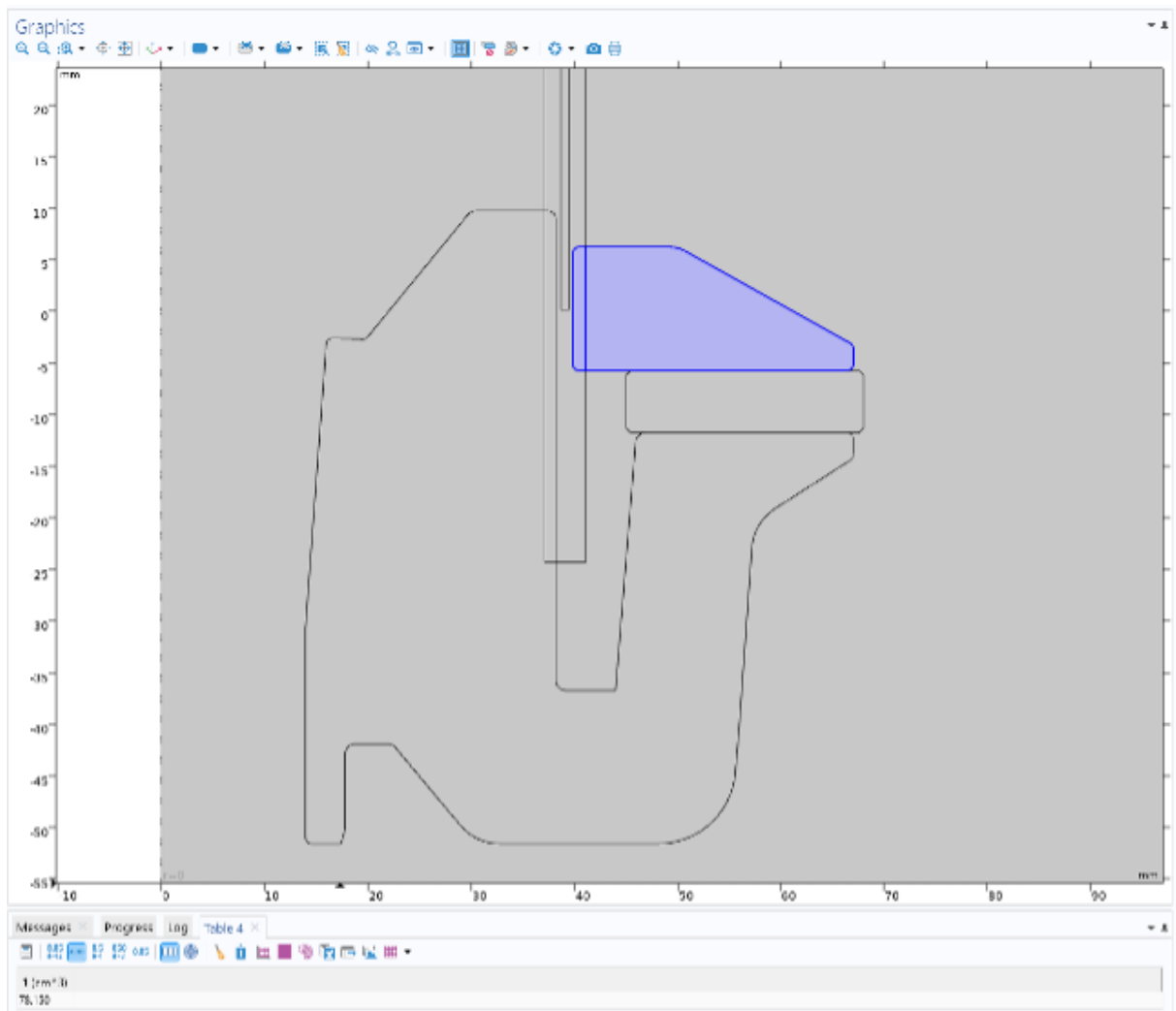
Figure 5.38: Nominal Volume for PPS

Nominal volume for the PPI is 402.25 m^3 while for the PPS is 78.15 m^3.

These values are reported in Figure 5.37 and 5.38 under the model representation.

A graphic representation of the two volumes comparison can be seen in Figure 5.39 :
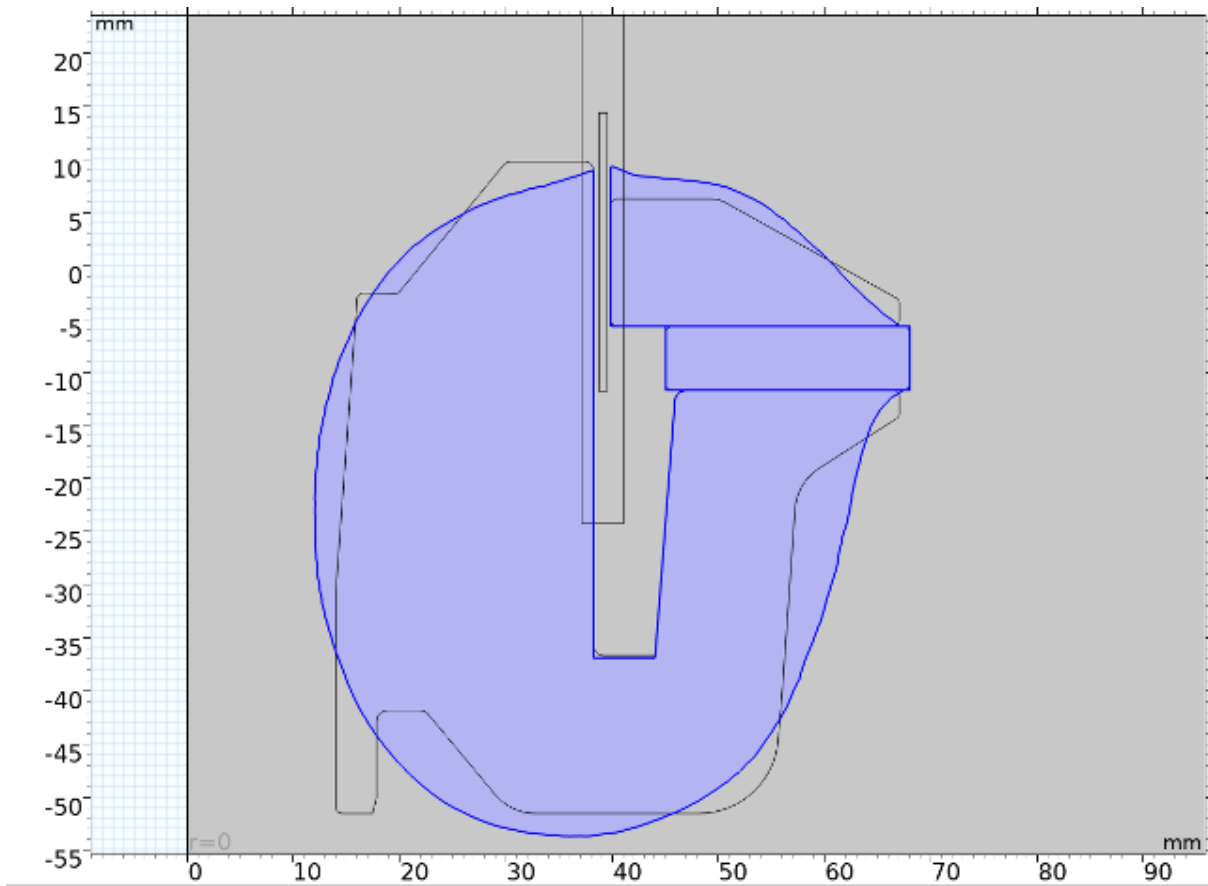
Figure 5.39: Comparison between optimized and nominal volume for FE3

6 | Conclusions and Future Developments

In this work, the objective was to improve the shape of the plates to enhance the performance of the magnetic circuit in terms of peak of the Bl curve at x=0, percentage of symmetry of the same curve by reducing the amount of material used, in terms of volume. Table 6.1 reports the results achieved in percentage terms after optimization, comparing them with the results of the nominal models.

	Bl(0)[Wb/m]			Bl Symmetry(%)			Volume [m^3]		
	Nominal	Final	$\Delta(\%)$	Nominal	Final	$\Delta(\%)$	Nominal	Final	$\Delta(\%)$
Woofer 1	3.7	3.9	**+6%**	97.8	98.7	**+1.5%**	32.7	24.7	**-30%**
Woofer 2	8.6	9.5	**+9.7%**	94.1	98.9	**+3%**	170.2	141.4	**-17%**
Woofer 3	24.5	27	**+10%**	96.8	98.5	**+1.2%**	480.5	521.4	**+8%**

Table 6.1: Results comparison between nominal and optimized model

For Woofer 1, the optimized geometry has met the requirements posed in Section 2. *Bl* in x=0 is 5% higher than the nominal one (3.9[Wb/m] against 3.7[Wb/m]),with a simmetry value of the curve more than 1.5% improved but with significantly less volume used. In fact, the optimized PPI is corresponding to almost 70% of the nominal one, while the optimized PPS almost 76%, with a significant reduction of volume used. For Woofer 2, the optimized geometry has met the requirements posed in 2. *Bl* in x=0 is almost 10% higher than the nominal one (9.5[Wb/m] against 8.5[Wb/m]), with a symmetry value of the curve more than 3% improved but with less volume used. In fact, the optimized PPI is corresponding to almost 95% of the nominal one, while the optimized PPS almost 63%, with a significant reduction of volume used overall. For Woofer 3, the optimized geometry has met two out of three of the requirements posed in 2. *Bl* in x=0 is almost 10% higher than the nominal one (27[Wb/m] against 24.5[Wb/m]), with a simmetry value of the curve more than 1.2% improved but this time two volumes are comparable. In fact, the optimized PPI is corresponding to almost 101% of the nominal one, while the optimized

PPS almost 103%, with no significant reduction of volume used overall, that means that the starting geometry in terms of volume was still the lightest shape possible, with a very little room for improvement. Even though volume requirements are not met, *Bl* maximum value and symmetry are really improved, this makes this solution to be taken into account anyway.

The methodology chosen to perform the topologic optimization was not a custom solution applied to magnetic circuits, but is a pre-built methodology with algorithms and solvers, that has many applications apart from the optimization of loudspeakers' components. Applying this kind of process to magnetic circuits led to some interesting results, obtaining better performances in terms of Bl factor and portability. The aim of this methodology is to provide a mean to optimize the magnetic circuit in a pre-design phase, FEM software like COMSOL Multiphysics are really useful in this because they can help build prototypes without enhancing costs and productivity requirements. Anyway, this method with the Density Model applied is not the unique way to deal with these kind of problems, but the goal of the project was to propose a solution without considering completely the feasibility; In fact, the plates' shape where the optimization process starts, are squared and don't leave space for the pin, also the basket and the modulation ring, where present, were not considered.

Obviously, there is always room for improvements, but this can be useful as a method to build the pre-design phase and consider every possible opportunity to make it feasible also in a factory process. A possible way to improve this kind of solution is also to consider variable the dimension of the magnet, that in this case had the same dimensions of the starting model in all design phases, and obtain the same performance results using yet less iron for the plates.

Bibliography

[1] E. A. *Master Handbook of Acoustics: 4th Edition*. McGraw-Hill, 2001.

[2] M. Audio. Magico news for summer 2020, 2020. URL `https://www.magicoaudio.com/news/qpml3rqd1prhpgedadyhhwm6j0fh9a`.

[3] A. N. Benoît Merit. Magnet-only loudspeaker magnetic circuits: A solution for significantly lower current distortion. *Journal of the Audio Engineering Society*, 2012.

[4] A. N. Benoît Merit. Magnet-only loudspeaker motors: linear behavior theoryvs. nonlinear measurements. *Societe Francaise d'Acoustique*, pages 463–474, 2015.

[5] Beranek. *L. L. Acoustics. 2nd ed. Acoustical Society of America*. Woodbridge,NY, 1993.

[6] L. Bortot. Optimization of demodulation rings in professional louspeakers. Master's thesis, Università di Padova, 2012.

[7] M. Cafaro. Loudspeaker motor: Design and non-ideality analysis. Master's thesis, Politecnico di Milano, 2021.

[8] M. Cobianchi. Progettazione altoparlanti parte 1,2,3. *Audio Review*, 2021.

[9] COMSOL. Comsol documentation, . URL `https://doc.comsol.com/6.1/docserver/#!/com.comsol.help.comsol/helpdesk/helpdesk.html`.

[10] COMSOL. Optimization module user's guide, . URL `https://doc.comsol.com/5.4/doc/com.comsol.help.opt/OptimizationModuleUsersGuide.pdf`.

[11] S. COMSOL AB, Stockholm.

[12] M. A. H.-F. A. Design. Electrical model for vented enclosure. URL `http://mh-audio.nl/Calculators/EM2.asp`.

[13] T. A. o. S. Eminence and Sound. Understanding loudspeaker data, 2023. URL `https://eminence.com/pages/support__understanding-loudspeaker-data`.

[14] G.L.Augspurger. The magnet, heart of the loudspeaker. *HiFi/Stereo Review*, pages 1–4, 1965.

[15] E. Guarin. Desing and optimization considerations for speaker magnets. URL `https://www.aes.org/tmpFiles/elib/20230319/5714.pdf`.

[16] A. Halliday. Navigating the intuitive comsol multiphysics® modeling environment, 2016. URL `https://www.comsol.com/blogs/navigating-the-intuitive-comsol-multiphysics-modeling-environment/`.

[17] K. E. Jensen. Performing topology optimization with the density method. URL `https://www.comsol.it/blogs/performing-topology-optimization-with-the-density-method/`.

[18] W. Klippel. Loudspeaker nonlinearities – causes, parameters, symptoms. .

[19] W. Klippel. Maximizing efficiency in active loudspeaker systems, . URL `https://www.aes.org/tmpFiles/elib/20230319/19425.pdf`.

[20] K. S. Marinescu M., Marinescu N. Optimization of magnetic circuits for loudspeakers 1970 and now. *ISFEE*, 2012.

[21] T. F. MFG.CO.Ltd. Basic properties of magnets, 2018. URL `https://www.tokyoferrite-ho.co.jp/en/technical_data/behavior/behavior.html`.

[22] mynewmicrophone. Full list: Thiele-small speaker parameters w/ descriptions. URL `https://mynewmicrophone.com/full-list-thiele-small-speaker-parameters-w-descriptions/`.

[23] M. Rémy. Innovative ironless loudspeaker motor adapted to automotive audio. *Acoustics*, 2011.

[24] K. Shaposhnikov. How to perform a nonlinear distortion analysis of a loudspeaker driver. *COMSOL Blog*, 2018.

[25] E. Sound. Ttc - tetracoil double voice coil. URL `https://www.eighteensound.it/en/technologies/ttc-tetracoil-double-voice-coil/`.

[26] SoundImports. Thiele/small parameters, a guide to the mysterious world of loudspeakers' specifications. URL `https://www.soundimports.eu/en/blogs/blog/thiele-small-parameters/`.

[27] W. X. Topology optimization for structural and fluid mechanics in comsol. URL `https://www.comsol.com/blogs/topology-optimization-for-structural-and-fluid-mechanics-in-comsol/`.

[28] C. Zuccatti. Optimizing the voice-coii-airgap geometry for maximum loudspeaker motor strength.

[1–16, 19, 21–28]

List of Figures

List of Tables

List of Symbols

Variable	Description	SI unit
$\boldsymbol{Bl}$	force factor	Wb/m
$\boldsymbol{B}$	magnetic induction field	T
$\boldsymbol{B_r}$	remanent flux density	T
$\vec{\boldsymbol{H}}$	magnetizing force field	Am^{-1}
$\vec{\boldsymbol{M}}$	magnetization field	Am^{-1}
$\boldsymbol{D}$	dielectric displacement field	C/m^2
$\vec{\boldsymbol{J}}$	current density	A/m^2
$\boldsymbol{\mu_r}$	relative permeability	1
$\boldsymbol{\epsilon_r}$	relative permittivity	1
$\boldsymbol{\sigma}$	conductivity	Sm^{-1}
$\vec{\boldsymbol{J}}$	current density	A/m^2
$\boldsymbol{i}$	current	A
$\boldsymbol{\theta_c}$	Control material volume factor	1
$\boldsymbol{\theta_f}$	Filtered material volume factor	1
$\boldsymbol{\theta_p}$	Penalized material volume factor	1
$\boldsymbol{\theta}$	Material volume factor	1
$\boldsymbol{\theta_{avg}}$	Average material volume factor	1
$\boldsymbol{S.I}$	Simmetry Index	%

Acknowledgements

I would like to thank Faital for the opportunity I was given and for the very formative months I spent in the company, especially to my mentor Grazia, who in addition to being an exceptional worker is a strong woman with character and a true inspiration to me as a person. I would also especially like to thank Marco D., Marco C., Tommaso and Mattia who made these months much more enjoyable and were always available for anything I needed.

I would like to thank Professor Giuseppe Bertuccio for the opportunity he gave me in doing this thesis, for his extremely interesting course and for all the precious advice he gave me.

I would like to thank my family, who have always supported me in any choice I have made and have allowed me to finish this study path, always believing in me.

I would like to thank i Kiwi, my lifelong friends, with whom I have shared many adventures and I know they will always be there for me as I will be there for them, and they have never let me miss a smile or a word of comfort even in the most dark moments.

I would like to thank Caballos e Puledritas, who in recent years have always made me feel at home in a large group, with whom I have shared moments that I will always carry with me.

I would like to thank the high school group, which I have known for more years than I care to admit, with which I grew up and shared many experiences that I will always carry in my heart, and in particular Mario, Giulia and Margherita, who have always been at my side and whose precious friendship I will preserve for the rest of my life.

I would like to thank the Crossfit Bullams guys, who have made my passion for sport ever stronger, and with whom I have established a bond that goes far beyond the gym,

with whom we have formed a splendid group over the years ready to support each other in the most tiring moments.

I would like to thank my Belle, Claudia and Silvia, who are always by my side, and with whom we are always ready to support each other on any occasion in life, and we are always ready to give advice when needed. They lifted me up in moments of discomfort and I owe them a lot, more than they imagine.

I would like to thank Marco and Teo, who in addition to having gone through the tortuous university path with me, making each other strong to finish, have become two precious people who I cannot do without and with whom we have shared wonderful experiences.

I would like to thank the guys at Axis Gym, with whom we have formed a splendid working group and friendship that goes beyond the weight room, and also the Panettoni group, with whom we have established a wonderful relationship that has made work a fun and stimulating, and with whom we have created a good friendship.

I would like to thank the guys from Cremona, Mattia, Jaime, Gianmarco, Andrea, Enrico, Laura, Luca and Enrico for making my study days much more pleasant by sweetening them with pleasant chats and fun evenings. In particular I wanted to thank Federico, who was a wonderful fellow student and is still a sincere friend, with a huge heart always willing to give all of himself for others.

I would like to thank my band, Jacopo and Francesco, with whom we have known each other for many years and although each of us has had different experiences in life we have never lost touch, always linked by the same indissoluble passion for music.

I would like to thank my sailing friends, in particular Andrea and Jacopo, with whom, in addition to a sincere friendship, we have shared a great passion for this sport since we were kids. I wanted to thank Monica, who is the indissoluble blonde part of me, a point of reference for longer than anyone else and whose friendship is a rare treasure that was given to me, and to which I will remain forever attached.

And last but not least, I wanted to thank my fiancée, Maddalena, who came into my life like a bolt from the blue, completely turning it upside down. In every dark moment, in every difficulty she has always been there and with a smile, a sweet word reminds me every day how much I am in love with her and she is my number one supporter and fan.

Every day she gives everything for me, as I do for her and is the true representation of Love in all forms, and I couldn't be luckier to have her by my side.